

# **IMPROVED DYNAMIC STABILITY USING FACTS DEVICES WITH PHASOR MEASUREMENT FEEDBACK**

by

**Mark Allen Smith**

Thesis submitted to the Faculty of the  
Virginia Polytechnic Institute and State University  
in partial fulfillment of the requirements for the degree of

**MASTER OF SCIENCE**

in

**Electrical Engineering**

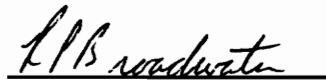
**APPROVED:**



**A. G. Phadke, Chairman**



**S. Rahman**



**R. P. Broadwater**

**December 1994  
Blacksburg, Virginia**

C.2

LD  
5655  
V855  
1994  
S659  
C.2

# **IMPROVED DYNAMIC STABILITY USING FACTS DEVICES WITH PHASOR MEASUREMENT FEEDBACK**

by

**Mark Allen Smith**

**Arun G. Phadke, Committee Chairman  
The Bradley Department of Electrical Engineering**

## **(ABSTRACT)**

With an increasing number of regulatory and economic factors making the operation of power systems more challenging, utilities must take full advantage of technological advances which allow more flexibility for operation. One of these advances is the combination of power electronic controllers and compensation devices known as Flexible AC Transmission Systems (FACTS) technology. This thesis will examine the ability of FACTS technology to improve dynamic stability when controlled with data obtained from another recent advancement, phasor measurement units (PMUs). Based on an overview of the relative capabilities of presently available FACTS devices, a specific device will be chosen to be modeled in a dynamic stability study. Eigenvalue sensitivity analysis will be used to determine the optimal placement for this FACTS device in regards to stability for a test power system. Then a state space model will be developed for the FACTS compensated test system, and eigenvalue sensitivity and time-domain methods will be used to determine the optimal controller characteristics for the modeled FACTS device. Stability results will be verified using eigenvalue analysis and time simulation techniques.

## **ACKNOWLEDGMENT**

I would like to thank my advisor, Dr. Arun G. Phadke, for all his support and guidance on this thesis and during my graduate studies at Virginia Tech. I would also like to thank my other committee members, Dr. Saifur Rahman and Dr. Robert P. Broadwater, for their guidance while I pursued my graduate degree. In addition, I would like to thank my fellow graduate students in the power area for their advice and friendship during my graduate studies. Finally, I want to thank my girlfriend, Jacqueline Homer, and my family for the constant support and understanding that have made this all worthwhile.

# TABLE OF CONTENTS

## **Chapter 1     Introduction**

1.1	Problem Statement.....	1
1.2	Power System Stability.....	2
1.3	Flexible AC Transmission Systems.....	3
1.4	Proposed Solution.....	4

## **Chapter 2     Power System Stability**

2.1	Definition of Stability.....	6
2.2	State Space Model.....	9
2.3	Eigenvalues and Stability.....	10

## **Chapter 3     FACTS Devices**

3.1	Background.....	12
3.2	Types of Devices.....	13
3.2.1	NGH-SSR Damper.....	14
3.2.2	Static VAR Compensator.....	15
3.2.3	Thyristor-Controlled Series Capacitor.....	15
3.2.4	Static Condenser.....	15
3.2.5	Thyristor-Controlled Phase Angle Regulator.....	16
3.2.6	Unified Power Controller.....	16
3.2.7	Thyristor-Controlled Dynamic Brake.....	17
3.3	Device Selection.....	17
3.4	Practical Applications.....	19

## **Chapter 4     Power System Model**

4.1	Description of Test System.....	22
4.2	Constant Impedance Load Model.....	24
4.3	Two-Axis Generator Model.....	26
4.4	Excitation System Model.....	29
4.5	Linearized State Equations.....	31
4.6	Current Coefficient Matrix.....	33

<b>Chapter 5</b>	<b>Response of the Uncompensated System</b>	
5.1	Assumed Conditions.....	40
5.2	Evaluation Techniques.....	41
5.3	Results.....	43
<b>Chapter 6</b>	<b>Addition of a FACTS Device To Power System Model</b>	
6.1	Optimal Placement of FACTS Device.....	48
6.2	FACTS Control Strategy.....	51
6.3	Effects On The Reduced Admittance Matrix.....	53
6.4	Augmented Current Coefficient Matrix.....	54
6.5	Optimization of FACTS Controller.....	58
<b>Chapter 7</b>	<b>Response of the Compensated System</b>	
7.1	Assumed Conditions.....	67
7.2	Mechanical Series Compensation.....	67
7.3	Modulated FACTS Compensation.....	71
7.4	Compensated System Loadability.....	76
<b>Chapter 8</b>	<b>Conclusions</b>	
8.1	Summary of Results.....	78
8.2	Future Work.....	80
<b>References</b> .....		82
<b>Appendix A</b>	<b>Numeric Coefficient Matrices</b>	
A.1	Current Coefficient Matrices.....	84
A.2	State Coefficient Matrices.....	84
<b>Appendix B</b>	<b>Source Code Listings</b>	
B.1	MATLAB Data Files.....	87
B.2	Uncompensated System Simulations.....	90
B.3	FACTS Compensated System Simulations.....	100
B.4	Sensitivity Studies.....	113
<b>Vita</b> .....		120

## LIST OF FIGURES

Figure 3.1:	Schematic of a Typical Single Phase TCSC Installation.....	18
Figure 4.1:	Nine Bus, Three Machine Power System.....	23
Figure 4.2:	IEEE Type I Excitation System.....	30
Figure 4.3:	Phasor Diagram of Machine and System Reference Frames.....	34
Figure 4.4:	Linearized Current Coefficient Matrix.....	39
Figure 4.5:	Reduced Linearized Current Coefficient Matrix.....	39
Figure 5.1:	Flowchart for Uncompensated Test System Simulations.....	42
Figure 5.2:	System Eigenvalues (Uncompensated System).....	43
Figure 5.3:	Close-up of Dominant Eigenvalues (Uncompensated System).....	44
Figure 5.4:	Electrical Power of Generator 1 (Uncompensated System).....	45
Figure 5.5:	Electrical Power of Generator 2 (Uncompensated System).....	45
Figure 5.6:	Electrical Power of Generator 3 (Uncompensated System).....	46
Figure 5.7:	Rotor Angle Difference, $\delta_{12}$ (Uncompensated System).....	46
Figure 5.8:	Rotor Angle Difference, $\delta_{13}$ (Uncompensated System).....	47
Figure 6.1:	Nine Bus Test System with Addition of FACTS Device.....	50
Figure 6.2:	Conceptual Diagram of FACTS Control Scheme.....	52
Figure 6.3:	Current Coefficient Matrix With Inclusion of FACTS State Variable.....	56
Figure 6.4:	Critical Eigenvalue Variation with FACTS Controller Gain.....	60
Figure 6.5:	Critical Eigenvalue Variation with FACTS Controller Time Constant.....	60

Figure 6.6:	Flowchart for FACTS Compensated Test System Simulations.....	63
Figure 6.7:	Response of FACTS Reactance for $K_X = -21$ and $T_X = 10$ .....	63
Figure 7.1:	System Eigenvalues (Mechanically Compensated System).....	69
Figure 7.2:	Close-up of Dominant Eigenvalues (Mechanically Compensated System)...	69
Figure 7.3:	Electrical Power of Generator 1 (Mechanically Compensated System).....	70
Figure 7.4:	Rotor Angle Difference, $\delta_{12}$ (Mechanically Compensated System).....	70
Figure 7.5:	System Eigenvalues (FACTS Compensated System).....	72
Figure 7.6:	Close-up of Dominant Eigenvalues (FACTS Compensated System).....	72
Figure 7.7:	Electrical Power of Generator 1 (FACTS Compensated System).....	73
Figure 7.8:	Electrical Power of Generator 2 (FACTS Compensated System).....	73
Figure 7.9:	Electrical Power of Generator 3 (FACTS Compensated System).....	74
Figure 7.10:	Rotor Angle Difference, $\delta_{12}$ (FACTS Compensated System).....	74
Figure 7.11:	Rotor Angle Difference, $\delta_{13}$ (FACTS Compensated System).....	75
Figure 7.12:	Change in TCSC Reactance, $\Delta X_{45}$ , versus Time.....	75
Figure 8.1:	Electrical Power of Generator 1 for All Compensation Conditions.....	79
Figure A.1:	Current Coefficient Matrix for Uncompensated Test System.....	84
Figure A.2:	Current Coefficient Matrix for FACTS Compensated Test System.....	84
Figure A.3:	Numeric State Matrix Coefficients for Uncompensated Test System.....	85
Figure A.4:	Numeric State Matrix Coefficients for FACTS Compensated Test System.	86



## LIST OF TABLES

Table 3.1:	FACTS Devices and Their Control Attributes.....	14
Table 4.1:	Per Unit Impedance Data for Nine Bus System.....	24
Table 4.2:	Initial Generation, Load, and Voltage Data for Nine Bus System.....	24
Table 4.3:	Converted Load Admittances for Nine Bus System.....	25
Table 4.4:	Two-Axis Generator Data for Nine Bus Test System.....	28
Table 4.5:	Two-Axis Generator Model Nomenclature.....	29
Table 4.6:	Summary of Excitation System Data for Nine Bus System.....	31
Table 4.7:	Generator Initial Conditions.....	33
Table 5.1:	System Eigenvalues for Uncompensated Test System.....	44
Table 6.1:	Average Critical Eigenvalue Sensitivity to Changes in Line Reactance.....	49
Table 6.2:	TCSC Response Characteristics for Various Controller Settings.....	65
Table 7.1:	System Eigenvalues for Mechanically Compensated System.....	68
Table 7.2:	System Eigenvalues for FACTS Compensated System.....	71
Table 8.1:	Critical System Eigenvalues For All Compensation Conditions.....	79

# CHAPTER 1

## Introduction

### 1.1 Problem Statement

Many factors in recent years have made the operation of power systems an increasingly complex and challenging task. The need to meet increased load growth has come in conflict with obtaining new rights-of-way for transmission lines. Regulatory constraints, including those governing the environmental impacts of power plants, have presented utilities with the possible dilemma of sacrificing system security levels in order to comply with federally mandated environmental regulations. Economic concerns have forced utilities to operate their plants and transmission systems for much longer lifetimes and closer and closer to the edge of their limits. With these changes, several traditional system concerns demand more attention. Among these is the problem of small-signal oscillations which, if they are not damped out, may damage equipment or interrupt electrical service. Technological advances in the area of power electronics now allow more flexible, dynamic control of power system compensation devices for use in

correcting this and several other network problems. This thesis will examine the implementation and control of this technology for improving the dynamic stability of a power system.

## 1.2 Power System Stability

The concept of stability is important in many fields and may be defined in slightly different ways depending on the application. In general, however, a system is regarded as stable if it either reaches a steady-state value in a finite amount of time or continues to oscillate at a fixed amplitude indefinitely. For power systems, a system is regarded as stable if it reaches steady-state after a disturbance within a finite amount of time. An infinitely oscillatory response to a disturbance, while regarded as stable from a theoretical point-of-view, is undesirable in a power system due to the impracticality of using and supplying electricity in such a manner.

The study of power system stability comprises three distinct areas of concern [1]. First, *steady-state* stability refers to the ability of a power system to yield a long-term stable response to ordinary changes in load and generation. On the other hand, if a power system has good *transient* stability, it will remain stable after large or sustained disturbances such as faults. The third area of concern within power system stability is known as *dynamic* stability. Dynamic stability is a measure of how well a power system responds to small disturbances such as unexpected changes in load or generation. If a power system is not dynamically stable, oscillations caused by these small disturbances will continue to increase in amplitude and not damp out.

### **1.3 Flexible AC Transmission Systems**

Series and shunt compensation have long been used by electric utilities for improving transmission voltage levels, increasing power transfer capabilities and reducing overall transmission losses [2]. However, in the past these tools have been basically static in nature since they were operated by some sort of mechanical means. Recently, improvements in power electronics and control technologies have led to improved options for controlling power system compensation devices such as series capacitors. Due to their ability to provide utilities with greater flexibility in operating their power systems, these devices have been dubbed “Flexible AC Transmission Systems” or FACTS devices. This term and the concept it represents have been credited to Narain G. Hingorani of the Electric Power Research Institute (EPRI) [3]. Devices in this category include a variety of high-power electronic controllers which may be used individually or in combinations depending on the application. Examples of FACTS devices include static VAR compensators (SVCs), unified power controllers (UPCs), and thyristor-controlled series capacitors (TCSCs). The major advantage of these new controllers over conventional control devices such as mechanical switches and phase shifters is their ability to quickly respond to power system changes without the inertial time delays inherent in mechanical devices. As a result of these advances, series compensation can now be controlled dynamically in order to respond quickly to changes in a power system. This includes the capability to damp power system oscillations.

## **1.4 Proposed Solution**

This thesis will examine the ability of FACTS technology to improve dynamic power system stability by damping oscillations. Specifically, the thesis will focus on how placement and control of a typical FACTS device can be chosen and designed in order to provide maximum improvement in the dynamic stability of a test power system. The focus will be the application and implementation of FACTS technology rather than on detailed modeling of the devices themselves.

Various FACTS devices will be examined to determine their power system control capabilities, and one device will be selected for modeling. To determine the effectiveness of the chosen FACTS device in improving dynamic stability, an example power system, including each generator's excitation system, will be modeled in detail. An initially stable system will be moved towards marginal stability by adjusting the time constants and gains in each generator's excitation system. The system will also be moved to an unstable state by a gradual change in reactive load. Then, a disturbance in the form of an instantaneous change in generator mechanical power will be applied to the system, and the response of the system will be evaluated.

In order to damp the oscillations caused by the disturbance, the selected FACTS device will be inserted into the test power system. Eigenvalue sensitivity analysis will be used to determine what FACTS device location will provide optimal compensation for the entire power system. An approach for including the FACTS device in a state space model of the test power system will be proposed and implemented. Then using eigenvalue and

time-domain techniques, a FACTS control strategy using remotely measured power system data will be developed and optimized for overall test system stability and device time-response desirability. Results for the uncompensated, mechanically compensated and FACTS compensated test systems will be evaluated using both eigenvalue analysis and numerical simulation.

## **CHAPTER 2**

### **Power System Stability**

#### **2.1 Definition of Stability**

An effective study of power system stability, a topic which includes several distinct areas of research, should be designed with a specific definition of this characteristic in mind. Failure to provide a narrow definition for stability can otherwise result in confusion. For example, the term stability when applied to an electric utility may have different meanings for power system planners who think in terms of months or years and system operations engineers who are more concerned with shorter periods of time such as seconds, minutes, or hours. For this thesis, it is therefore important to start with a general definition for stability and then refine the definition to reflect the specific attributes that are being examined in this research study.

In general, stability deals with the time-domain response of a system to some type of disturbance. A disturbance in a power system can be defined as a “sudden change or sequence of changes in one or more of the operating quantities” [4]. This could be a

momentary change in conditions in a system (an impulse) or a sudden but sustained change in system parameters (a step function). A response to a disturbance may exhibit overdamped or underdamped oscillations and may include exponential growth or decay. The responses of “operating quantities” such as generator rotor angle, electrical power output, and frequency are often used in determining the stability of a power system. In relating the general concept of stability to a power system, a well-known textbook author defines stability as the following:

“Power system stability may be defined as that property of the system which enables the synchronous machines of the system to respond to a disturbance from a normal operating condition so as to return to a condition where their operation is again normal.” [5]

This definition is sufficiently general to allow three sub-categories of power system stability which are defined by the time period of a study as well as the magnitude of a disturbance. *Steady-state* stability refers to the ability of a power system to yield a stable response to ordinary changes in operating conditions. As the name implies, steady-state stability studies examine the overall long-term behavior of power systems under normal expected conditions. As such, these studies generally use very simplified power system models and assume that all transients have died out. On the other hand, the study of *transient* stability examines the response of a power system to sudden large changes in system conditions such as faults or the loss of generating units. These disturbances may cause sudden changes in system response within a few cycles of the network power



oscillation. Consequently, transient stability deals with time periods measured in milliseconds through periods of a few seconds.

The third area of concern within power system stability is known as *dynamic* stability, the major area of interest in this study. Dynamic stability is determined by assessing a system's response to disturbances that are small enough to allow linearization of the equations describing the system's dynamics. Studies in this area usually include detailed generator and excitation system models. Dynamic stability bridges the time period between transient and steady-state stability. Thus, the time period covered by dynamic stability studies is generally measured in minutes. If a power system is not dynamically stable, disturbances can cause small signal fluctuations that may gradually increase in amplitude and become sustained oscillations.

In performing studies of stability on a power system, several assumptions are usually made to simplify analysis. Three assumptions generally apply to all types of stability studies [5]. First, only synchronous frequency currents and voltages are considered. Thus, harmonic components and dc offsets are neglected. Also, symmetrical components are used for representing unbalanced faults. Finally, generated voltages are assumed to be unaffected by variations in machine speed. In addition to these basic assumptions, further simplifying assumptions may be applied to power systems depending on the specific type of stability being considered. For dynamic stability, one crucial assumption is that all variables can be linearized around an initial operating point.

## 2.2 State Space Model

In order to model a power system for a dynamic stability study, generator and excitation system differential equations must be formulated for each machine. The forms of these equations depend on what models are used. Perhaps the most commonly used model for a synchronous generator is an emf in series with a reactance. For this general model, the dynamics of the rotor of each machine are described by what is known as the swing equation. This may be written in several forms depending on whether it is expressed in terms of power or torque and whether the units used to express each term are absolute or per unit. One useful form in terms of per unit power is:

$$\left( \frac{2H}{\omega_R} \right) \frac{d^2\delta}{dt^2} = P_m - P_e - D\omega \quad (2.1)$$

where  $H$  is related to stored energy in the rotor at rated speed  $\omega_R$  and  $D$  is a damping coefficient. Detailed generator and excitation system differential equations are discussed in Chapter 4, but equation (2.1) is useful in demonstrating the state space model.

For the state space representation of a power system, all of the generator and excitation system equations are linearized and formulated into a format in which the time derivatives of each state variable are grouped in a vector. Then the right hand side of each equation may be grouped in matrices containing combinations of initial conditions and other state variables. The state and input variables are then factored out, leaving matrices of coefficients acting on state variables (the **A** matrix) and the system inputs (the **B** matrix). Realizing that angular frequency ( $\omega$ ) equals the time derivative of rotor angle ( $\delta$ )

and that  $P_m$  is assumed constant while  $P_e$  is linearized around its initial operating point, equation (2.1) can be arranged in the form:

$$\begin{aligned}\dot{\delta} &= \omega \\ \dot{\omega} &= -\left(\frac{\omega_R}{2H}\right)(P_e + D\omega) + \left(\frac{\omega_R}{2H}\right)P_m\end{aligned}\quad (2.2)$$

Summarizing this format for an entire system of equations:

$$\dot{\mathbf{x}} = \mathbf{Ax} + \mathbf{Bu} \quad (2.3)$$

where  $\mathbf{x}$  and  $\mathbf{u}$  are variable vectors and  $\mathbf{A}$  and  $\mathbf{B}$  are coefficient matrices. Equation (2.3) represents the state space equation for the system. The content of this state matrix, in the form of the matrix eigenvalues, can be used to determine the stability of the system.

### 2.3 Eigenvalues and Stability

From matrix theory, the eigenvalues  $\lambda_i$  of a square matrix  $\mathbf{A}$  are defined as all non-trivial solutions to the following equation:

$$\mathbf{Ax} = \lambda\mathbf{x} \quad (2.4)$$

This equation can be solved using the relationship:

$$\det(\mathbf{A} - \lambda\mathbf{I}) = 0 \quad (2.5)$$

where  $\mathbf{I}$  is the identity matrix which contains ones on its diagonal and zeros for every off-diagonal term. Expanding the equation for a  $n \times n$  matrix:

$$\det \begin{vmatrix} a_{11} - \lambda & a_{12} & \cdots & a_{1n} \\ a_{21} & a_{22} - \lambda & \cdots & a_{2n} \\ \vdots & \vdots & \ddots & \vdots \\ a_{n1} & a_{n2} & \cdots & a_{nn} - \lambda \end{vmatrix} = 0 \quad (2.6)$$

Thus, there will be  $n$  eigenvalues for a  $n \times n$  matrix. These eigenvalues may be completely real numbers or complex conjugate pairs.

Eigenvalues provide very meaningful information about the stability of a system, and they are often plotted in a complex plane to provide a graphical representation of the system's stability characteristics. In this graphical sense, eigenvalues which are to the left of the imaginary axis are regarded as stable while those that appear on or to the right of the imaginary axis reflect unstable conditions. The time response of a linear system to a disturbance is equal to a summation of components containing constants multiplied by terms of the form  $e^{\lambda t}$  [6]. The eigenvalues with the largest real components have the most impact on this response and are thus referred to as the dominant or critical eigenvalues. Accordingly, a system with only a single, positive real-valued critical eigenvalue will exhibit exponential growth while a system with a single, negative real-valued critical eigenvalue will exhibit a response with an exponential decay. In a similar manner, dominant eigenvalues which are complex conjugates of each other and have negative real parts will provide an oscillatory response inside the envelope of an exponential decay. This oscillation will have an angular frequency ( $\omega$ ) equal to the imaginary portion of the critical eigenvalue(s). Thus, it is the real component of each eigenvalue which determines if a system is stable while the imaginary part (if it exists) determines the form of the response.

## **CHAPTER 3**

### **FACTS Devices**

#### **3.1 Background**

As stated previously, FACTS devices consist of power electronic controllers used in conjunction with power system compensation devices such as series capacitors. The fundamental component of most FACTS device controllers is the thyristor. Various combinations of designs using these thyristors comprise the types of FACTS devices discussed in this chapter. Since, the focus of this thesis is the application of FACTS devices rather than the details of how the actual controller components work, the following general discussion of FACTS devices is included merely to provide background information.

FACTS devices may be used to influence the state of a power system in three ways [7]. First, they can be used to control the series impedance of a transmission line through series compensation. In a similar manner, FACTS devices can be used to control system voltage characteristics by parallel compensation. Finally, the phase angle between two

points on the transmission system can be altered by the insertion of FACTS devices which incorporate phase-shifting transformers.

From the nature of their electronic controllers, FACTS devices have a number of inherent advantages over any existing electromechanical counterparts [7]. By definition, FACTS devices allow for *flexible* control of power systems. Probably the most important attribute of these devices which allows this flexibility is their speed of operation. Since the power electronic controllers have no massive mechanical components to introduce physical time delays in switching, they can operate very rapidly in order to react to the changing conditions on a power system. Also due to the lack of mechanical parts which inevitably wear over time, FACTS devices allow virtually limitless repeatability and require very little maintenance. In addition, as further advances in power electronics technology make FACTS technology less expensive, the ability of these devices to be used for multiple purposes will make them even more economically attractive for use by electric utilities.

### **3.2 Types of Devices**

A variety of FACTS devices are now in use. Table 3.1 provides a summary of these devices and their major control capabilities. A brief discussion of each of these devices is provided below. As stated above, this section is intended as an overview rather than a detailed description of each FACTS device.

### 3.2.1 NGH-SSR Damper

This device is specifically designed to compensate for subsynchronous resonance (SSR). SSR occurs at a frequency typically between 15-30 Hz when the natural frequencies of a generator's rotational shaft are the same as the electrical resonance frequency of a transmission line [3]. This device is comprised of an AC thyristor switch connected in series with a resistor and small inductor. This combination is then placed in parallel with a series capacitor.

**Table 3.1: FACTS Devices and Their Control Attributes (Adapted from [3])**

FACTS Device	Areas of Increased Control						
	Power	Voltage	VARs	Phase Angle	Oscillation Damping	Transient Stability	Series Impedance
NGH-SSR Damper					X	X	X
Static VAR Compensator		X	X		X		
Thyristor-Controlled Series Capacitor	X	X			X	X	X
Static Condenser		X	X		X	X	X
Thyristor-Controlled Phase Angle Regulator	X			X	X	X	
Unified Power Controller	X	X	X		X	X	
Thyristor-Controlled Dynamic Brake					X	X	

### 3.2.2 Static VAR Compensator

Static VAR compensators (SVCs) have been used by some electric utilities since the mid-1970s for voltage stability control [3]. This device, which also utilizes thyristors in its design, allows for quick insertion or removal of shunt combinations of reactors (inductors) and capacitors. SVCs have also been used in conjunction with power system stabilizers to improve overall power system damping [8].

### 3.2.3 Thyristor-Controlled Series Capacitors

One of the most versatile of the FACTS devices listed in Table 3.1 is the thyristor-controlled series capacitor (TCSC). This device allows variation in the series impedance of a transmission line by the series insertion or removal of capacitor banks. With this capability, TCSCs can be used to respond to sudden changes in a power system such as a fault (transient stability). Also, this device allows damping of oscillations that may be produced by small but frequently occurring disturbances such as load changes. These disturbances may push a marginally stable system to the point of instability. In this case, the TCSC can be a great tool for improving dynamic power system stability.

### 3.2.4 Static Condenser

The static condenser or Statcon is a device which has attributes similar to the static VAR compensator discussed above with the addition of improved stability control capabilities. The Statcon functions like a three phase AC-DC inverter which is driven by a



DC storage capacitor. The output voltages of this device are in phase with the AC system voltages and may be higher or lower in magnitude than the system depending on how the device is controlled. The difference between the Statcon and system voltage magnitudes causes the flow of output current from the device to be either leading or lagging. Thus, the polarity and magnitude of reactive power can be influenced by controlling the voltage of the Statcon. The Statcon's improved stability control as compared to the SVC is due in part to its ability to have equal compensation impact at a lower power rating [3].

#### 3.2.5 Thyristor-Controlled Phase Angle Regulator

As the name implies, this device allows control of power system phase angle. This is accomplished by addition or subtraction of a variable voltage component to each phase voltage that is 90 degrees out of phase. This voltage component can be obtained from a transformer connected across the other two phases. Variation in the amount of phase change is determined by switching in transformer windings with different turns ratios.

#### 3.2.6 Unified Power Controller

Unified power controllers (UPCs) have the greatest variety of control attributes of all present FACTS devices. UPCs accomplish these control attributes through the addition of a series voltage vector to a typical AC system voltage. This voltage, which is produced through a rectifier-inverter combination, may have variable magnitude and may

or may not be in phase with the system voltage. Thus, this injected variable voltage, if controlled correctly, can have a positive effect on several power system characteristics.

### **3.2.7 Thyristor-Controlled Dynamic Brake**

The thyristor-controlled dynamic brake consists of a resistive load which is connected in a shunt configuration and controlled by thyristors. This resistive load can be applied as needed to damp out or “brake” power system oscillations. This device has a strong application in reducing the risk of loss of synchronism in generators [3].

## **3.3 Device Selection**

As discussed above, there are several FACTS devices which have a variety of power system control capabilities. These attributes, as summarized in Table 3.1, include the capability to control voltage level, power flow, and power system oscillations. The two devices in this table which exhibit the widest range of control capabilities are the thyristor-controlled series capacitor (TCSC) and the unified power controller (UPC). Since the TCSC is basically a conventional series capacitor with an advanced switching system, it is more simple to describe and model than the UPC. Thus, the TCSC will be the device modeled in this thesis.

A circuit diagram for one phase of a typical TCSC installation is shown in Figure 3.1. It consists of a large number of small thyristor-controlled capacitors in series with a larger capacitor which is normally switched mechanically. The TCSC being modeled in

this thesis will be assumed to have thirty 1% thyristor-controlled compensation segments in series with one 20% mechanically switched capacitor bank. This will allow incremental changes in the TCSC reactance between 0 and 30% of normal line reactance and a total compensation capability of 50%.

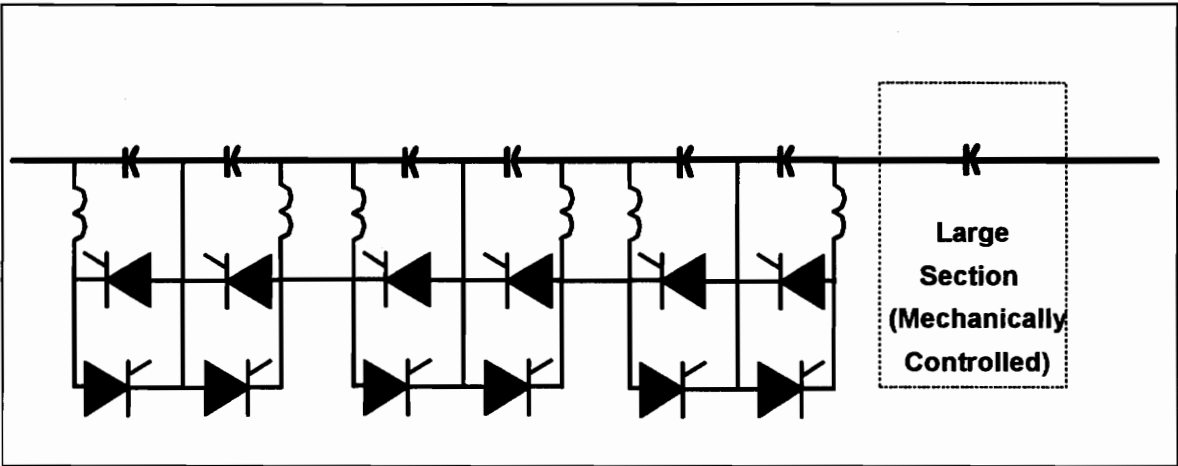


**Figure 3.1: Schematic of a Typical Single Phase TCSC Installation**

One important characteristic of traditional series capacitor installations without advanced control systems is their ability to withstand overvoltages from the high currents observed during faults. Early installations used air gaps placed in parallel with the capacitor modules for protecting the device during faults. More recently, gap-type protection schemes have been replaced with metal oxide varistors (MOVs) which have highly non-linear resistance characteristics due to their zinc oxide content [9]. This protection scheme allows the device to be reinserted instantaneously without transients. Even more recently, electronic control of switches which bypass both the capacitors and MOV during prolonged periods of overvoltage has been proposed [10].

Overvoltage protection is obviously important for TCSC installations. The ability for instantaneous reinsertion is a requirement for damping oscillations and quickly adjusting compensation to meet the dynamic needs of a power system. Since the emphasis of this thesis is towards the application of FACTS devices for improvements in dynamic stability rather than the detailed characteristics of the device, the TCSC modeled here will have an assumed overvoltage protection scheme consistent with the above discussion. Specifically, the TCSC will be assumed to have both MOV and electronic bypass switching protection, although these features will not be expressly modeled in this thesis.

### **3.4 Practical Applications**

A number of studies have been published recently regarding the practical application of FACTS devices on power systems. Several studies refer to the increased line loading capabilities realized using FACTS devices [11,12]. The capability for fast repeated switching of compensation devices using FACTS controllers also allows damping of oscillations that are both dynamic and transient in nature. Since the focus of this study is stability, the concentration in this section will be on the uses of FACTS technology to improve power system stability.

For transient stability, Mihalic et al evaluated the effectiveness of various FACTS devices including thyristor-controlled phase angle regulators, unified power controllers, and static VAR compensators [7]. Their criteria in damping transients were to maintain system synchronism during the first swing of the transient, to damp subsequent oscillations

as much as possible, and to prevent the system from persevering near the maximum of the first transient swing. Various control strategies were used for different FACTS devices. For the SVC, the control strategy involved the use of frequency deviation during the initial transient swing to operate the device in a “bang-bang” manner. In following swings, the output of the controller was proportional to the frequency deviation squared. Series compensation was also examined, but no active damping control strategy was presented. The results of their SVC simulations showed that synchronism could be maintained after a three phase fault using their proposed control strategy.

In the area of dynamic stability concerns, coordinated control of static VAR compensators through the use of dominant eigenvalue optimization has been proposed as an effective method for enhancing small-signal stability [8]. Also, control of thyristor-controlled phase shifters (TCPSs) in coordination with generators using optimal control techniques has shown promise for improving small-disturbance stability [13]. In this particular study, localized bus frequency and voltage deviations due to a small disturbance were used as control system input signals.

Mountford et al showed that a thyristor-controlled series capacitor could be used effectively for increased power flow, improved voltage performance, and, more relevant to this thesis, damping small-signal system oscillations [12]. For their work on dynamic stability, the selection of TCSC sites was based on desired improvements in power transfer levels. This study used Z-domain post-processing of time simulations rather than state eigenvalue analysis in the determination of a control scheme for the TCSC. The devised

control scheme used local bus frequencies and voltages as inputs to the various transfer functions devised from the Z-domain techniques.

For this thesis, the goal is improved dynamic stability along the lines of what has been studied by Mountford and others, but with particular emphasis on the design of the device controller. Network reduction will be utilized to simplify the topology of a test system so that a state matrix of the power system can be readily formulated. Optimal TCSC placement for improved stability will be determined using eigenvalue sensitivity methods. An augmented state matrix which includes this FACTS device will be derived. Then, a control strategy using remote phasor measurements as input signals will be designed to optimize both the stability and time response characteristics of the TCSC to a disturbance. Final results will be verified using both eigenvalue and numerical simulation techniques.

## **CHAPTER 4**

### **Power System Model**

#### **4.1 Description of Test System**

The power system used in this study of dynamic stability and FACTS control is a nine bus, three machine system adapted from [14]. The layout for the system is shown in Figure 4.1. As shown, each of the three generators is connected to a bus and step-up transformer which transforms the voltage to the 230 kV level on the transmission system. This transmission system serves three loads which are designated as *A*, *B*, and *C*. Line impedance data for this system is shown in Table 4.1. Generation, load, and voltage data are provided in Table 4.2. All per unit values for this test system have been calculated on a base of 100 MVA.

In modeling this power system, several assumptions were made. First, loads were modeled as constant impedances. Each generator was represented using the two-axis model discussed by Anderson and Fouad [14]. In order to be able to adjust the overall system stability before insertion of FACTS devices, the excitation systems of each

generator were modeled in detail. Finally, in order to formulate a linear state matrix for this system, all equations and variables were linearized around the initial operating point to account for incremental changes in their values. A discussion of each of these modeling assumptions is presented in the following sections.

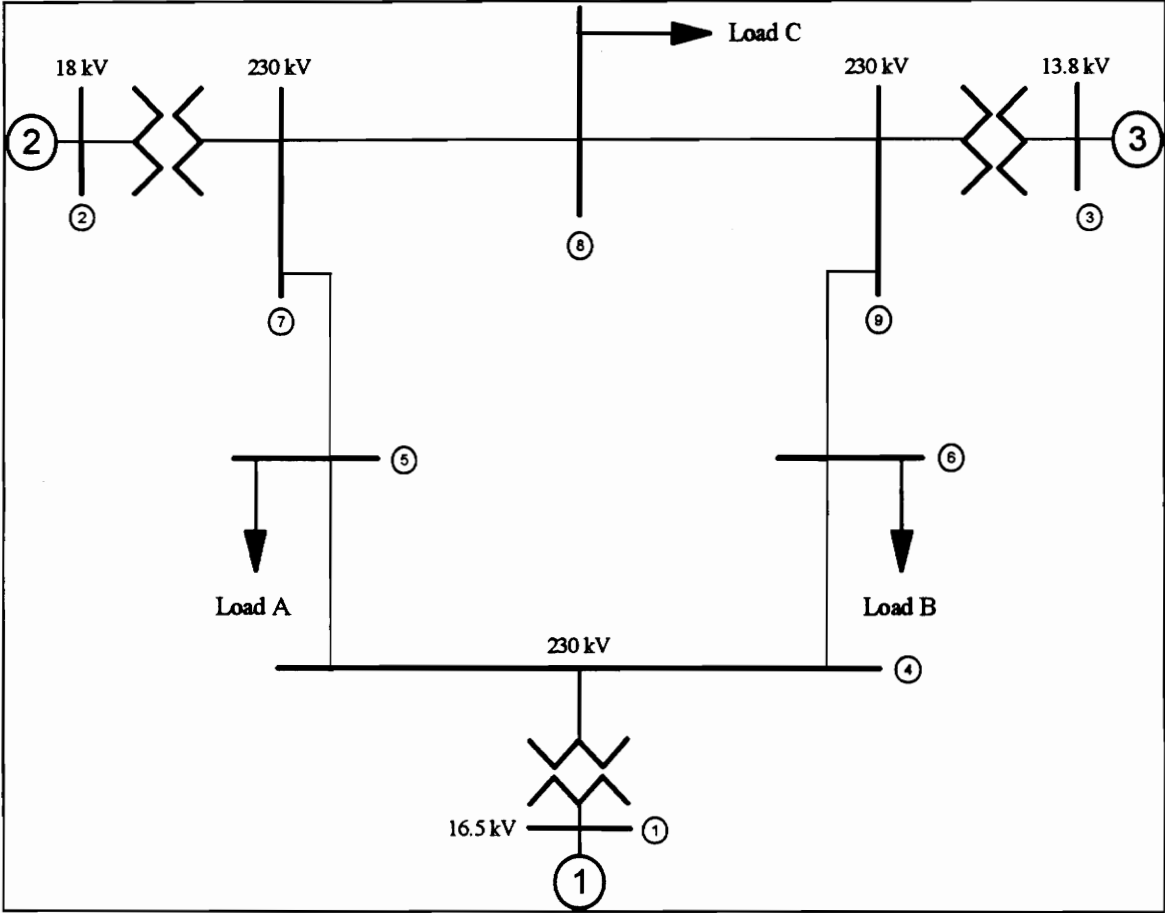


**Figure 4.1: Nine Bus, Three Machine Power System [14]**



**Table 4.1: Per Unit Impedance Data for Nine Bus System**

<b>From Bus</b>	<b>To Bus</b>	<b>R</b>	<b>X</b>	<b>B/2</b>
1	4	0	0.1184	--
2	7	0	0.1823	--
3	9	0	0.2399	--
4	5	0.0100	0.0850	0.0880
4	6	0.0170	0.0920	0.0790
5	7	0.0320	0.1610	0.153
6	9	0.0390	0.1700	0.1790
7	8	0.0085	0.0720	0.0745
8	9	0.0119	0.1008	0.1045

**Table 4.2: Initial Generation, Load, and Voltage Data for Nine Bus System**

<b>Generator or Load</b>	<b>Voltage Magnitude (Per Unit)</b>	<b>Voltage Phase Angle (Degrees)</b>	<b>Real Power (Per Unit)</b>	<b>Reactive Power (Per Unit)</b>
Generator 1	1.040	0.0°	0.716	0.270
Generator 2	1.025	9.3°	1.630	0.067
Generator 3	1.025	4.7°	0.850	-0.109
Load A	0.996	-4.0°	1.250	0.500
Load B	1.013	-3.7°	0.900	0.300
Load C	1.016	0.7°	1.000	0.700

## 4.2 Constant Impedance Load Model

In order to reduce the test power system network to a more manageable level of detail for performing simulations, a constant impedance load model was employed. This

model converts all loads to admittances based on initial load flow data using the following relationships:

$$P_L + jQ_L = \bar{V}_L \bar{I}_L^* = \bar{V}_L [\bar{V}_L^* (G_L - jB_L)] = V_L^2 (G_L - jB_L) \quad (4.1)$$

$$\bar{Y}_L = P_L / V_L^2 - j(Q_L / V_L^2) \quad (4.2)$$

Table 4.3 shows the converted load admittances for the nine bus test system.

**Table 4.3: Converted Load Admittances for Nine Bus System**

Load	Converted Admittance (Per Unit)
A	1.2601 - j0.5040
B	0.8770 - j0.2923
C	0.9688 - j0.6781

Once the equivalent admittances for each load have been calculated, they can be added to the network as shunt admittances. Also, the reactance of each transformer can be added to the transient reactance of its associated generator to form the effective unit reactance. Using these values in conjunction with the line impedance data, the overall bus admittance matrix  $Y$  can be formed. To simplify the system,  $Y$  is partitioned in order to formulate the reduced admittance matrix for the network. All nodes except for the internal generator nodes are eliminated by partitioning the current matrix in terms of those nodes which inject current into the system (generators) and those which do not (all other

nodes). Accordingly, the bus admittance and voltage matrices are partitioned to match the current matrix:

$$\begin{bmatrix} \mathbf{I}_n \\ \dots \\ 0 \end{bmatrix} = \begin{bmatrix} \mathbf{Y}_{nn} & \vdots & \mathbf{Y}_{nr} \\ \dots & \dots & \dots \\ \mathbf{Y}_{rn} & \vdots & \mathbf{Y}_{rr} \end{bmatrix} \begin{bmatrix} \mathbf{V}_n \\ \dots \\ \mathbf{V}_r \end{bmatrix} \quad (4.3)$$

The subscript  $n$  is used to denote generator nodes while  $r$  refers to remote non-generator nodes. Expanding the above equation yields:

$$\begin{aligned} \mathbf{I}_n &= \mathbf{Y}_{nn} \mathbf{V}_n + \mathbf{Y}_{nr} \mathbf{V}_r \\ 0 &= \mathbf{Y}_{rn} \mathbf{V}_n + \mathbf{Y}_{rr} \mathbf{V}_r \end{aligned} \quad (4.4)$$

Finally, the reduced network admittance matrix can be obtained by eliminating  $\mathbf{V}_r$  from the current equations:

$$\mathbf{I}_n = (\mathbf{Y}_{nn} - \mathbf{Y}_{nr} \mathbf{Y}_{rr}^{-1} \mathbf{Y}_{rn}) \mathbf{V}_n = \mathbf{Y}_{red} \mathbf{V}_n \quad (4.5)$$

Thus, a network with  $n$  generators can be reduced to an  $n \times n$  admittance matrix  $\mathbf{Y}_{red}$ . For the nine bus test system,  $\mathbf{Y}_{red}$  was found to be:

$$\mathbf{Y}_{red} = \begin{bmatrix} 0.8341 - j3.0120 & 0.2719 + j1.4788 & 0.1982 + j1.2006 \\ 0.2719 + j1.4788 & 0.3994 - j2.7727 & 0.1979 + j1.0521 \\ 0.1982 + j1.2006 & 0.1979 + j1.0521 & 0.2655 - j2.3944 \end{bmatrix}$$

### 4.3 Two-Axis Generator Model

There are several different models which are used in modeling synchronous machines for stability studies. These include models where the damper windings and/or transient flux linkages are neglected as well as the so-called one and two-axis models. The

two-axis model was chosen for use in simulating this system based on the prevalence of this model in several technical references on stability studies [14, 15, 16].

In a synchronous machine, the modeling of actual winding variables may be greatly simplified by transforming the variables to a new frame of reference which moves with the rotor. This is accomplished through the use of Park's transformation [14]. This transformation projects phase  $a$ ,  $b$ , and  $c$  quantities onto three axes. These axes are along the direct axis of the rotor field winding (*direct* or  $d$ -axis), the neutral axis of the field winding (*quadrature* or  $q$ -axis), and along a stationary axis which produces quantities proportional to their zero-sequence counterparts [14].

In the two-axis model of a synchronous machine, the transient behavior of the generator is included while the subtransient behavior is neglected. Transient behavior resides largely in the field circuit of the  $d$ -axis and an equivalent circuit in the  $q$ -axis formed by the solid rotor. Also, in the stator voltage equations, the leakage flux linkage terms for each axis are assumed to be negligible compared to the speed based voltage terms in the equations. These assumptions lead to the following relationships between the internal generator emf and terminal voltage for each axis:

$$\begin{aligned} V_d &= E'_d - x'_q I_q \\ V_q &= E'_q + x'_d I_d \end{aligned} \quad (4.6)$$

As discussed in [14, 15, 16], the following differential equations apply to each  $i$ th generator modeled using the two-axis model:

$$\tau'_{q0i} \dot{E}'_{di} = -E'_{di} - (x_{qi} - x'_{qi}) I_{qi} \quad (4.7)$$

$$\tau'_{d0i} \dot{E}'_{qi} = E_{fdi} - E'_{qi} + (x_{di} - x'_{di}) I_{di} \quad (4.8)$$

$$\frac{2H_i}{\omega_R} \dot{\omega}_i = P_{mi} - (I_{di} E'_{di} + I_{qi} E'_{qi}) - D_i \omega_i \quad (4.9)$$

$$\dot{\delta}_i = \omega_i \quad (4.10)$$

Although these equations represent four generator state variables per machine, the overall system order will be  $4i-1$  since the rotor angle equation can be written in terms of two angles:

$$\dot{\delta}_{ij} = \omega_i - \omega_j \quad (4.11)$$

Finally, electrical power, which is the middle term in parentheses in equation (4.9), may be calculated in terms of the above variables using the expression:

$$P_{ei} = V_{qi} I_{qi} + V_{di} I_{di} \approx E'_{qi} I_{qi} + E'_{di} I_{di} \quad (4.12)$$

The approximation in the above equation comes from the assumption that  $x'_d \approx x'_q$ . This is a moderately good approximation in terms of accuracy, but it greatly simplifies the equation for angular frequency, especially once it is linearized in section 4.5. Table 4.4 summarizes the two-axis model data for the nine bus system. Table 4.5 provides a summary of the meanings of each term used in these equations.

**Table 4.4: Two-Axis Generator Data for Nine Bus Test System**

Parameter	Generator 1	Generator 2	Generator 3
$x_d$	0.1460	0.8958	1.3125
$x'_d$	0.0608	0.1198	0.1813
$x_q$	0.0969	0.8645	1.2578
$x'_q$	0.0969	0.1969	0.2500
$\tau_{d0}$	8.96	6.00	5.89
$\tau_{q0}$	0.5000	0.5350	0.6000
H	23.64	6.40	3.01

**Table 4.5: Two-Axis Generator Model Nomenclature (Compiled from [14,16])**

Term	Units	Definition
$V_d, V_q$	pu	d- and q-axes components of terminal voltage
$I_d, I_q$	pu	d- and q-axes components of armature current
$E_d, E_q$	pu	magnitudes of d- and q-axes components of voltages behind d- and q-axes transient reactances respectively
$x_d, x_q$	pu	d- and q-axes synchronous reactances
$x_d', x_q'$	pu	d- and q-axes transient reactances
$\tau_{d0}, \tau_{q0}$	sec	d- and q-axes transient open circuit time constants
$\delta$	rad	generator rotor angle
$\omega$	rad/sec	generator rotor angle velocity
$D$	pu	Damping Coefficient
$\omega_R$	rad/sec	rated generator speed
$P_m$	pu	mechanical input power to generator
$E_{fd}$	pu	applied field voltage
$H$	pu•sec	stored energy at rated speed (inertia constant)

#### 4.4 Excitation System Model

For the test system under study, IEEE Type 1 excitation systems were assumed for each generator [17]. Figure 4.2 below shows a block diagram for this type of excitation control system. Based on this block diagram, the following equations describe the excitation system for each  $i$ th generator [15]:

$$\dot{V}_{Ri} = (K_{Ai} V_{ei} - V_{Ri}) / T_{Ai} \quad (4.13)$$

$$\dot{E}_{fdi} = (V_{Ri} - S_{Ei} - K_{Ei} E_{fdi}) / T_{Ei} \quad (4.14)$$

$$\dot{V}_{SLi} = (K_{Si} / T_{Si}) E_{fdi} - V_{SLi} \quad (4.15)$$

$$V_{ei} = V_{refi} - V_i - V_{Si} \quad (4.16)$$

$$V_{Si} = (K_{Si} / T_{Si}) E_{fdi} - V_{SLi} \quad (4.17)$$

$$V_{RLi} = \begin{cases} V_{Ri} & \text{if } V_{Rmini} \leq V_{Ri} \leq V_{Rmaxi} \\ V_{Rmini} & \text{if } V_{Ri} < V_{Rmini} \\ V_{Rmaxi} & \text{if } V_{Ri} > V_{Rmaxi} \end{cases} \quad (4.18)$$

$$S_{Ei} = f(E_{fdi}) = A_i e^{B_i E_{fdi}} \quad (4.19)$$

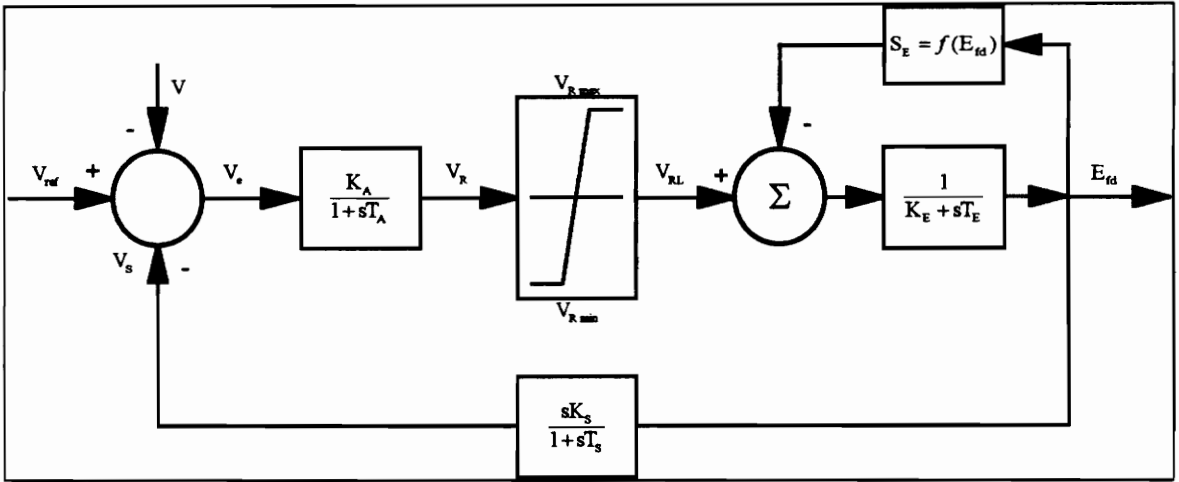


**Figure 4.2: IEEE Type I Excitation System [16]**

Since  $S_{Ei}$  is a non-linear function, it must be linearized in order to solve the above differential equations using conventional numerical methods. For this simulation, conditions were assumed to be below saturation so that  $S_{Ei}$  was equal to one.

The terminal voltage  $V_i$  in the equations above is a function of the  $d$  and  $q$  axis voltages:

$$V_i^2 = V_{di}^2 + V_{qi}^2 \quad (4.20)$$

Linearizing  $V_i$  and defining the two-axis voltages in terms of the generator state variables  $E_q'$  and  $E_d'$ :

$$V_i = \left( \frac{V_{di0}}{V_{i0}} \right) (E_{di}' - x_{qi}' I_{qi}) + \left( \frac{V_{qi0}}{V_{i0}} \right) (E_{qi}' + x_{di}' I_{di}) \quad (4.21)$$

This equation is crucial in providing coupling between the generator and excitation system equations in the state matrix. Table 4.6 contains excitation system data for the nine bus test system.

**Table 4.6: Summary of Excitation System Data for Nine Bus System**

Parameter	Generator 1	Generator 2	Generator 3
$K_A$	25	15	20
$K_E$	-1.155	-0.1071	-0.1071
$K_S$	0.405	0.091	0.108
$T_A$	5.6	2.0	1.2
$T_E$	0.5140	0.8700	1.5140
$T_S$	0.85	0.85	0.85

#### 4.5 Linearized State Equations

In order to formulate a linear state matrix model of the nine bus power system, all non-linearities must be removed from the equations in sections 4.3 and 4.4. This may be accomplished by replacing each variable by its initial value plus an incremental change:

$$x_i = x_{i0} + x_{i\Delta} \quad (4.22)$$

The generator and excitation system equations discussed above exhibit nonlinearity from products of variables and from trigonometric functions. For products, reduction is made



by assuming higher order terms (e.g.  $x_{i\Delta}x_{j\Delta}$ ) are sufficiently small to be neglected. In addition, initial condition products (e.g.  $x_{i0}x_{j0}$ ) cancel from the right and left hand sides of the linearized product equation. For trigonometric functions of incremental angles (expressed in radians), the following approximations can be made:

$$\begin{aligned}\cos\delta_{\Delta} &\cong 1 \\ \sin\delta_{\Delta} &\cong \delta_{\Delta}\end{aligned}\quad (4.23)$$

Following these approximations, the linearized state equations for each generator may now be written:

$$\tau'_{q0i}\dot{E}'_{di\Delta} = -E'_{di\Delta} - (x_{qi} - x'_{qi})I_{qi\Delta} \quad (4.24)$$

$$\tau'_{d0i}\dot{E}'_{qi\Delta} = E_{fdi\Delta} - E'_{qi\Delta} + (x_{di} - x'_{di})I_{di\Delta} \quad (4.25)$$

$$\frac{2H_i}{\omega_R}\dot{\omega}_{i\Delta} = P_{mi\Delta} - I_{di0}E'_{di\Delta} - I_{qi0}E'_{qi\Delta} - E'_{di0}I_{di\Delta} - E'_{qi0}I_{qi\Delta} - D_i\omega_{i\Delta} \quad (4.26)$$

$$\dot{\delta}_{ij\Delta} = \omega_{i\Delta} - \omega_{j\Delta} \quad (4.27)$$

$$\dot{E}_{fdi\Delta} = (V_{Ri\Delta} - (1 + K_{Ei})E_{fdi\Delta}) / T_{Ei} \quad (4.28)$$

$$\dot{V}_{SLi\Delta} = (K_{Si} / T_{Si})E_{fdi\Delta} - V_{SLi\Delta} \quad (4.29)$$

$$\dot{V}_{Ri\Delta} = (K_{Ai}(V_{refi} - V_{i\Delta} - (K_{Si} / T_{Si})E_{fdi\Delta} + V_{SLi\Delta}) - V_{Ri\Delta}) / T_{Ai} \quad (4.30)$$

where

$$V_{i\Delta} = \left( \frac{V_{di0}}{V_{i0}} \right) (E'_{di\Delta} - x'_{qi}I_{qi\Delta}) + \left( \frac{V_{qi0}}{V_{i0}} \right) (E'_{qi\Delta} + x'_{di}I_{di\Delta}) \quad (4.31)$$

In addition, the linearized expression for electrical power is:

$$P_{ei\Delta} = I_{di0}E'_{di\Delta} + I_{qi0}E'_{qi\Delta} + E'_{di0}I_{di\Delta} + E'_{qi0}I_{qi\Delta} \quad (4.32)$$

The calculated initial conditions required in these equations and those which are developed in the next section are provided in Table 4.7. For equations using initial rotor angle differences, these values may be obtained by subtracting the individual initial rotor angles shown below.

**Table 4.7: Generator Initial Conditions**

	<b>Generator 1</b>	<b>Generator 2</b>	<b>Generator 3</b>
$I_{q0}$	0.6709	0.9319	0.6196
$I_{d0}$	-0.3021	-1.2903	-0.5614
$E_{d0}$	0.0000	-0.6221	-0.6244
$E_{q0}$	1.0563	0.7883	0.7676
$V_{d0}$	-0.0650	-0.8056	-0.7793
$V_{q0}$	1.0380	0.6338	0.6659
$\delta_0$	3.5838	61.1084	54.1876

#### 4.6 Current Coefficient Matrix

As discussed previously, a great deal of simplification in a synchronous machine model can be achieved by transforming variables to a common reference frame. Further simplifications can be made by ensuring that all variables are measured based on a common system-wide reference. For example, in order to apply the admittance form of Ohm's law, currents and voltages for the entire network must be based on the same

reference. If currents and voltages are all based on a common system reference frame and are denoted by  $\hat{\mathbf{I}}$  and  $\hat{\mathbf{V}}$ , respectively, then:

$$\hat{\mathbf{I}} = \mathbf{Y}\hat{\mathbf{V}} \quad (4.33)$$

Now the two-axis current coefficient matrix can be derived as discussed in [14].

It now becomes necessary to determine if the expressions for two-axis currents and voltages developed in the previous sections are all based on a common reference frame. Figure 4.3 shows a phasor diagram which relates the  $d$  and  $q$  axis components of a voltage phasor to a system reference denoted by  $D_{REF}$  and  $Q_{REF}$ . As shown, there is a phase shift of  $\delta_i$  between these two reference frames. Since rotor angles are different for each generator, the two axis voltages and currents previously derived are all in the same coordinate system, but with a phase shift between them. The new overall system reference frame eliminates this offset between generators, and thus provides a consistent system reference frame.

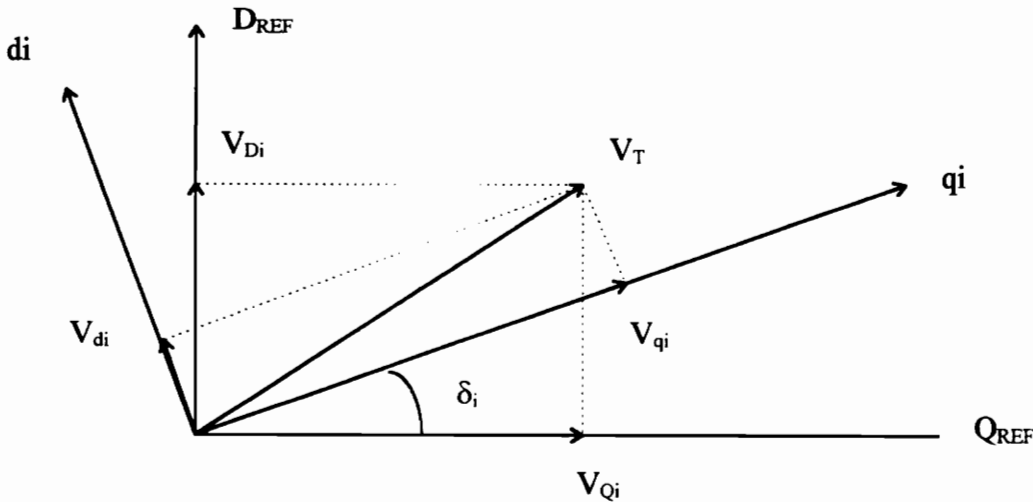


**Figure 4.3: Phasor Diagram of Machine and System Reference Frames [14]**

In order to utilize equation (4.33), it is therefore necessary to transform all  $d$  and  $q$  axis quantities ( $\bar{V}_i = V_{qi} + jV_{di}$ ) to the common rotating reference frame ( $\hat{V}_i = V_{Qi} + jV_{Di}$ ).

This transformation can be accomplished by the following relationship:

$$\hat{V}_i = \bar{V}_i e^{j\delta_i} \quad (4.34)$$

For a matrix of voltages, the transformation may be defined in terms of a matrix  $\mathbf{T}$ :

$$\mathbf{T} = \begin{bmatrix} e^{j\delta_1} & 0 & \dots & 0 \\ 0 & e^{j\delta_2} & \dots & 0 \\ \vdots & \vdots & \ddots & \vdots \\ 0 & 0 & \dots & e^{j\delta_n} \end{bmatrix} \quad (4.35)$$

Using this transformation matrix, the relationship between two-axis voltage and current matrices and their system reference frame counterparts can be derived:

$$\begin{aligned} \hat{\mathbf{I}} &= \mathbf{T} \bar{\mathbf{I}} \\ \hat{\mathbf{V}} &= \mathbf{T} \bar{\mathbf{V}} \end{aligned} \quad (4.36)$$

Now, substituting the results of (4.36) in (4.33) and performing matrix pre-multiplication to solve for the current matrix:

$$\mathbf{T} \bar{\mathbf{I}} = \mathbf{Y} \mathbf{T} \bar{\mathbf{V}} \quad (4.37)$$

$$\bar{\mathbf{I}} = (\mathbf{T}^{-1} \mathbf{Y} \mathbf{T}) \bar{\mathbf{V}} = \bar{\mathbf{M}} \bar{\mathbf{V}} \quad (4.38)$$

If  $\Theta_{ij}$  is defined as the phase angle of each reduced network admittance matrix element, then for the nine bus power system under study:

$$\overline{\mathbf{M}} = \begin{bmatrix} Y_{11}e^{j\Theta_{11}} & Y_{12}e^{j(\Theta_{12}-\delta_{12})} & Y_{13}e^{j(\Theta_{13}-\delta_{13})} \\ Y_{21}e^{j(\Theta_{21}-\delta_{21})} & Y_{22}e^{j\Theta_{22}} & Y_{23}e^{j(\Theta_{23}-\delta_{23})} \\ Y_{31}e^{j(\Theta_{31}-\delta_{31})} & Y_{32}e^{j(\Theta_{32}-\delta_{32})} & Y_{33}e^{j\Theta_{33}} \end{bmatrix} \quad (4.39)$$

Thus, an expression for two-axis currents in terms of two-axis voltages is now available for application to the test system. Since the reduced nine bus power system is assumed to include generator transient reactances, the voltages at each of the three remaining buses (generator nodes) are  $\overline{E}_1'$ ,  $\overline{E}_2'$ , and  $\overline{E}_3'$ . Therefore, in order to solve the differential equations in section 4.3,  $\overline{E}'$  can be substituted for  $\overline{V}$  in equation (4.38). However, in order to model the small signal perturbations associated with dynamic stability studies, equation (4.38) now must be linearized in order to formulate a state matrix for linearized state variables:

$$\begin{aligned} \overline{\mathbf{I}}_0 + \overline{\mathbf{I}}_\Delta &= (\overline{\mathbf{M}}_0 + \overline{\mathbf{M}}_\Delta)(\overline{\mathbf{E}}'_0 + \overline{\mathbf{E}}'_\Delta) \\ \overline{\mathbf{I}}_\Delta &= \overline{\mathbf{M}}_0\overline{\mathbf{E}}'_\Delta + \overline{\mathbf{M}}_\Delta\overline{\mathbf{E}}'_0 \end{aligned} \quad (4.40)$$

The  $\overline{\mathbf{M}}_0$  matrix is the nominal transformation matrix evaluated with each generator rotor angle equal to its initial value,  $\delta_{i0}$ . Similarly, the initial voltage behind transient reactance matrix,  $\overline{\mathbf{E}}'_0$ , is evaluated at its initial conditions. The incremental voltage matrix,  $\overline{\mathbf{E}}'_\Delta$ , contains the incremental state variables. The incremental transformation matrix  $\overline{\mathbf{M}}_\Delta$ , however, involves several of the linearization approximations discussed above. First, all rotor angles are linearized:

$$\delta_i = \delta_{i0} + \delta_{i\Delta} \quad (4.41)$$

Since the diagonal terms of  $\overline{\mathbf{M}}$  contain no terms related to the rotor angle, these diagonal elements are not affected by the linearization of  $\delta$  and appear only in the  $\overline{\mathbf{M}}_0$  matrix. Thus,  $\overline{\mathbf{M}}_\Delta$  contains only off-diagonal elements.

The general form of the off-diagonal elements in the transformation matrix  $\overline{\mathbf{M}}$  is:

$$\overline{m}_{ij} = Y_{ij} e^{j(\Theta_{ij} - \delta_{ij0})} e^{-j\delta_{ij\Delta}} \quad (4.42)$$

Using Euler's equation and the trigonometric linearizations discussed above, the incremental portion of this expression can be approximated as:

$$e^{-j\delta_{ij\Delta}} = \cos(\delta_{ij\Delta}) - j\sin(\delta_{ij\Delta}) \cong (1 - j\delta_{ij\Delta}) \quad (4.43)$$

and the general linearized form for the entries of this matrix becomes:

$$\overline{m}_{ij\Delta} \cong -jY_{ij} e^{j(\Theta_{ij} - \delta_{ij0})} \delta_{ij\Delta} \quad (4.44)$$

Using this fact and substituting into equation (4.38), the linearized current coefficient matrix can now be written (see Figure 4.4) which relates the  $d$  and  $q$  axis coefficients for each generator in terms of the linearized state variables discussed in section 4.5. Eliminating the redundant rotor angle difference variable using  $\delta_{23\Delta} = \delta_{13\Delta} - \delta_{12\Delta}$  and using the fact that  $\delta_{21} = -\delta_{12}$  and  $\delta_{31} = -\delta_{13}$ , the final form for the reduced two-axis current coefficient matrix can be determined. This matrix and the relationship between two-axis currents and state variables are shown in Figure 4.5. The real and imaginary parts of all the variables are then separated to avoid complications from dealing with complex variables. After separation of real and complex variables is complete, the current coefficient matrix can be used in conjunction with the linearized state variables discussed

in section 4.5 to form the state matrix  $\mathbf{A}$ . The numeric coefficients of both the reduced linearized current coefficient and state matrices are provided for reference in Appendix A.

$$\begin{bmatrix} \bar{I}_{1\Delta} \\ \bar{I}_{2\Delta} \\ \bar{I}_{3\Delta} \end{bmatrix} = \begin{bmatrix} Y_{11}e^{j\Theta_{11}} & Y_{12}e^{j(\Theta_{12}-\delta_{120})} & Y_{13}e^{j(\Theta_{13}-\delta_{130})} & -j\bar{E}'_{20}Y_{12}e^{j(\Theta_{12}-\delta_{120})} & -j\bar{E}'_{30}Y_{13}e^{j(\Theta_{13}-\delta_{130})} & 0 \\ Y_{21}e^{j(\Theta_{21}-\delta_{210})} & Y_{22}e^{j\Theta_{22}} & Y_{23}e^{j(\Theta_{23}-\delta_{230})} & -j\bar{E}'_{10}Y_{21}e^{j(\Theta_{21}-\delta_{210})} & 0 & -j\bar{E}'_{30}Y_{23}e^{j(\Theta_{23}-\delta_{230})} \\ Y_{31}e^{j(\Theta_{31}-\delta_{310})} & Y_{32}e^{j(\Theta_{32}-\delta_{320})} & Y_{33}e^{j\Theta_{33}} & 0 & -j\bar{E}'_{10}Y_{31}e^{j(\Theta_{31}-\delta_{310})} & -j\bar{E}'_{20}Y_{32}e^{j(\Theta_{32}-\delta_{320})} \end{bmatrix} \begin{bmatrix} \bar{E}'_{1\Delta} \\ \bar{E}'_{2\Delta} \\ \bar{E}'_{3\Delta} \\ \delta_{12\Delta} \\ \delta_{13\Delta} \\ \delta_{23\Delta} \end{bmatrix}$$

**Figure 4.4: Linearized Current Coefficient Matrix**

$$\begin{bmatrix} \bar{I}_{1\Delta} \\ \bar{I}_{2\Delta} \\ \bar{I}_{3\Delta} \end{bmatrix} = \begin{bmatrix} Y_{11}e^{j\Theta_{11}} & Y_{12}e^{j(\Theta_{12}-\delta_{120})} & Y_{13}e^{j(\Theta_{13}-\delta_{130})} & -j\bar{E}'_{30}Y_{13}e^{j(\Theta_{13}-\delta_{130})} \\ Y_{21}e^{j(\Theta_{21}+\delta_{120})} & Y_{22}e^{j\Theta_{22}} & Y_{23}e^{j(\Theta_{23}-\delta_{230})} & -j\bar{E}'_{30}Y_{23}e^{j(\Theta_{23}-\delta_{230})} \\ Y_{31}e^{j(\Theta_{31}+\delta_{130})} & Y_{32}e^{j(\Theta_{32}+\delta_{230})} & Y_{33}e^{j\Theta_{33}} & -j\bar{E}'_{10}Y_{31}e^{j(\Theta_{31}+\delta_{130})} \\ & & & +j\bar{E}'_{20}Y_{32}e^{j(\Theta_{32}+\delta_{230})} \end{bmatrix} \begin{bmatrix} \bar{E}'_{1\Delta} \\ \bar{E}'_{2\Delta} \\ \bar{E}'_{3\Delta} \\ \delta_{12\Delta} \\ \delta_{13\Delta} \end{bmatrix}$$

**Figure 4.5: Reduced Linearized Current Coefficient Matrix**



## **CHAPTER 5**

### **Response of the Uncompensated System**

#### **5.1 Assumed Conditions**

In evaluating the response of the nine bus test system, the following assumptions were made about system conditions prior to, during, and after the disturbance was simulated. Prior to the disturbance, the system was assumed to have gradually migrated to an unstable state due to a slow increase of reactive power at one of the loads. For this study, the initial excitation system parameters were chosen so as to make the most critical eigenvalues have negative real parts that were close to zero. Thus, the gradual change in reactive power is enough to move these marginal eigenvalues into the right-half plane. This condition will be assumed to remain throughout the study period. Then a disturbance is applied to the system in the form of a step function increase in mechanical power in one of the generators. Eigenvalue analysis will show that the system will have an unstable response to this disturbance. This will be verified with a numerical simulation of the response of electrical power and the difference in rotor angles between generating units.

## 5.2 Evaluation Techniques

For this thesis, eigenvalue analysis was used for several purposes, including the determination of the optimal location for the FACTS device in the test system which will be discussed in Chapter 6. This frequent usage of eigenvalue analysis and matrix operations required the use of a specialized software package. As a result, the computer program MATLAB<sup>®</sup> (a registered trademark of The MathWorks, Inc.) was used for all matrix calculations [18]. MATLAB<sup>®</sup> script files were written to input power system data, perform network reduction, and calculate the coefficients of the system state matrix  $A$ . Once this matrix was formulated, eigenvalues were calculated by MATLAB<sup>®</sup>. Similar scripts files were used for the determination of FACTS placement and numerical derivative calculations (see Chapter 6).

For time simulation of results, a combination of MATLAB<sup>®</sup> script files and a C program were used. The same script files as listed above were used to determine the state matrix. These coefficients were written to a text file which was then read by a C program which was used to solve the set of differential equations represented by the system state variables and state matrix. This was done chiefly for speed of solution and for providing flexibility in choosing time steps and data compression parameters. Although MATLAB<sup>®</sup> does have the capability to solve differential equations using Runge-Kutta methods, the size of even the nine bus test system made the calculation of the system response very time consuming. The C program, utilizing Euler's method for ease of programming, yielded virtually identical time response results in approximately one tenth of the time of

MATLAB®. Since the response curves have a relatively low frequency, good results can be obtained using Euler's method with a moderate to small step size. The solutions to the differential equations were then written to a text file in MATLAB® format so the results could be read by MATLAB® for final calculation of incremental power and data plotting. Figure 5.1 shows a flowchart of both the eigenvalue and numerical simulation processes. Source code listings for the referenced C program and MATLAB® script files are provided in Appendix B.

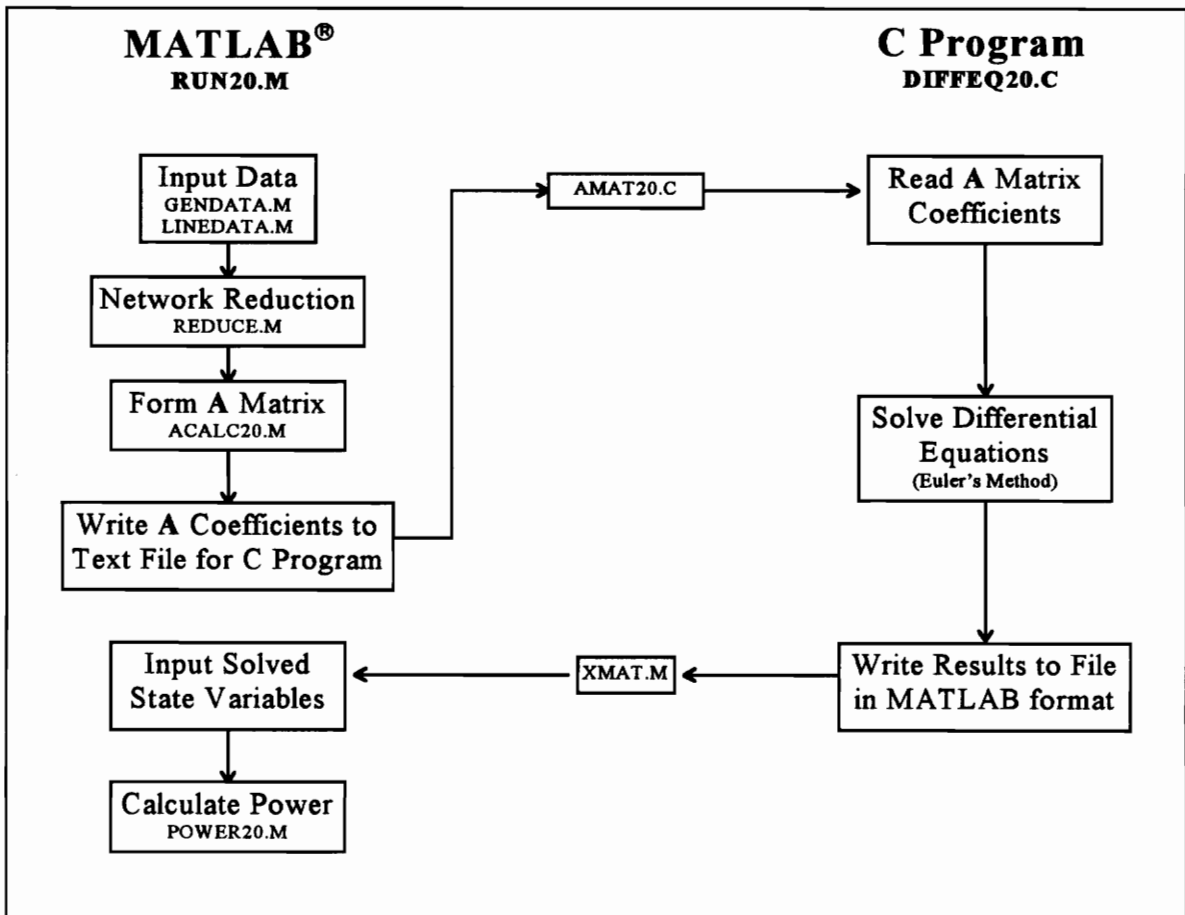


**Figure 5.1: Flowchart for Uncompensated Test System Simulations**

### 5.3 Results

The uncompensated nine bus power system exhibited an unstable system response to the simulated disturbance. Figure 5.2 shows the overall system eigenvalues while Figure 5.3 provides a close-up of the two eigenvalues which became unstable from the reactive load change. Table 5.1 provides a summary of the system eigenvalues for the uncompensated system with the unstable eigenvalues highlighted in bold. For numerical simulations, the system was initially at steady-state before the disturbance occurred at 10 seconds. Electrical power, which is plotted for each generator in Figures 5.4 through 5.6, shows slowly growing oscillations. This is also observed in Figures 5.7 and 5.8 which show rotor angle difference between generators.

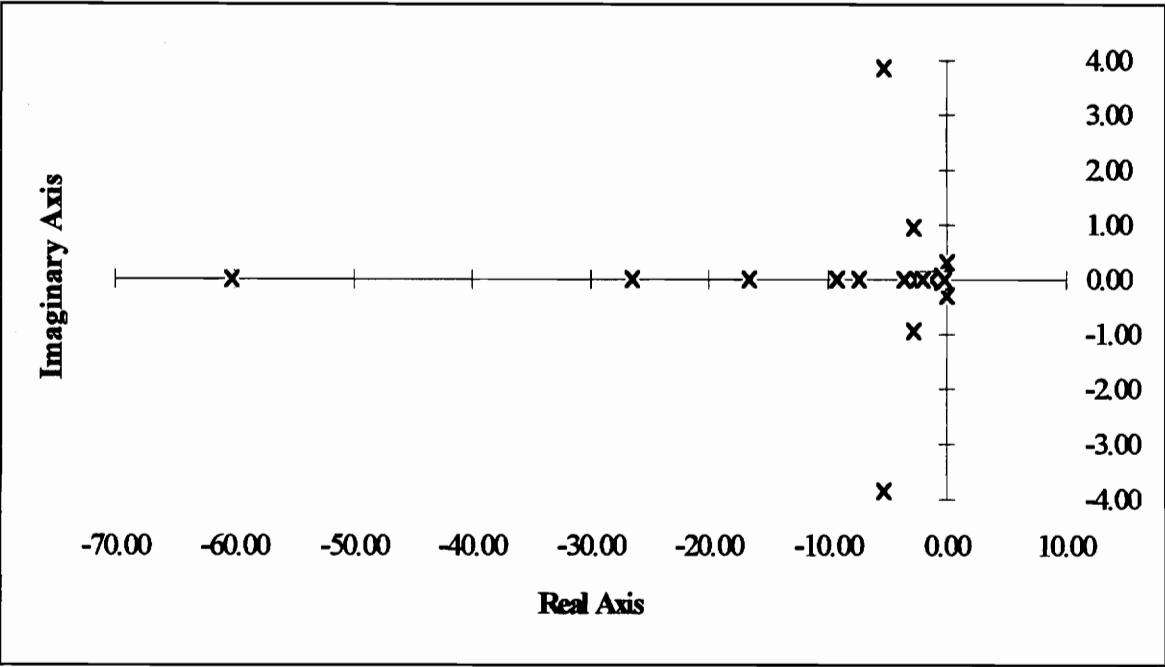
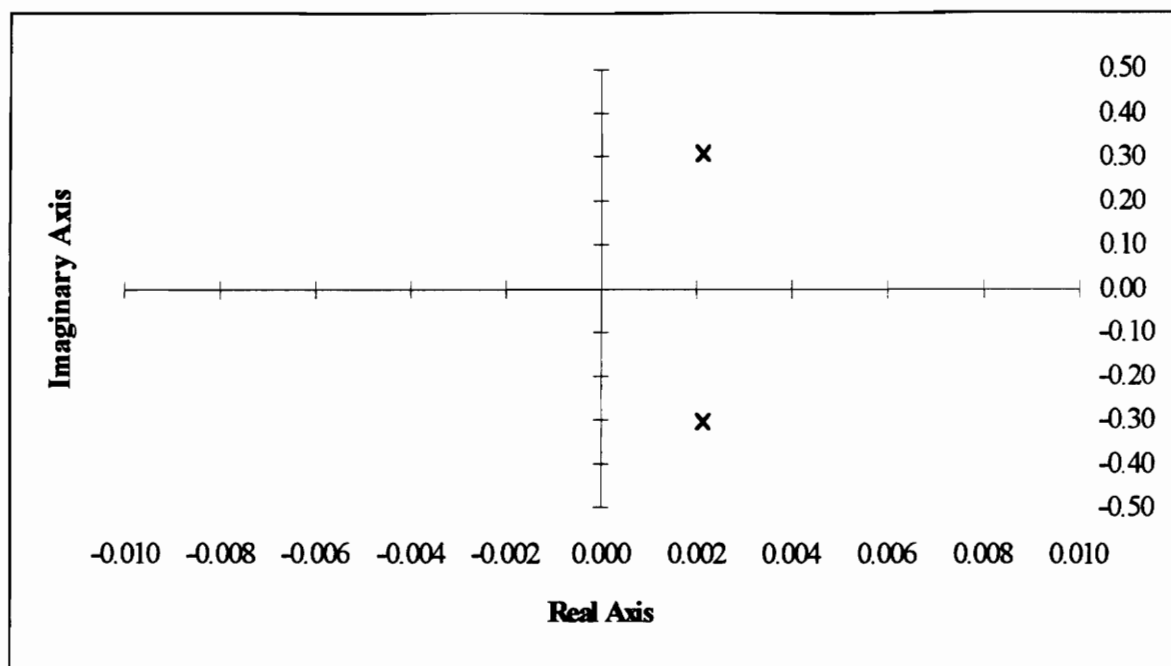


Figure 5.2: System Eigenvalues (Uncompensated System)



**Figure 5.3: Close-up of Dominant Eigenvalues (Uncompensated System)**

**Table 5.1: System Eigenvalues for Uncompensated Test System**

System Eigenvalues	
-60.2202	-2.5341
-26.5061	<b>0.0021 + 0.3043i</b>
-16.5755	<b>0.0021 - 0.3043i</b>
-9.2083	-1.5769
-5.2454 + 3.8478i	-0.6959
-5.2454 - 3.8478i	-0.3805 + 0.0494i
-7.3475	-0.3805 - 0.0494i
-3.5514	-1.3394
-2.7664 + 0.9461i	-0.1747
-2.7664 - 0.9461i	-2.0000

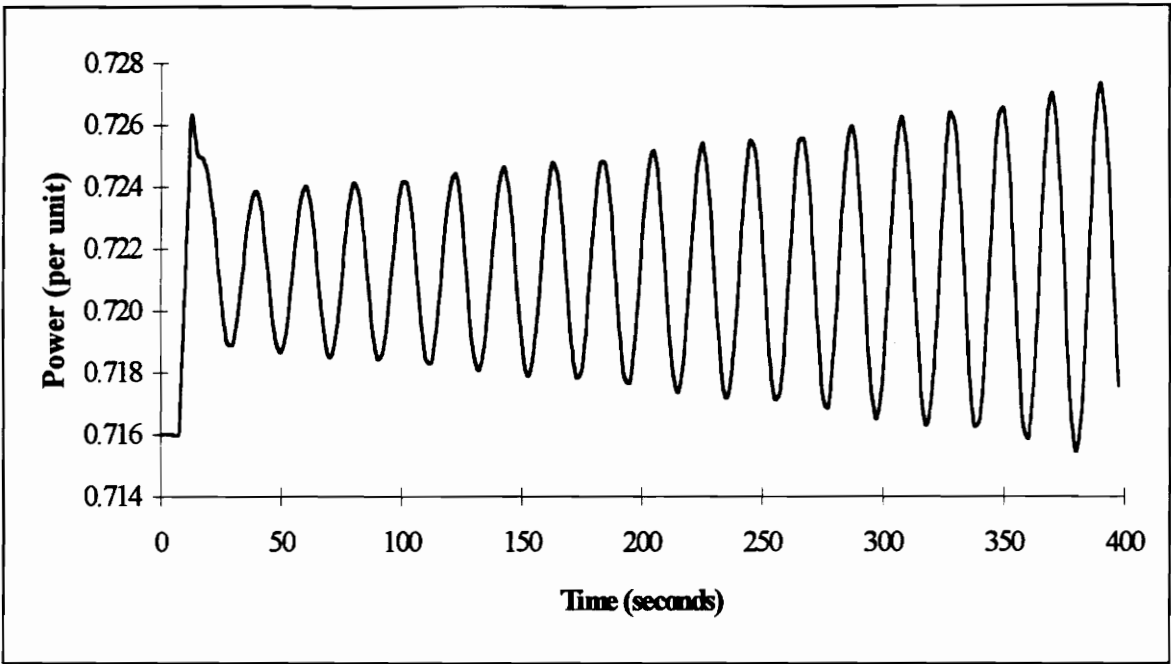


**Figure 5.4: Electrical Power of Generator 1 (Uncompensated System)**

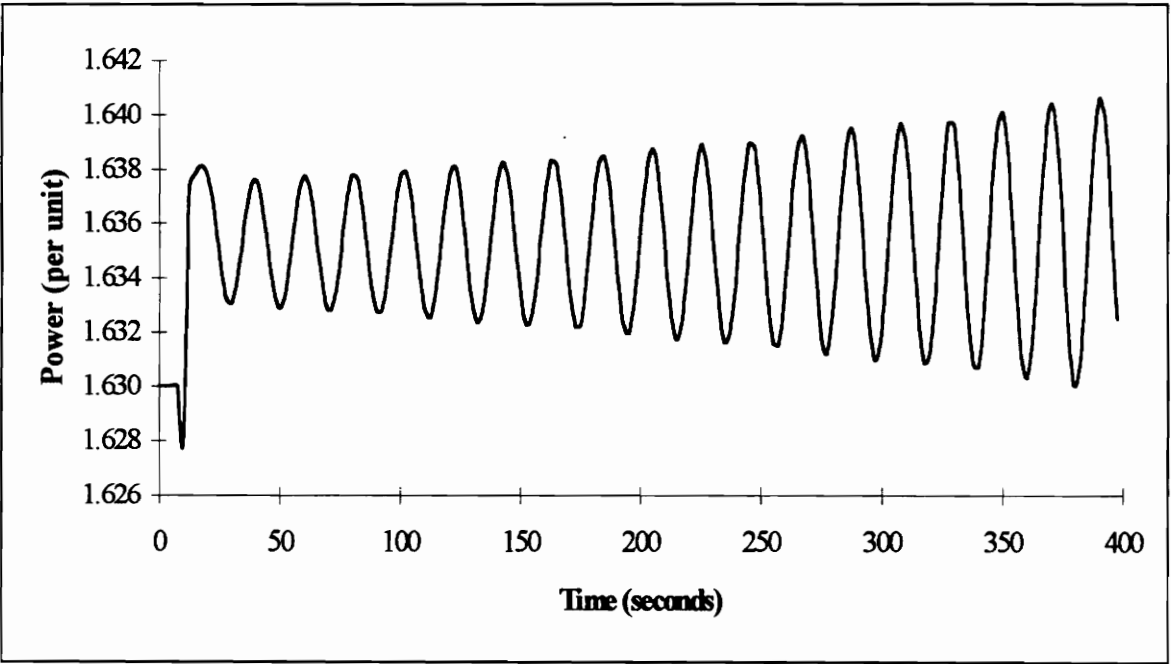


**Figure 5.5: Electrical Power of Generator 2 (Uncompensated System)**

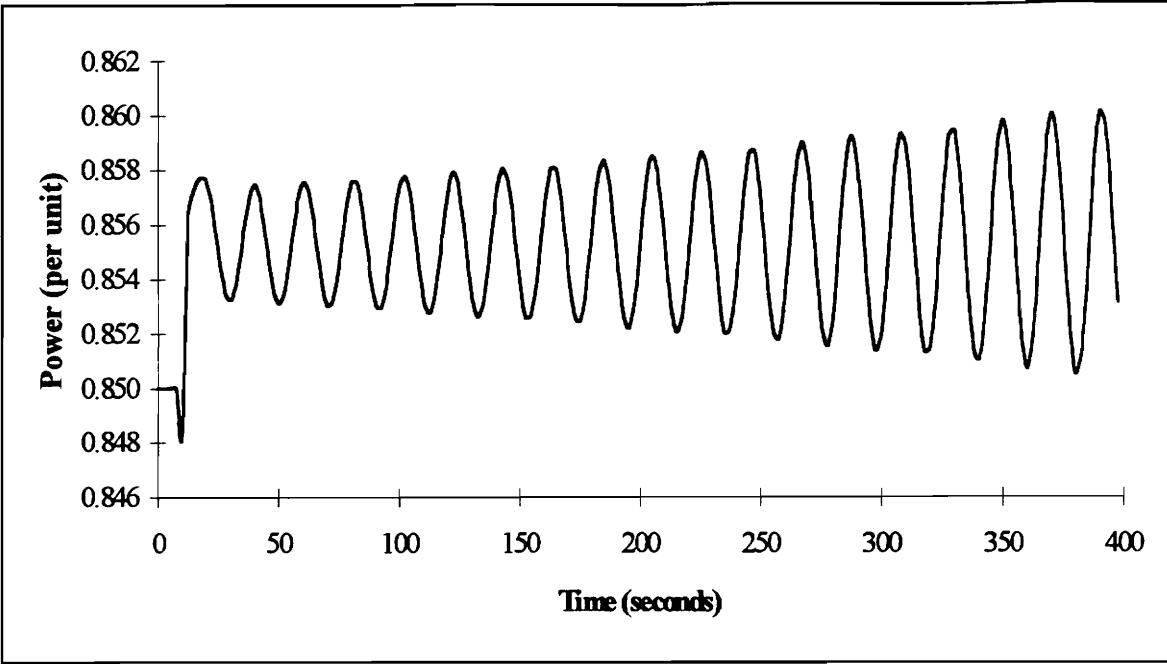


**Figure 5.6: Electrical Power of Generator 3 (Uncompensated System)**

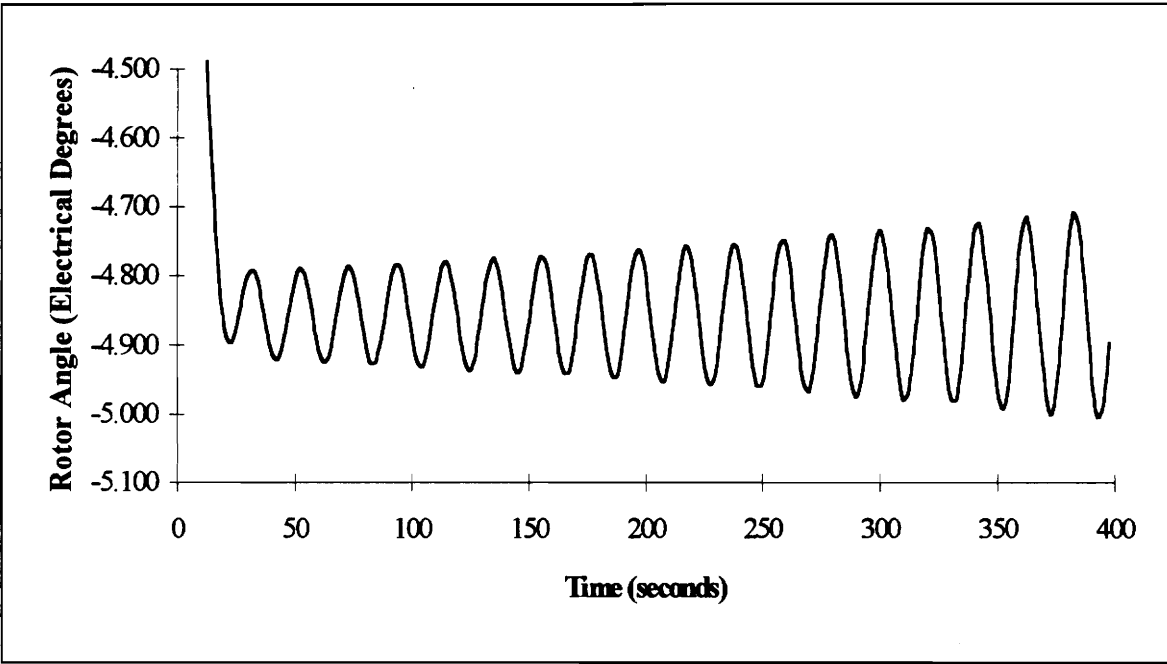


**Figure 5.7: Rotor Angle Difference,  $\delta_{12}$  (Uncompensated System)**

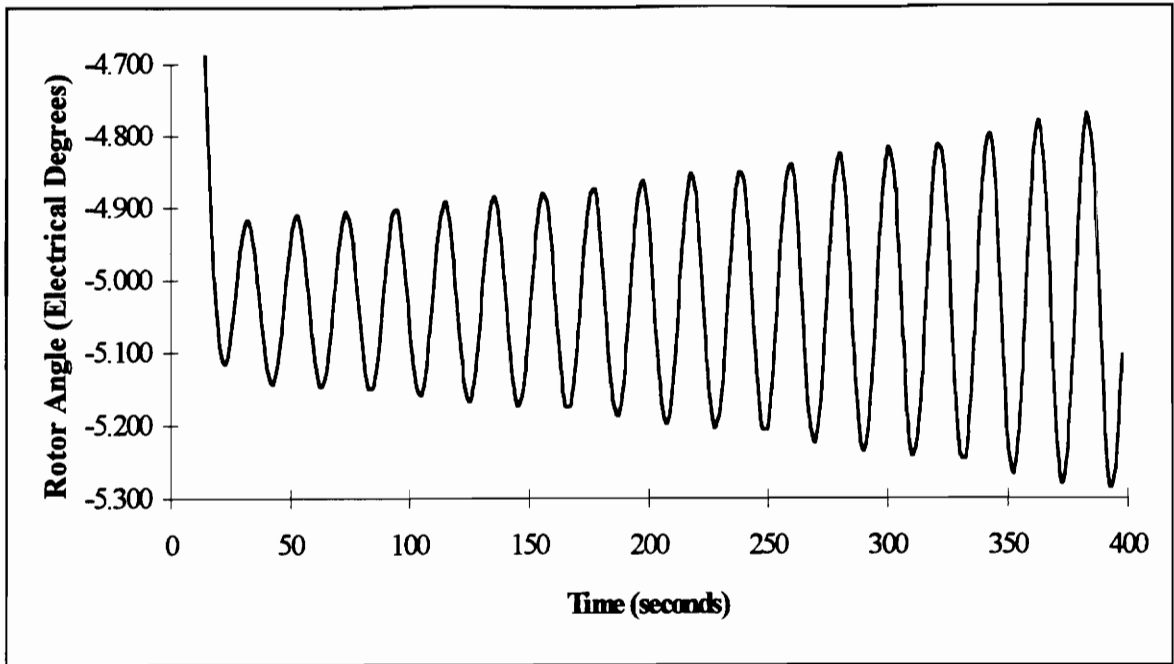


**Figure 5.8: Rotor Angle Difference,  $\delta_{13}$  (Uncompensated System)**

Results from the numerical simulations verified the instability of the system to a disturbance as predicted by eigenvalue analysis. In addition, the period of the oscillations on the time simulation plots appears to be roughly 20-25 seconds. This compares well with the 20.65 second period calculated from the imaginary part of the critical eigenvalues.



## **CHAPTER 6**

### **Addition of a FACTS Device to Power System Model**

#### **6.1 Optimal Placement of FACTS Device**

In order to improve the dynamic stability of the nine bus test system described in Chapter 4, a TCSC is to be inserted into the power network. Since FACTS devices and controllers are very expensive, it is important to limit the number of devices and to choose their placement for optimal stability improvement. For the purposes of this thesis, only one FACTS device will be used due to the cost factor listed above and the relatively small size of the nine bus test system. In order to evaluate the best placement of the TCSC, the response of the  $A$  matrix eigenvalues to changes in the reactance of each line will be examined.

In the nine bus test system, there are six transmission lines in which the FACTS device may be inserted. To evaluate the effectiveness of FACTS insertion on each line, an array was formed containing the real portion of the dominant eigenvalue of the  $A$  matrix versus incremental changes in reactance for each transmission line. Since the real portion

of all eigenvalues must be negative in order for a system to have a stable response to a disturbance, tracking the most marginal eigenvalue provides an indication of whether a system is becoming more stable or more unstable. From this data array of critical real eigenvalues versus incremental changes in line reactance, a numerical derivative of the critical real eigenvalue ( $\lambda_c$ ) with respect to reactance ( $X_{ij}$ , the reactance in the line between buses  $i$  and  $j$ ) was calculated for each of the six lines. These derivative values were then averaged over the range between the normal line reactance and half of the initial line reactance for each line. This 50% compensation is assumed as a TCSC compensation limit throughout this thesis. The resulting derivatives for each line are shown in Table 6.1.

**Table 6.1: Average Critical Eigenvalue Sensitivity to Changes in Line Reactance**

Average Numerical Derivative	Value
$\frac{\partial \lambda_c}{\partial X_{45}}$	-0.0268
$\frac{\partial \lambda_c}{\partial X_{57}}$	-0.0169
$\frac{\partial \lambda_c}{\partial X_{78}}$	-0.0002
$\frac{\partial \lambda_c}{\partial X_{89}}$	-0.0010
$\frac{\partial \lambda_c}{\partial X_{69}}$	-0.0160
$\frac{\partial \lambda_c}{\partial X_{46}}$	-0.0170

The numbers in Table 6.1 may be interpreted as a measure of the sensitivity of the network to changes in line reactance, such as those caused by insertion of a TCSC. More specifically, these numerical derivatives provide an evaluation of how much stability increase can be obtained by insertion of capacitive series compensation in each transmission line. Since all of the line positions provide increased stability (negative eigenvalue derivatives) for insertion of a TCSC, it is logical to use the magnitude of these numerical derivatives in order to judge which line will provide the most dramatic increase in stability. Thus, based on the above numeric data, a TCSC inserted in the line between buses 4 and 5 will provide the most increased stability. Figure 6.1 shows the nine bus test system with the addition of the FACTS device.

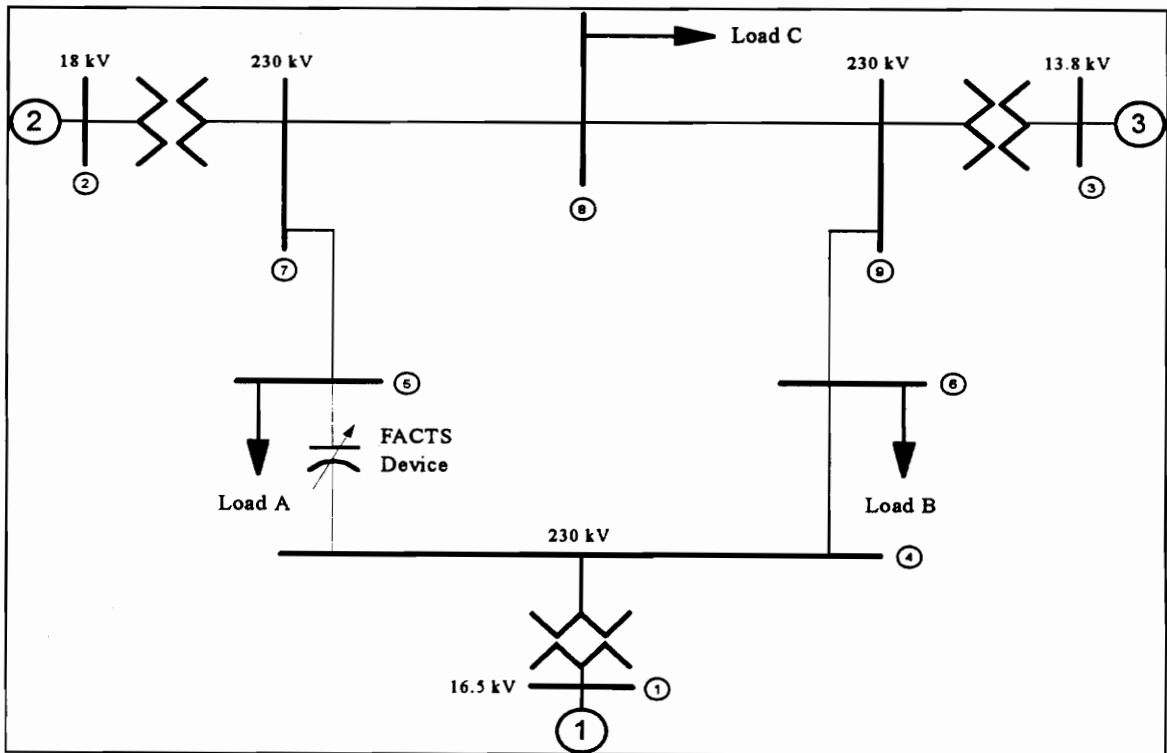


**Figure 6.1: Nine Bus Test System with Addition of FACTS Device**

## 6.2 FACTS Control Strategy

In order to minimize the amount of compensation needed and automate FACTS response to small signal disturbances, a control scheme was developed. One good measure of power system dynamic stability is the generator rotor angle,  $\delta$ . Any small signal disturbance on a power system will cause some variation in rotor angle. In order to consider rotor angle as a possible control input signal for the TCSC, accurate synchronized measurements of the voltage phasors of generators at remote sites must be available for transmission to the controller at the FACTS installation. Recent advancements in monitoring technologies now allow reliable phase angle measurements through the use of phasor measurement units (PMUs) [19, 20]. Thus, with reliable phase angle information available, it becomes possible to use rotor angle in the control of the FACTS device.

For this thesis, only conventional PID type controllers were considered. For simplicity a first order transfer function between compensated reactance ( $\Delta X$ ) and rotor angle difference ( $\delta_{ij}$ ) between the two closest generators was initially evaluated:

$$\frac{\Delta X_{45}}{\delta_{12}} = \frac{K_x}{1 + sT_x} \quad (6.1)$$

However, by the final value theorem, as  $s$  approaches zero, the compensated reactance will assume a steady state value of  $K_x \delta_{12}$ . Since the purpose of the FACTS device is to damp out oscillations and return to the normal line reactance value ( $\Delta X=0$ ), this final value

is obviously undesirable. To correct this problem, a differentiation operator  $s$  was added to the numerator of the transfer function:

$$\frac{\Delta X_{45}}{\delta_{12}} = \frac{K_X s}{1 + sT_X} \quad (6.2)$$

This transfer function provides the desired zero steady-state value for  $\Delta X$ . Note that frequency difference between generators is now the effective control input signal. Figure 6.2 provides a conceptual overview of the proposed control scheme for the TCSC.

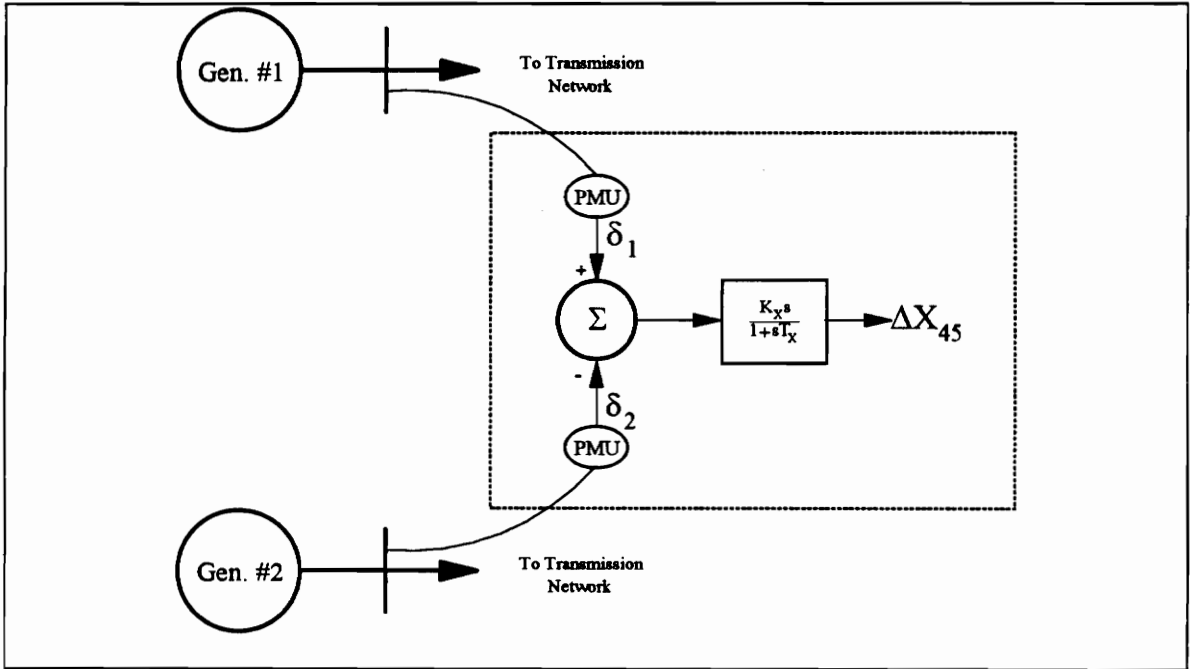


**Figure 6.2: Conceptual Diagram of FACTS Control Scheme**

The reliability of frequency as a measure of system oscillation, except for those measurements which are collected near a coherent generator, has been questioned [12]. However, since PMUs allow synchronized phasor measurements from remote generators,

remote rotor angle data can be collected and transmitted to the TCSC installation for differentiation. Thus, the aforementioned reliability issue can be avoided.

### 6.3 Effects On The Reduced Admittance Matrix

Since a FACTS device changes the effective reactance of a transmission line, it has a corresponding effect on the admittance matrix for the network. This obviously affects the A matrix and thus the eigenvalues of the state matrix. In order to account for this impact, each element of the reduced admittance matrix  $\bar{Y}_{red}$  was linearized in the following manner:

$$\bar{Y}_{ij} = \bar{Y}_{ij0} + \bar{Y}_{ij\Delta} \quad (6.3)$$

To formulate an exact relationship between changes in X and changes in the reduced admittance matrix would require network reduction of the nine bus power system for each incremental change in FACTS reactance. Since network reduction involves matrix inversion, this method could be too computation intensive for calculations on a large power system. Therefore, in order to express the incremental admittance change in terms of changes in line reactance, a numerical derivative of each admittance matrix element with respect to changes in X was used. Using this derivative, each admittance matrix element can now be linearized as:

$$\bar{Y}_{ij} = \bar{Y}_{ij0} + \frac{\partial \bar{Y}_{ij}}{\partial X_{45}} \Delta X_{45} \quad (6.4)$$

Note that since each element of the reduced admittance matrix is complex, the numerical derivative of each term with respect to FACTS compensation is also complex. This derivative exhibits nearly linear behavior over the range of 0 to 50% compensation. As a result, each admittance matrix element is averaged over this range to obtain the following numerical derivative matrix:

$$\frac{\partial \mathbf{Y}_{red}}{\partial \mathbf{X}_{45}} = \begin{bmatrix} 1.8648 + j2.9674 & -0.3972 - j2.4039 & 0.1767 - j0.3851 \\ -0.3972 - j2.4039 & -0.3920 + j1.6479 & -0.2169 + j0.1994 \\ 0.1767 - j0.3851 & -0.2169 + j0.1994 & -0.0507 + j0.0076 \end{bmatrix}$$

Using this derivative matrix in conjunction with the linearization equation for  $\mathbf{Y}_{ij}$  above, the augmented current coefficient matrix may now be formed.

#### 6.4 Augmented Current Coefficient Matrix

Now that  $\mathbf{Y}_{ij}$  can be expressed in terms of the incremental change in  $\mathbf{X}_{45}$ , the linearization of the current coefficient matrix as presented in Chapter 4 must be adapted. Recall the relationship between two-axis voltages and currents and the reference frame transformation matrix  $\bar{\mathbf{M}}$  defined in Chapter 4:

$$\bar{\mathbf{I}} = \bar{\mathbf{M}} \bar{\mathbf{E}}' \quad (6.5)$$

$$\bar{\mathbf{M}} = \begin{bmatrix} \mathbf{Y}_{11} e^{j\Theta_{11}} & \mathbf{Y}_{12} e^{j(\Theta_{12} - \delta_{12})} & \mathbf{Y}_{13} e^{j(\Theta_{13} - \delta_{13})} \\ \mathbf{Y}_{21} e^{j(\Theta_{21} - \delta_{21})} & \mathbf{Y}_{22} e^{j\Theta_{22}} & \mathbf{Y}_{23} e^{j(\Theta_{23} - \delta_{23})} \\ \mathbf{Y}_{31} e^{j(\Theta_{31} - \delta_{31})} & \mathbf{Y}_{32} e^{j(\Theta_{32} - \delta_{32})} & \mathbf{Y}_{33} e^{j\Theta_{33}} \end{bmatrix} \quad (6.6)$$

This system was linearized using the following relationship:

$$\bar{\mathbf{I}}_{\Delta} = \bar{\mathbf{M}}_{\Delta} \bar{\mathbf{E}}'_{\Delta} + \bar{\mathbf{M}}_{\Delta} \bar{\mathbf{E}}'_{\Delta} \quad (6.7)$$

Now, linearization of the system proceeds taking into account the new expression for each admittance matrix element in terms of incremental TCSC reactance as shown in equation (6.4). Substitution reveals that the admittance matrix entries which are expressed in terms of incremental FACTS reactance have no effect on the initial transformation matrix,  $\overline{\mathbf{M}}_{\bullet}$ . Therefore, all of the impact of FACTS compensation on the current will come from  $\overline{\mathbf{M}}_{\Delta}$ . From Chapter 4,  $\overline{\mathbf{M}}$  was found to contain only off-diagonal non-zero entries of the form:

$$\overline{\mathbf{m}}_{ij} = Y_{ij} e^{j(\Theta_{ij} - \delta_{ij0})} e^{-j\delta_{ij\Delta}} \quad (6.8)$$

If equation (6.4) is now substituted into this general form with the “0” subscript of  $Y_{ij0}$  dropped for convenience, and  $\alpha_{ij}$  is defined as the phase angle of the complex numerical derivative in this equation, the following expanded general form is found:

$$\overline{\mathbf{m}}_{ij} = (Y_{ij} e^{j\Theta_{ij}} + \left| \frac{\partial Y_{ij}}{\partial X_{45}} \right| e^{j\alpha_{ij}} \Delta X_{45}) e^{-j\delta_{ij0}} e^{-j\delta_{ij\Delta}} \quad (6.9)$$

Using Euler’s equation and the trigonometric linearizations discussed previously, the incremental portion of this expression due to  $\delta_{ij\Delta}$  can be approximated as:

$$e^{-j\delta_{ij\Delta}} = \cos(\delta_{ij\Delta}) - j\sin(\delta_{ij\Delta}) \cong (1 - j\delta_{ij\Delta}) \quad (6.10)$$

Ignoring higher order products (specifically the product of  $\delta_{ij\Delta}$  and  $\Delta X_{45}$ ) and grouping terms other than rotor angles and FACTS reactance in  $\overline{\mathbf{M}}_{\bullet}$ , the general linearized form for the entries of  $\overline{\mathbf{M}}_{\Delta}$  now becomes:

$$\overline{\mathbf{m}}_{ij\Delta} \cong \left| \frac{\partial Y_{ij}}{\partial X_{45}} \right| e^{j(\alpha_{ij} - \delta_{ij0})} \Delta X_{45} - jY_{ij} e^{j(\Theta_{ij} - \delta_{ij0})} \delta_{ij\Delta} \quad (6.11)$$



Since  $\Delta X_{45}$  is a new state variable in the **A** matrix, the current coefficient matrix is expanded by one column, and it now acts on a variable vector in which  $\Delta X_{45}$  has been added. Using the previous current coefficient matrix from Chapter 4 (the final form in which the redundant angle difference variable was eliminated) in conjunction with the new terms due to  $\Delta X_{45}$  yields the new current coefficient matrix which relates the  $d$  and  $q$  axis variables to the new expanded set of state variables (see Figure 6.3).

Now, the complete set of state variables for the nine bus system including the controlled FACTS device on the line between buses 4 and 5 can be summarized. From the discussion in Chapter 4, the linearized generator and excitation system state equations are:

$$\tau'_{q0i} \dot{E}'_{di\Delta} = -E'_{di\Delta} - (x_{qi} - x'_{qi}) I_{qi\Delta} \quad (6.12)$$

$$\tau'_{d0i} \dot{E}'_{qi\Delta} = E_{fdi\Delta} - E'_{qi\Delta} + (x_{di} - x'_{di}) I_{di\Delta} \quad (6.13)$$

$$\frac{2H_i}{\omega_R} \dot{\omega}_{i\Delta} = P_{mi\Delta} - I_{di0} E'_{di\Delta} - I_{qi0} E'_{qi\Delta} - E'_{di0} I_{di\Delta} - E'_{qi0} I_{qi\Delta} - D_i \omega_{i\Delta} \quad (6.14)$$

$$\dot{\delta}_{i\Delta} = \omega_{i\Delta} \quad (6.15)$$

$$\dot{E}_{fdi\Delta} = (V_{Ri\Delta} - (1 + K_{Ei}) E_{fdi\Delta}) / T_{Ei} \quad (6.16)$$

$$\dot{V}_{SLi\Delta} = (K_{Si} / T_{Si}) E_{fdi\Delta} - V_{SLi\Delta} \quad (6.17)$$

$$\dot{V}_{Ri\Delta} = (K_{Ai} (V_{refi} - V_{i\Delta} - (K_{Si} / T_{Si}) E_{fdi\Delta} + V_{SLi\Delta}) - V_{Ri\Delta}) / T_{Ai} \quad (6.18)$$

where

$$V_{i\Delta} = \left( \frac{V_{di0}}{V_{i0}} \right) (E'_{di\Delta} - x'_{qi} I_{qi\Delta}) + \left( \frac{V_{qi0}}{V_{i0}} \right) (E'_{qi\Delta} + x'_{di} I_{di\Delta}) \quad (6.19)$$

The additional state variable  $\Delta X_{45}$  is defined by the following equation:

$$\Delta \dot{X}_{45} = \frac{1}{T_x} (K_x \omega_{1\Delta} - K_x \omega_{2\Delta} - \Delta X_{45}) \quad (6.20)$$

$$\begin{bmatrix} \bar{I}_{1\Delta} \\ \bar{I}_{2\Delta} \\ \bar{I}_{3\Delta} \end{bmatrix} = \begin{bmatrix} Y_{11}e^{j\Theta_{11}} & Y_{12}e^{j(\Theta_{12}-\delta_{120})} & Y_{13}e^{j(\Theta_{13}-\delta_{130})} & -j\bar{E}'_{30}Y_{13}e^{j(\Theta_{13}-\delta_{130})} & -j\bar{E}'_{20}Y_{12}e^{j(\Theta_{12}-\delta_{120})} & \left| \frac{\partial Y_{11}}{\partial X_{45}} e^{j\alpha_{12}} + \bar{E}'_{20} \right| \left| \frac{\partial Y_{12}}{\partial X_{45}} e^{j(\alpha_{12}-\delta_{120})} \right| \\ Y_{21}e^{j(\Theta_{21}+\delta_{120})} & Y_{22}e^{j\Theta_{22}} & Y_{23}e^{j(\Theta_{23}-\delta_{210})} & -j\bar{E}'_{10}Y_{23}e^{j(\Theta_{23}-\delta_{210})} & -j\bar{E}'_{30}Y_{21}e^{j(\Theta_{21}+\delta_{120})} + \bar{E}'_{20} \left| \frac{\partial Y_{13}}{\partial X_{45}} e^{j(\alpha_{13}-\delta_{130})} \right| \\ Y_{31}e^{j(\Theta_{31}+\delta_{130})} & Y_{32}e^{j(\Theta_{32}+\delta_{210})} & Y_{33}e^{j\Theta_{33}} & -j\bar{E}'_{10}Y_{31}e^{j(\Theta_{31}+\delta_{130})} & -j\bar{E}'_{20}Y_{32}e^{j(\Theta_{32}+\delta_{210})} + \bar{E}'_{30} \left| \frac{\partial Y_{23}}{\partial X_{45}} e^{j(\alpha_{23}-\delta_{230})} \right| \\ & & & + j\bar{E}'_{20}Y_{32}e^{j(\Theta_{32}+\delta_{210})} & + j\bar{E}'_{30}Y_{33}e^{j(\Theta_{33}+\delta_{230})} & + \bar{E}'_{30} \left| \frac{\partial Y_{33}}{\partial X_{45}} e^{j\alpha_{33}} \right| \end{bmatrix} \begin{bmatrix} \bar{E}'_{1\Delta} \\ \bar{E}'_{2\Delta} \\ \bar{E}'_{3\Delta} \\ \delta_{12\Delta} \\ \delta_{13\Delta} \\ \Delta X_{45} \end{bmatrix}$$

**Figure 6.3: Current Coefficient Matrix With Inclusion of FACTS State Variable**

For the three machine system, the number of generator and excitation system equations is  $(7 \times 3) - 1$  or 20. With the addition of the incremental FACTS reactance variable, the final system order is increased by one. Thus, the overall state matrix is  $21 \times 21$  in size. The actual numeric coefficients for the current coefficient and state matrices of the FACTS compensated test system may be found in Appendix A.

## 6.5 Optimization of FACTS Controller

With a control scheme now implemented and included in the state matrix for the system, selection of the optimal time constant and gain for the FACTS control system must be made. In order to determine which combination of gain and time constant optimizes the stability and response of the FACTS device, both eigenvalue and time simulation techniques were used. First, a discussion of the general form of the FACTS control transfer function is appropriate:

$$\frac{\Delta X_{45}}{\delta_{12}} = \frac{K_X s}{1 + sT_X} \quad (6.21)$$

or equivalently, written as a state equation:

$$\Delta \dot{X}_{45} = \frac{1}{T_X} (K_X \omega_{1\Delta} - K_X \omega_{2\Delta} - \Delta X_{45}) \quad (6.22)$$

The relationship between the incremental reactance and rotor angle difference (effectively frequency difference due to the differentiation operator  $s$ ) appears to be first order, so a very simple step response would be expected. However, there are hidden dependencies in

this transfer function which give it a much higher order. Rotor angle is a function of frequency which in turn is a function of the  $d$  and  $q$  axis voltages and currents. Changes in the reactance in the system change the reduced admittance matrix and consequently the generator currents. This combination of interactions results in higher order dependency between the input and output variables in equation (6.21). Given this level of complexity in the relationship between rotor angle difference and FACTS reactance, it is difficult if not impossible to develop a complete transfer function in terms of all system variables. Therefore, in order to determine the stability and response characteristics of the system, other techniques such as eigenvalue analysis and numerical simulation must be used.

In order to use eigenvalue analysis to determine the best controller parameters in terms of stability, arbitrary values for  $K_x$  and  $T_x$  were chosen as starting guesses. Then one parameter was varied while the other remained fixed, and the critical eigenvalues ( $\lambda_c$ ) for the system were stored in an array versus the changing parameter. For the first trial run in this study, the time constant was held fixed at 10 seconds and the gain was varied to observe what effects it had on stability. Results showed that a negative gain was required for the system to be stable. Plots of  $\lambda_c$  versus  $K_x$  were used to determine the value of  $K_x$  that made the critical eigenvalue most negative (stable) for the given time constant. This plot is shown in Figure 6.4. As shown in the figure, a gain of -21 was found to provide the maximum stability for the given time constant of 10 seconds.

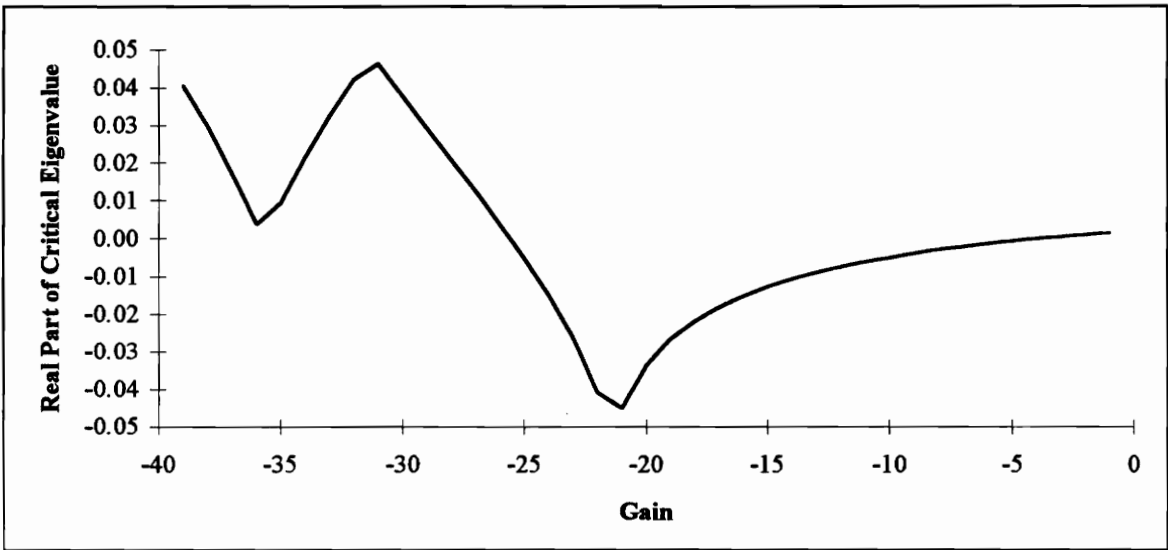


**Figure 6.4: Critical Eigenvalue Variation with FACTS Controller Gain**

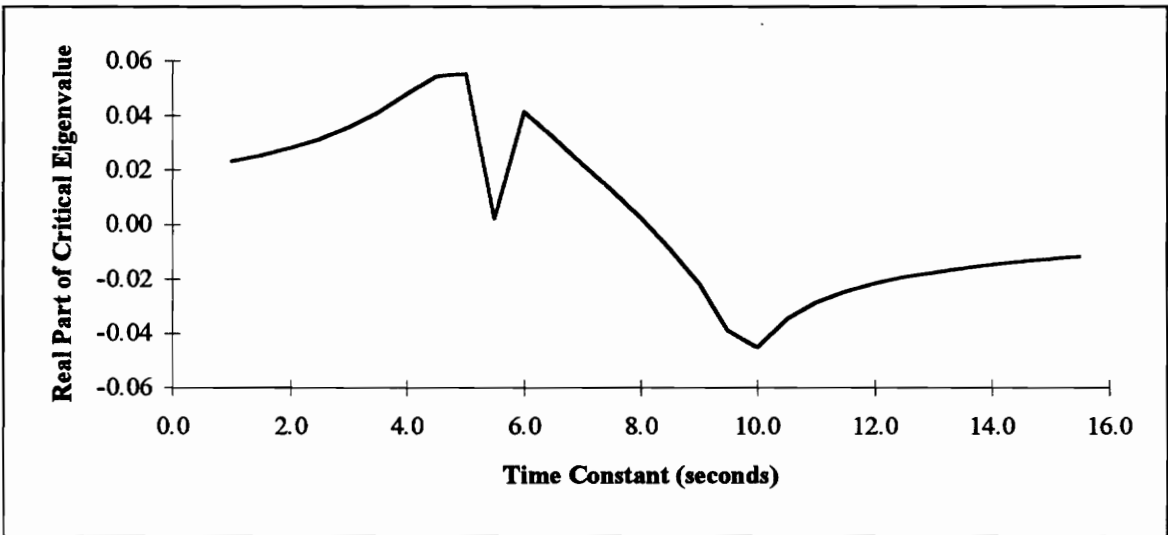


**Figure 6.5: Critical Eigenvalue Variation with FACTS Controller Time Constant**

Using this new value of gain and varying  $T_x$  in a manner similar to that discussed above, a new plot was developed (see Figure 6.5). From this new plot, the optimal time constant for the given gain of -21 was determined to be 10 seconds, the initially assumed

value. This consistency ensures that an iterative process is not necessary to determine the most stable pair of controller parameters. Given the stable characteristics of this set of parameters, the next step is to observe the time response of the system to a disturbance.

In evaluating the response of the FACTS device several characteristics must be observed. First and foremost, the response of the electrical power output and rotor angle from each generator must be stable. Since compensated reactance is a function of rotor angle, once the reactance response has become stable, the rotor angle and thus electrical power output of the generators must also be stable. Therefore, the time response of the FACTS device can be used to evaluate the overall system time response. Since a series capacitor is being modeled, only negative reactance changes should be observed ideally. Some inductive change can be achieved by insertion of a permanent inductor in series with the FACTS device and switching all capacitor modules out of the line. However, in order to maintain the initial line reactance specified in the model, capacitance with impedance magnitude equal to that of the series inductance would have to be inserted at all times. This portion of the FACTS capacitance would therefore not be available for damping oscillations. In addition, to minimize the cost of such an installation, the magnitude of the maximum capacitive swing must be within the limits of the assumed compensation range (50% for this thesis). Finally, the amount of time it takes for the system to stabilize to the normal line reactance (zero change in TCSC reactance) should be minimized in order to produce maximum damping of the disturbance.

Summarizing the three main criteria for an acceptable FACTS response in arbitrary rank and order:

1. Minimize positive (inductive) swings in reactance
2. Minimize disturbance settling time
3. Minimize capacitive compensation requirement

Since the system is highly nonlinear, it is difficult at best to determine the step response of this transfer function analytically. Control theory provides analytical expressions for the response attributes of a second order system. However, since the test system has several eigenvalues that are similar in magnitude and close to the imaginary axis, a second order approximation for the transfer function cannot be made accurately. Therefore, these attributes must be determined using time simulation techniques.

The same simulation methods as those discussed in Chapter 5 were used for analysis of the compensated system with the addition of a module in the C program for calculating FACTS maxima, minima, and settling time. This process is shown in Figure 6.6. The resulting FACTS reactance response for the gain and time constants selected using eigenvalue analysis above is shown in Figure 6.7. This response does show a rather dramatic damping of the oscillations within a short settling time. However, the amount of capacitive compensation required is somewhat high (above 30%) and the response has a large inductive swing of nearly 20%. So, two of the desired response characteristics have not been met. At this point, eigenvalue analysis was repeated for a different time constant value.

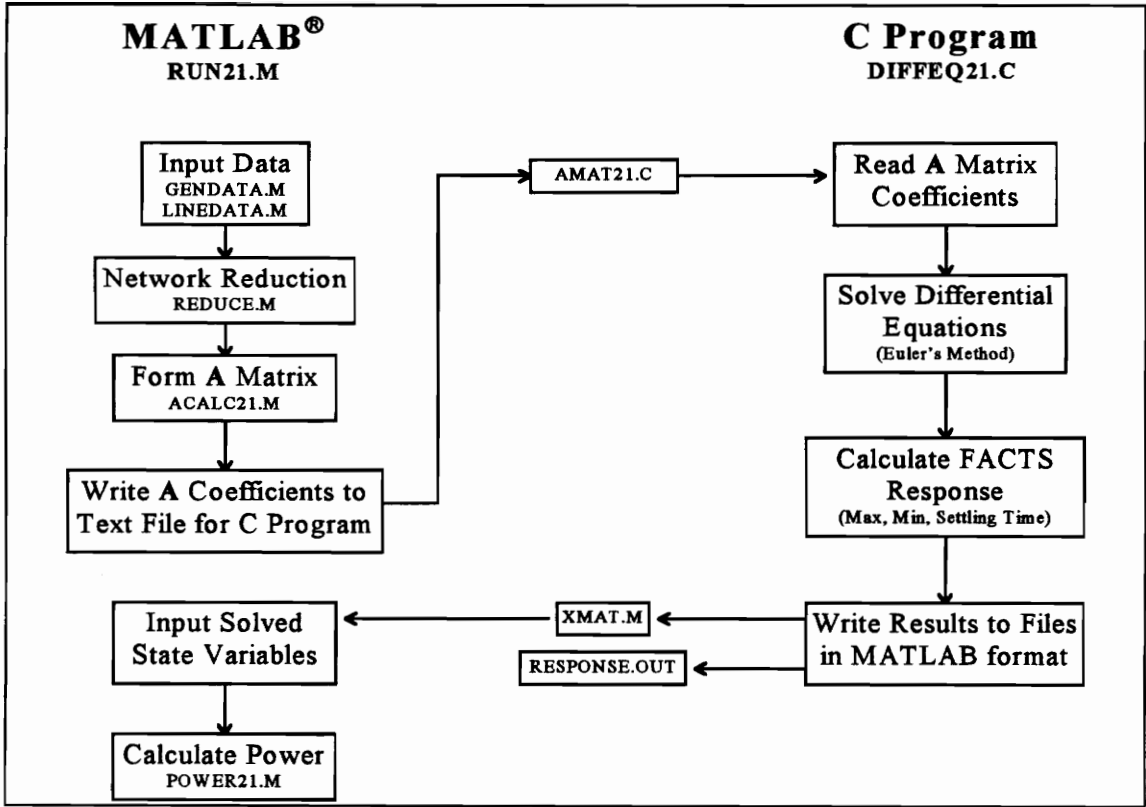


**Figure 6.6: Flowchart for FACTS Compensated Test System Simulations**

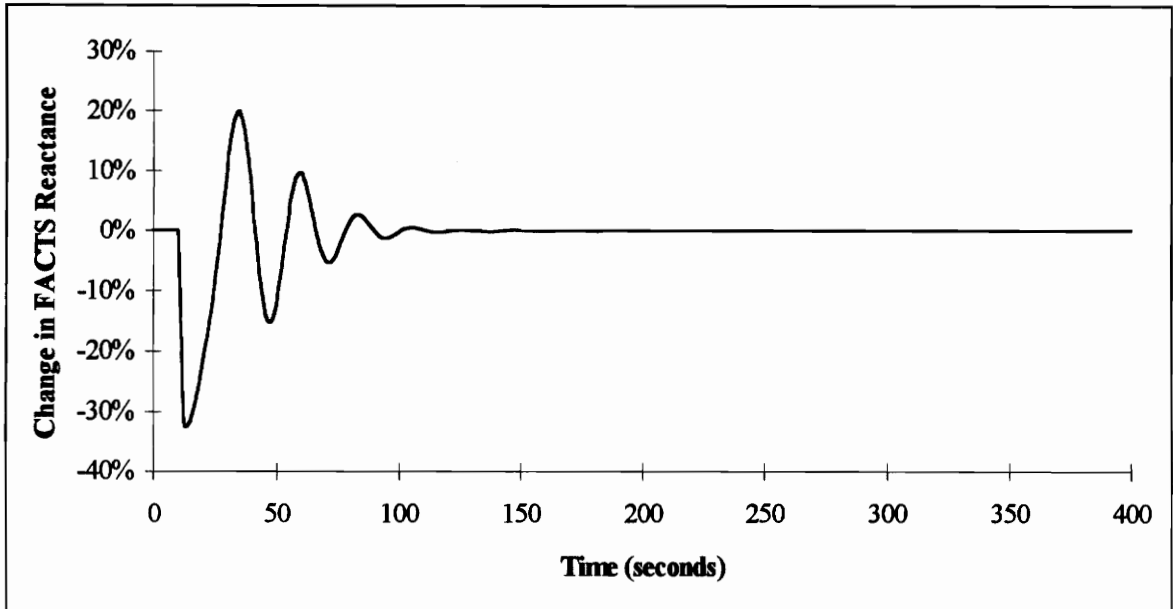


**Figure 6.7: Response of FACTS Reactance for  $K_X = -21$  and  $T_X = 10$**



As the response in Figure 6.7 shows, the compensation requirements in both the inductive and capacitive modes make a TCSC installation with these characteristics economically unattractive to construct. The lesson observed here is that good stability results based on eigenvalue analysis alone are not enough to make a practical evaluation of the controller time constant and gain. In other words, favorable response characteristics of the FACTS device are required in order to constitute an acceptable gain-time constant pair for the proposed control scheme. For this thesis, the required response information was obtained using time simulation techniques since analytical determination of these attributes cannot be made easily. The process used to evaluate the FACTS response for a variety of time constants and gains again starts with eigenvalue analysis. The time constant was held fixed while the gain was varied in order to determine what values of the gain yielded stable results for the given time constant. Then time simulations were performed for each of the stable gain-time constant pairs. A routine within the differential equation-solving C program was then used to calculate and tabulate the FACTS response characteristics for each combination of  $K_x$  and  $T_x$ . Maxima and minima for the FACTS response characteristic were calculated. In addition, the time required for the response amplitude, including all local extrema, to settle to 1% of the uncompensated line reactance was determined. This settling time criteria was an arbitrary conservative choice which was strictly used as a point of comparison among the various control parameter combinations. The entire simulation process was then repeated starting with the selection of a new time constant and the evaluation of stable values of gain.

Several trends emerge from the tabulated TCSC response data. In general, the maximum of the time response characteristic tends to decrease with increasing time constant while the minimum value, the amount of capacitive compensation, tends to increase. Settling time, on the other hand, exhibits fluctuations which cannot be easily expressed in terms of a general trend. Since the maximum and minimum peaks vary in opposite directions, some sort of compromise must be found which also minimizes settling time. Only generalizations can be made about the trends in each response characteristic and their relative importance compared to each other, so a tabulation was used to choose the best design combination manually. Selective gain and time constant combinations which produced capacitive compensation swings of less than 30% and inductive peaks of less than 3% are shown in Table 6.2.

**Table 6.2: TCSC Response Characteristics for Various Controller Settings**

<b>K<sub>x</sub></b>	<b>T<sub>x</sub></b>	<b>Inductive Compensation Requirement (%)</b>	<b>Capacitive Compensation Requirement (%)</b>	<b>Time(seconds)</b>
-10	10	1.1941	9.5851	275.000000
-11	10	1.7131	10.9212	255.000000
-12	10	2.3597	12.3563	257.500000
-24	20	1.8056	16.1142	215.000000
-26	20	2.2171	18.3400	215.000000
-28	20	2.6027	20.7990	192.500000
<b>-50</b>	<b>50</b>	<b>0.5526</b>	<b>17.0519</b>	<b>212.500000</b>
-55	50	0.6234	20.0084	212.500000
-60	50	0.7585	23.4077	212.500000
-65	50	0.9133	27.3155	212.500000
-100	100	0.1792	20.1835	275.000000
-110	100	0.1640	23.8803	275.000000
-120	100	0.1707	28.1473	255.000000

Arbitrary guidelines were chosen for determining the best gain and time constant combination. In order to keep oscillations in the capacitive region as much as possible, a maximum allowable inductive peak of 1% was chosen. Based on this criteria, the qualifying entries in Table 6.2 were evaluated in terms of the amount of capacitive compensation needed and the time it took for the response to settle. The final choice was  $K_x = -50$  and  $T_x = 50$  which exhibited a settling time of 212.5 seconds, a 0.55% inductive overshoot, and required 17.1% capacitive compensation (see Figure 7.12 in the next chapter). Thus, design objectives 1 and 3 from above have been greatly improved upon over the initial design choice while maintaining a relatively low settling time.

This simulation method could be used for determining controller parameters for a variety of design objectives. Although a table was generated to allow manual determination of the best controller, a sufficiently sophisticated system of weighting factors could be added to the C program to describe the importance of each factor and thus determine the best combination automatically. One possible method for automating this process is the Analytic Hierarchical Process (AHP) which utilizes pair-wise weighting of attributes in a matrix format [21]. This process was briefly investigated for use in completing the above task, but it was not implemented due to time limitations.

## **CHAPTER 7**

### **Response of the Compensated System**

#### **7.1 Assumed Conditions**

For simulation of the nine bus test system with the addition of the TCSC, all assumptions about the power system conditions made in the simulation of the uncompensated system remained unchanged. Specifically, the system was assumed to have undergone a gradual reactive load change, and a disturbance in the form of a small step change in mechanical power input to one of the generators was applied to the system ten seconds after the start of the simulation. In order to evaluate the effects of the controlled FACTS device on this system as compared to traditional series compensation, simulations of mechanically and electronically controlled compensation were made.

#### **7.2 Mechanical Series Compensation**

In order to illustrate the improved stability control of a TCSC over a conventional series capacitor installation with mechanical switching, a simulation of this conventional

installation was made. Since the oscillations observed on this system have a reasonably long period (roughly 20-25 seconds) it is reasonable to assume that a mechanical switch could insert a large block of capacitance within the period of the oscillations. Furthermore, to provide maximum damping from the conventional device, a total of 50% capacitive compensation (the assumed maximum compensation for the TCSC) was assumed to be inserted into the network.

Results from this simulation showed that mechanical series compensation would reduce the oscillation growth rate as compared to the uncompensated system. However, the overall system is still obviously unstable. Eigenvalues for the mechanically compensated system are listed in Table 7.1 and plotted in Figures 7.1 and 7.2. Time simulation results are presented for electrical power of generator 1 (Figure 7.3) and rotor angle difference between units 1 and 2 (Figure 7.4). The responses for the other units exhibited similar characteristics and were thus omitted for brevity.

**Table 7.1: System Eigenvalues for Mechanically Compensated System**

<b>System Eigenvalues</b>	
-60.2144	-2.5397
-26.3754	<b>0.0010 + 0.3034i</b>
-16.5755	<b>0.0010 - 0.3034i</b>
-9.2845	-1.5792
-5.3001 + 4.0078i	-0.7008
-5.3001 - 4.0078i	-0.3764 + 0.0250i
-7.3472	-0.3764 - 0.0250i
-3.5954	-1.3395
-2.7674 + 0.9460i	-0.1755
-2.7674 - 0.9460i	-2.0000

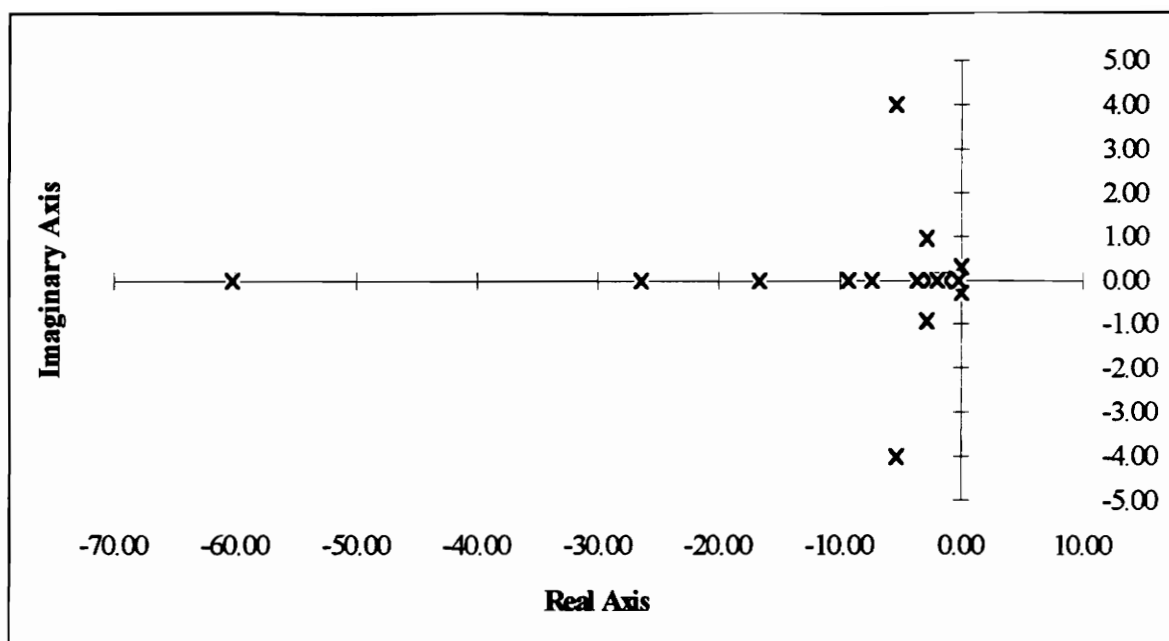


**Figure 7.1: System Eigenvalues (Mechanically Compensated System)**

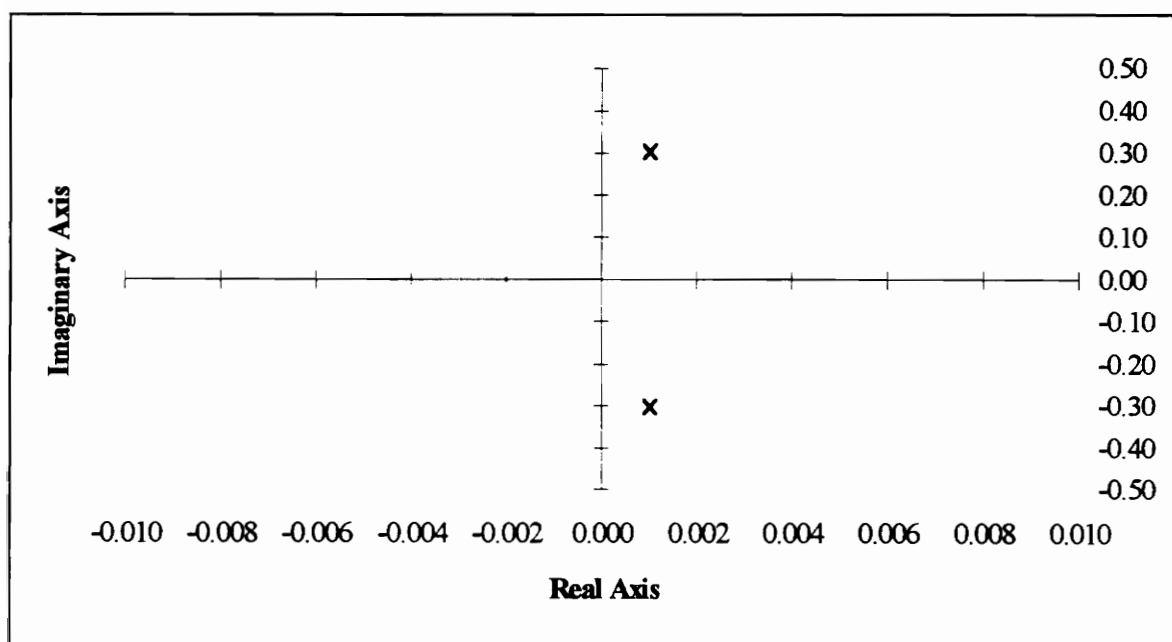


**Figure 7.2: Close-up of Dominant Eigenvalues (Mechanically Compensated System)**

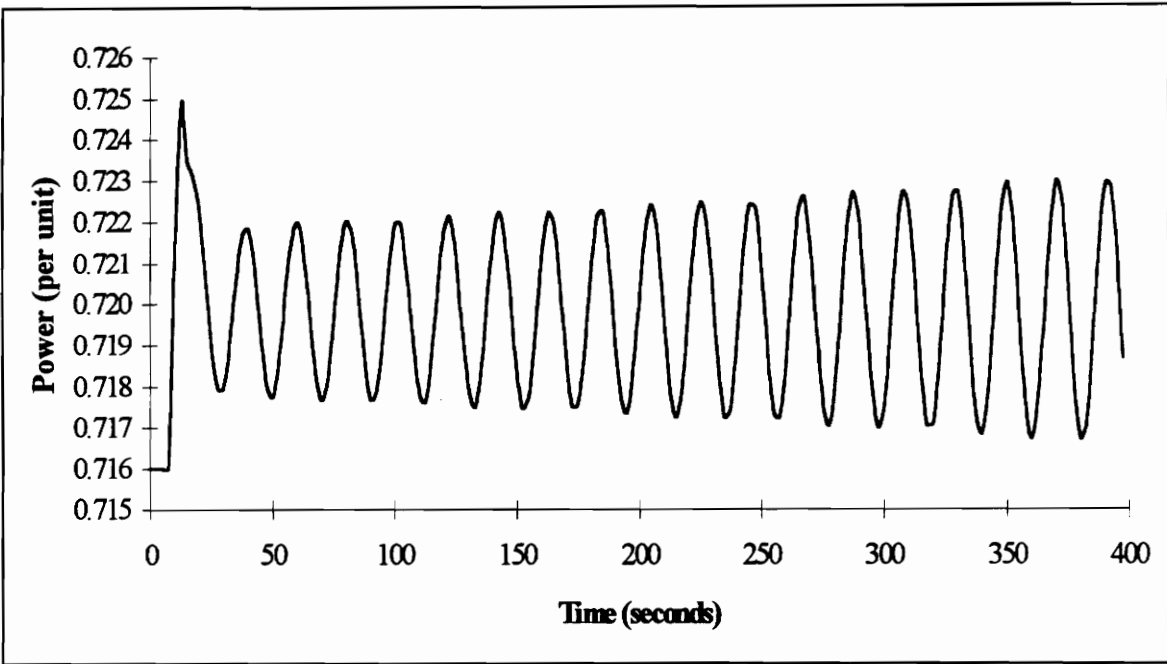


**Figure 7.3: Electrical Power of Generator 1 (Mechanically Compensated System)**

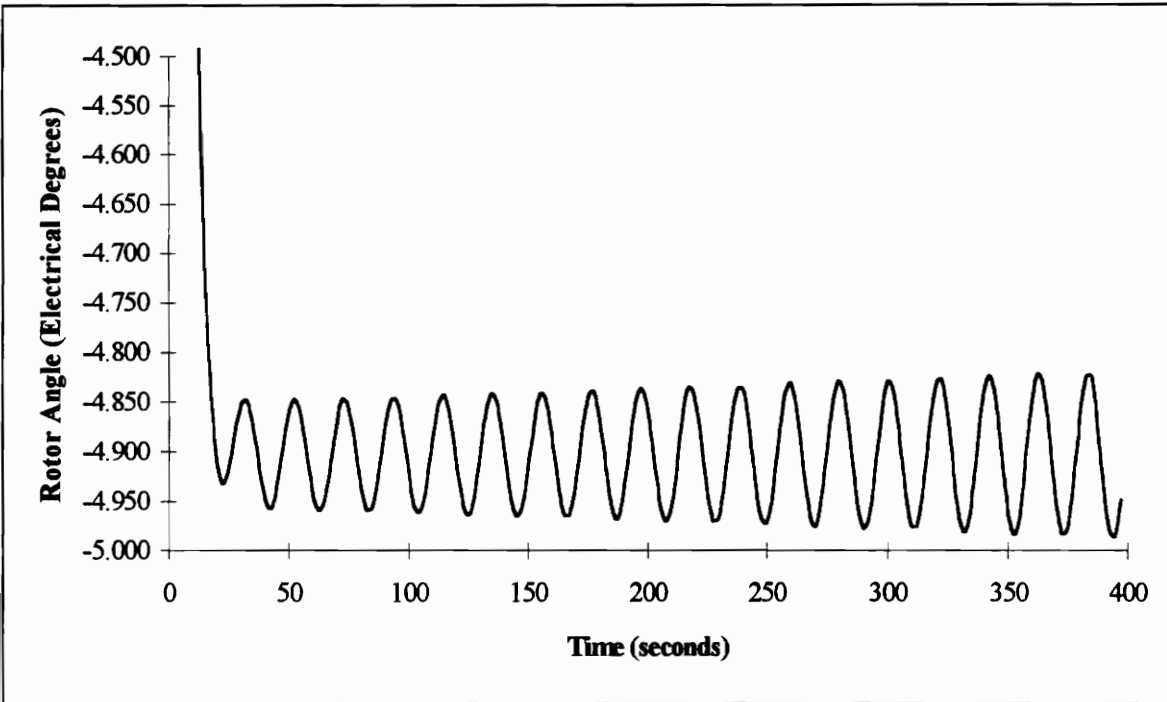


**Figure 7.4: Rotor Angle Difference,  $\delta_{12}$  (Mechanically Compensated System)**

### 7.3 Modulated FACTS Compensation

Using the values for  $K_X$  and  $T_X$  derived in Chapter 6, eigenvalue analysis and numerical simulations were completed for stability evaluation. Table 7.2 summarizes the overall system eigenvalues which are also plotted in Figure 7.5. A close-up of the dominant eigenvalues is shown in Figure 7.6. This second plot clearly shows that the critical eigenvalues remain in the left-half plane after the gradual reactive load change.

**Table 7.2: System Eigenvalues for FACTS Compensated System**

System Eigenvalues	
-60.2178	-1.7545 + 0.0716i
-26.6717	-1.7545 - 0.0716i
-16.5755	-1.3408
-9.2247	-0.7897
-5.7742 + 3.0820i	-0.0064 + 0.3031i
-5.7742 - 3.0820i	-0.0064 - 0.3031i
-7.3474	-0.4685
-2.7573 + 0.9558i	-0.1793 + 0.0362i
-2.7573 - 0.9558i	-0.1793 - 0.0362i
-2.5639 + 0.1415i	-0.0404
-2.5639 - 0.1415i	

Results from numerical simulations also verified the overall stability of the compensated system. The electrical power output of each generator is shown in Figures 7.7 through 7.9. Rotor angle differences are shown in Figures 7.10 and 7.11 and the TCSC reactance response is shown in Figure 7.12.



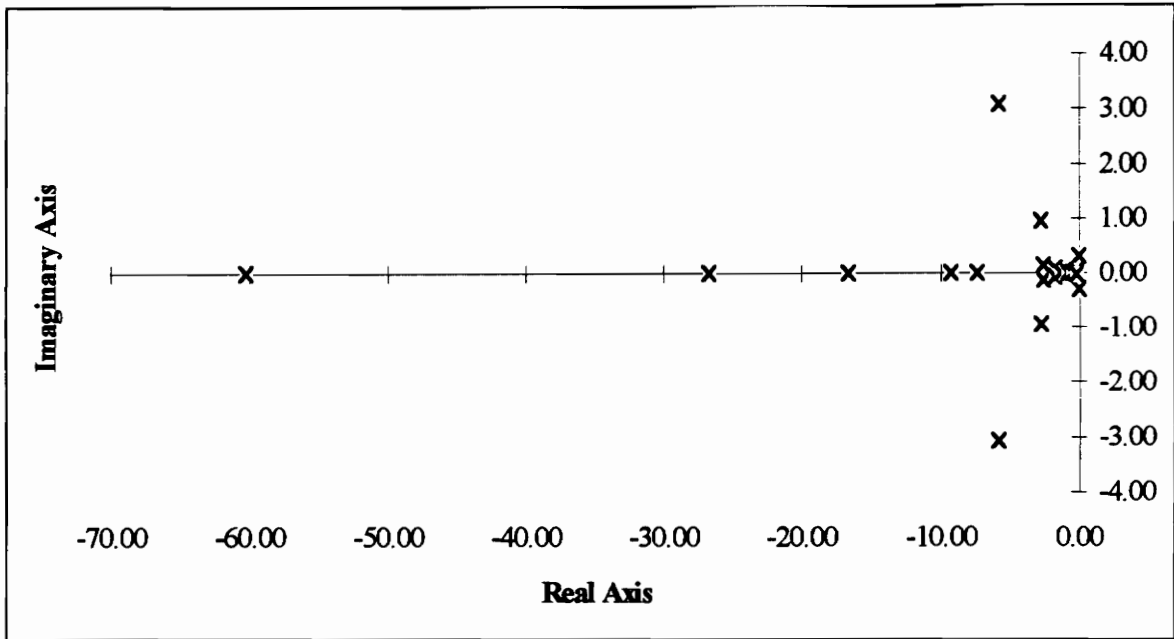


**Figure 7.5: System Eigenvalues (FACTS Compensated System)**

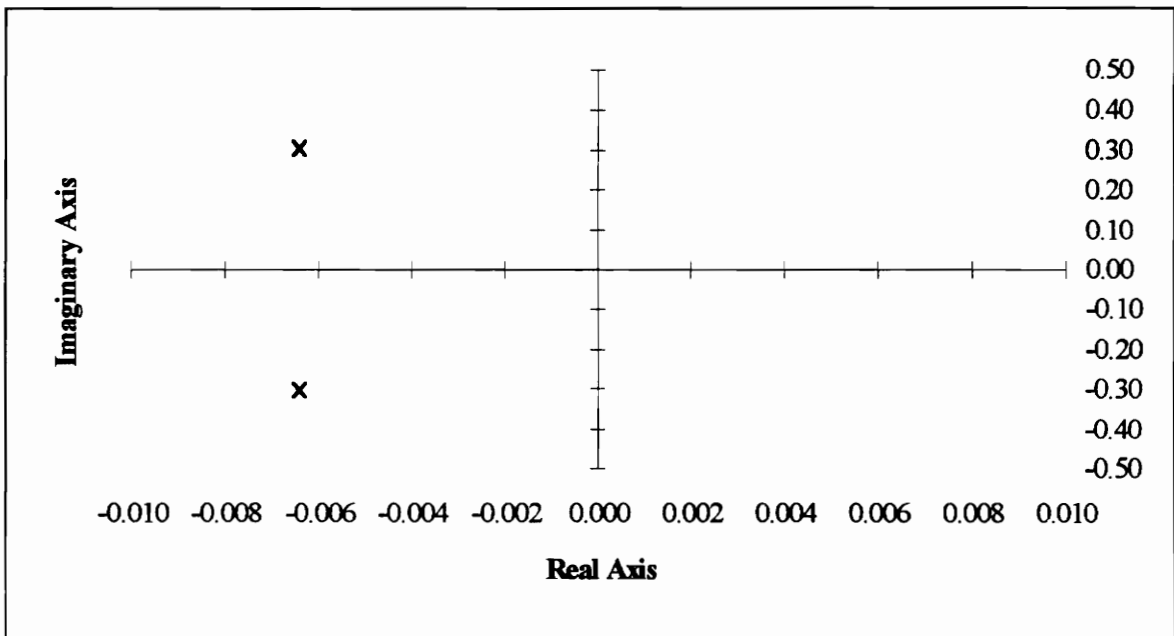


**Figure 7.6: Close-up of Dominant Eigenvalues (FACTS Compensated System)**

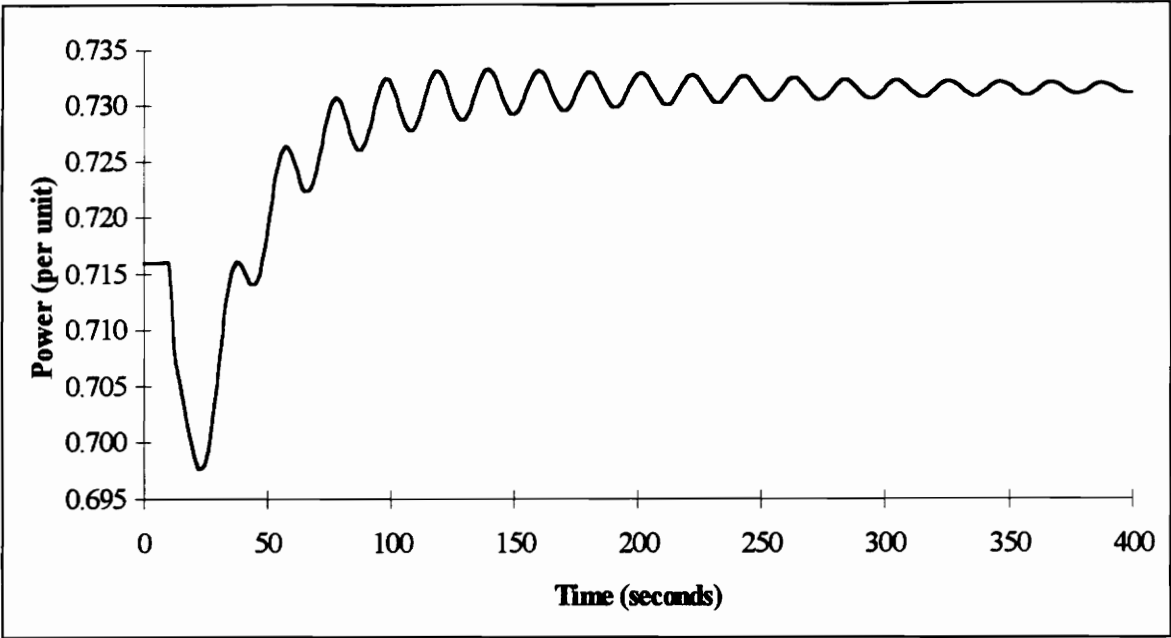


**Figure 7.7: Electrical Power of Generator 1 (FACTS Compensated System)**

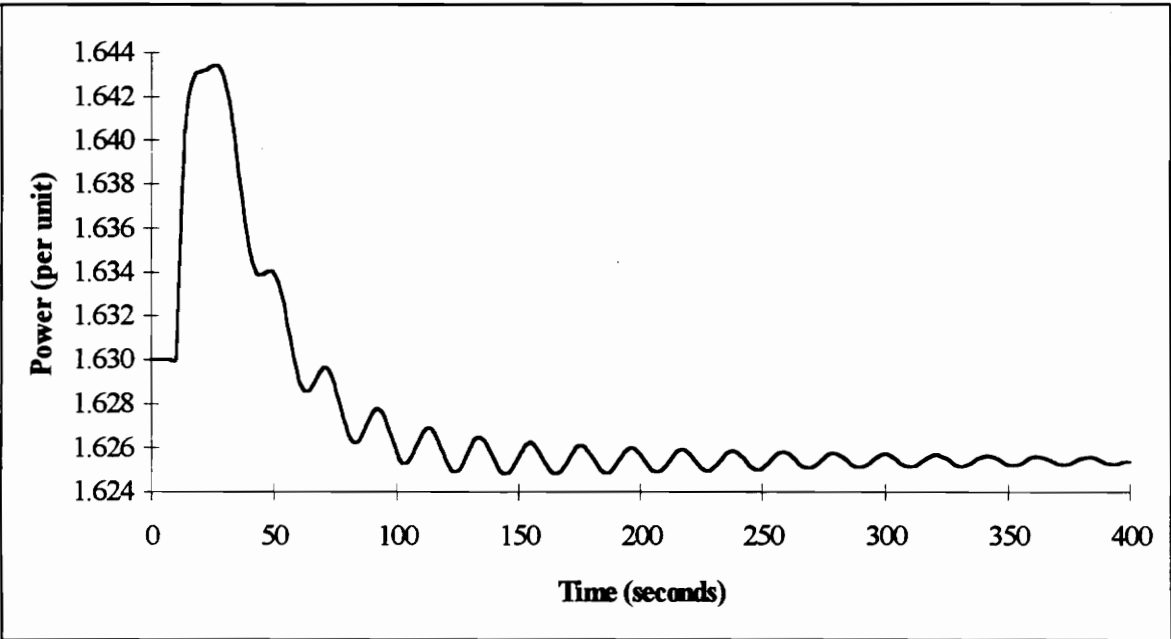


**Figure 7.8: Electrical Power of Generator 2 (FACTS Compensated System)**

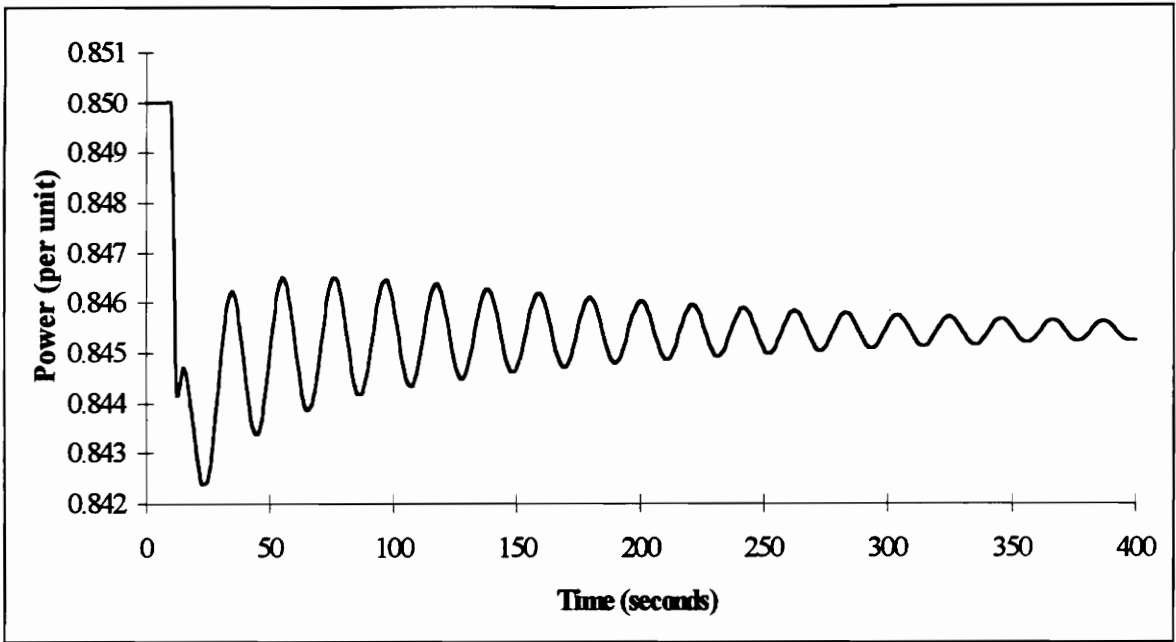


**Figure 7.9: Electrical Power of Generator 3 (FACTS Compensated System)**

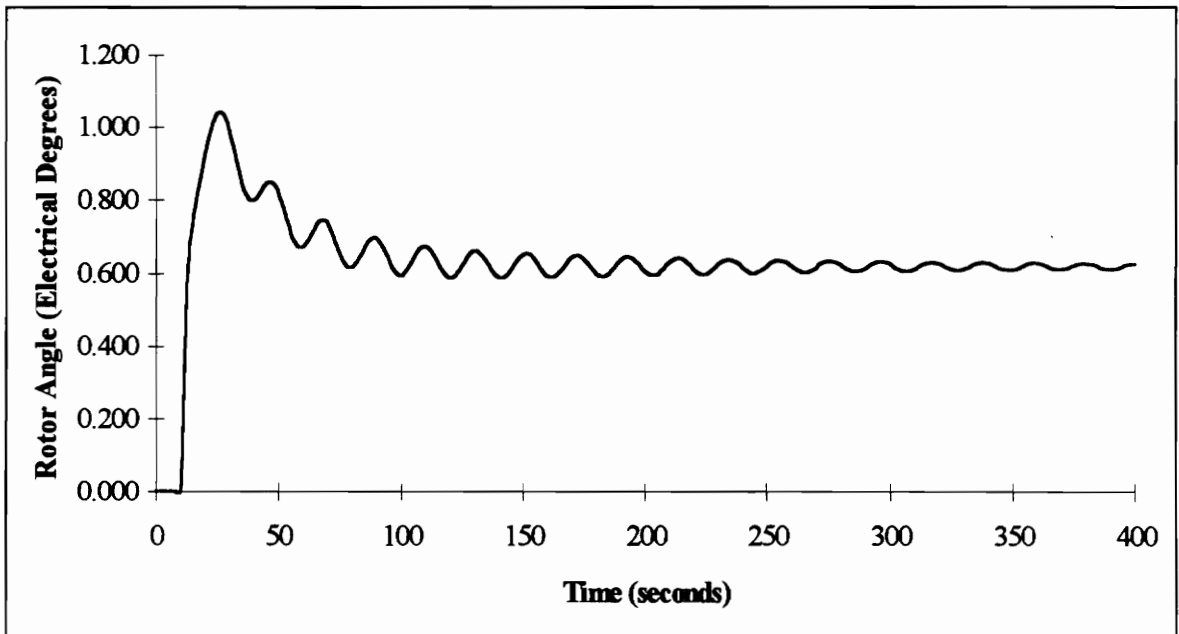


**Figure 7.10: Rotor Angle Difference,  $\delta_{12}$  (FACTS Compensated System)**

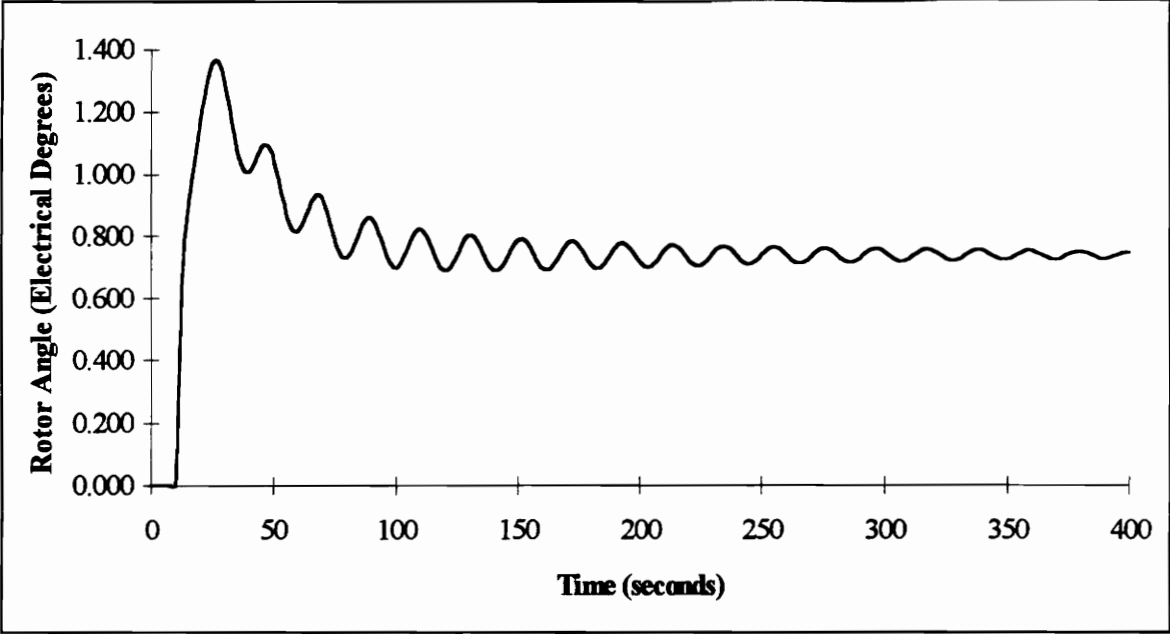


**Figure 7.11: Rotor Angle Difference,  $\delta_{13}$  (FACTS Compensated System)**

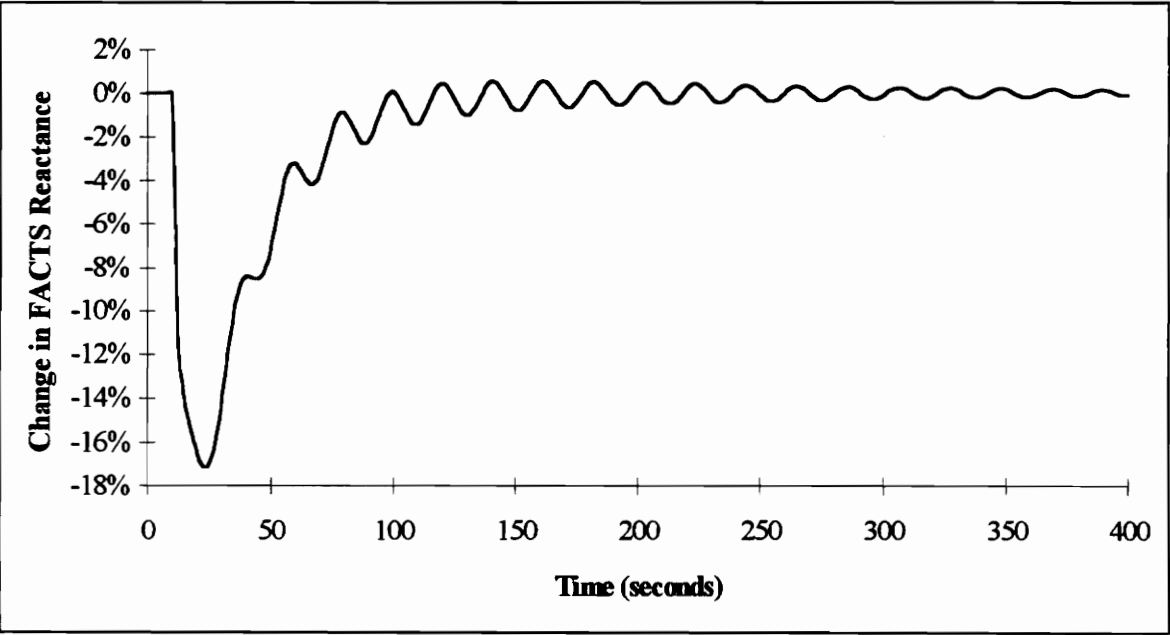


**Figure 7.12: Change in TCSC Reactance,  $\Delta X_{45}$ , versus Time**

#### 7.4 Compensated System Loadability

Although stability is the main focus of this study, the ability of FACTS devices to increase the amount of power that can be delivered on a transmission system deserves mention. In the case of the TCSC, increased loadability is achieved by increasing capacitive compensation in order to lower the overall line reactance. This can be illustrated by the following relationship:

$$P_e = \frac{E_1 E_2}{X_{12}} \sin \delta \quad (7.1)$$

where  $E_1$  and  $E_2$  are the voltages of two buses which are connected by a reactance  $X_{12}$  and have phase angle difference  $\delta$ . Thus, if the line reactance is lowered, the power transfer capability between buses 1 and 2 increases. From the maximum response of the TCSC characteristic shown in Figure 7.12, the peak of 17.1% compensation provides a 20.6% increase in transmission capability between generator 1 and load A, assuming all other variables are approximately constant. However, to realize a permanent increase in load transfer capability, some modules must always be inserted in the system.

In a related area, the stability of the test system network topology was greatly increased with the addition of the FACTS controller. Without the controller, the system was unstable at the initial load conditions. A rough study of the effects of the TCSC on the stability of the network was conducted by increasing the real power at each load and observing the eigenvalue response. Results showed that the FACTS compensated system could not be forced into instability by ordinary load changes. This shows that transmission

line thermal ratings and generation reserves limit the stability of the loads rather than the topology of this test system with the FACTS controller in place.

## **CHAPTER 8**

### **Conclusions**

#### **8.1 Summary of Results**

This thesis has shown the viability of modulating TCSC reactance in order to improve the dynamic stability of a power system. A method has been proposed and evaluated for optimal placement of FACTS devices for the purpose of oscillation damping. In addition, a PID controller using phasor measurement feedback has been shown to be quite effective at damping small-signal oscillations. Although model complexity significantly increases with the size of a network, the methods used in this thesis may be readily applied to any power system. The use of numerical eigenvalue derivatives in determining optimal location of a FACTS device, as presented in this thesis, could be a useful technique for this purpose in any network, regardless of size. Also, the state model which was adapted to include the FACTS device has applications for much larger power systems. Finally, the use of phasor measurements from PMUs has been shown to provide another useful purpose in the control of power systems. Numerical results for this study

are summarized in Table 8.1 which lists the critical eigenvalues for the test system in each compensation scenario and Figure 8.1 which provides a composite plot of the time response of electrical power for each compensation condition.

**Table 8.1: Critical System Eigenvalues For All Compensation Conditions**

Compensation Condition	Critical System Eigenvalues
Uncompensated System	$0.0021 \pm 0.3043i$
Mechanically Compensated System	$0.0010 \pm 0.3034i$
FACTS Compensated System	$-0.0064 \pm 0.3031i$

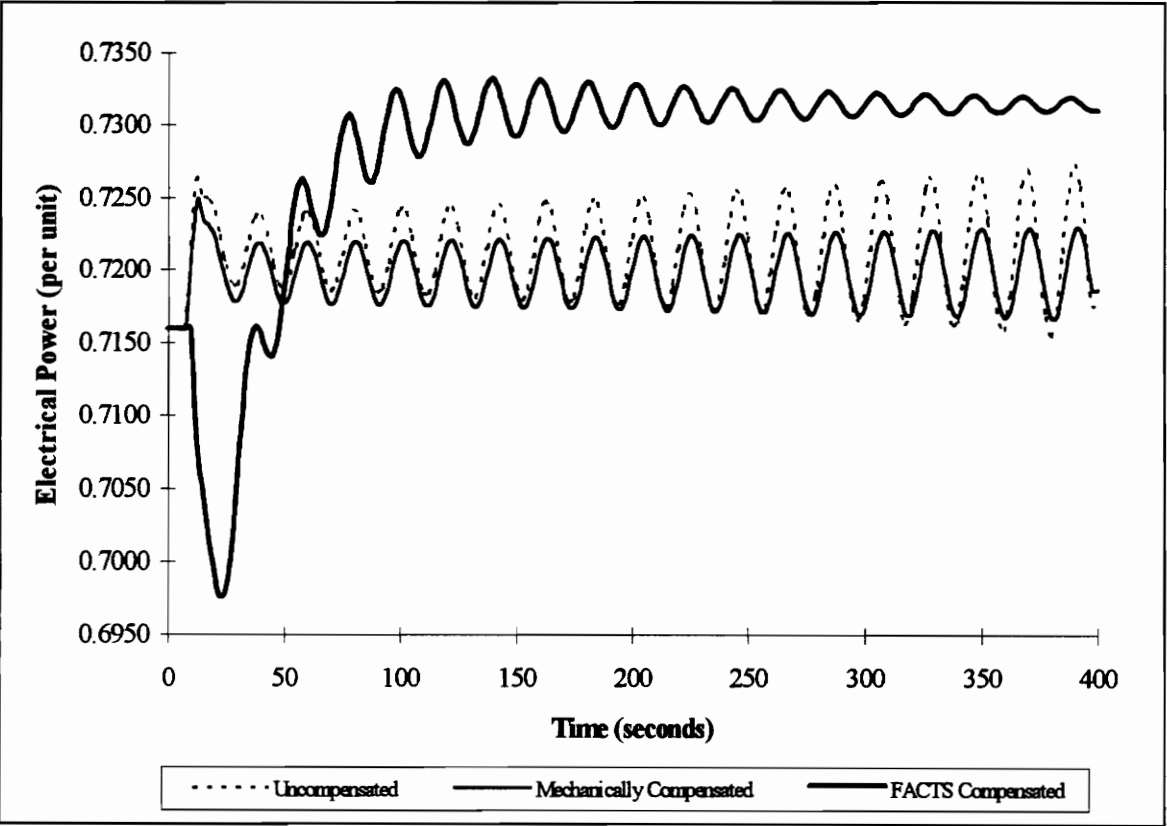


**Figure 8.1: Electrical Power of Generator 1 for All Compensation Conditions**



## **8.2 Future Work**

The assessment of damping strategies for dynamic oscillations in power systems, though much studied, remains an interesting and important area of research for the power engineering community. The factors discussed in the introduction of this thesis will continue to force utilities to push the operation of their power systems ever closer to their absolute security and stability limits. With this in mind, several areas of research may be extended from this thesis.

In the area of device modeling, more detailed models of the actual FACTS devices that are inserted into a network could be implemented into the power system model. This could include modeling overvoltage protection devices and incorporating any delays that may be observed between measurement of the rotor angles and insertion of the TCSC into the power network. In a broader examination of dynamic stability, phasor measurement feedback control of the excitation systems for generators could also be modeled for its impact on damping power system oscillations.

Also of interest would be application of the FACTS controller proposed in this thesis to a larger power system. This could include how multiple FACTS devices interact with each other to affect the damping of power system oscillations. As the costs of these devices continue to decrease with advances in technology, the combined capabilities of multiple FACTS installations could provide an incentive for broader uses of these devices

in the power industry. In addition, a more dynamic load model could be implemented to provide a more realistic simulation of actual power system behavior.

In the area of control theory, several items could be explored. First, investigation of more analytical approaches to determining the time response characteristics of the FACTS device in high order power system models could be valuable. Also, in order for a control system to work properly and consistently under realistic and variable conditions, the robustness of the controller must be evaluated. Development of a robust FACTS control system would be a crucial step in leading to practical implementations of these installations for dynamic stability control.

## REFERENCES

- [1] J. D. Glover and M. Sarma. *Power System Analysis and Design*. Boston: PWS-KENT Publishing Company, 1989, pp. 428-462.
- [2] G. Jancke, N. Fahlen, and O. Nerf. "Series Capacitors in Power Systems," *IEEE Transactions on Power Apparatus and Systems* Vol. PAS-94, May/June 1975, pp. 915-919.
- [3] N. G. Hingorani. "Flexible AC Transmission," *IEEE Spectrum* Vol. 30, April 1993, pp. 40-45.
- [4] P. L. Dandeno. "Overview of Steady-State (Small Signal) Stability In Bulk Electricity Systems," *Electrical Power and Energy Systems*, Vol. 4, No. 4, October 1982.
- [5] W. D. Stevenson, Jr. *Elements of Power System Analysis*, Fourth Edition, New York: McGraw-Hill, Inc., 1982, pp. 373-420.
- [6] R. T. Stefani, C. J. Savant, Jr., B. Shahian, and G. H. Hostetter. *Design of Feedback Control Systems*, Third Edition, New York: Saunders College Publishing, 1994, pp. 502-569.
- [7] R. Mihalic, P. Zunko, I. Papic and D. Povh. "Improvement of Transient Stability By Insertion of FACTS Devices," Paper APT 172-10-29, IEEE/NTUA Athens Power Tech Conference, September, 1993.
- [8] A. Roman-Messina and B. J. Cory. "Enhancement of Dynamic Stability By Coordinated Control of Static VAR Compensators," *Electrical Power and Energy Systems*, Vol. 15, No. 2, 1993, pp. 85-93.
- [9] D. L. Goldsworthy. "A Linearized Model for MOV-Protected Series Capacitors," *IEEE Transactions on Power Systems*, Vol. PWRS-2, No. 4, November, 1987, pp. 953-958.

- [10] B. Pilvelait, T. H. Ortmeyer, D. Maratukulam. "Advanced Series Compensation For Transmission Systems Using A Switched Capacitor Module," *IEEE Transactions on Power Delivery*, Vol. 8, No. 2, April 1993, pp. 584-590.
- [11] R. M. Maliszewski, B. M. Pasternack, H. N. Scherer Jr., M. Chamia, H. Frank, and L. Paulsson. "Power Flow Control In A Highly Integrated Transmission Network," CIGRE 1990 Session, Paper 37-303.
- [12] J. D. Mountford, R. J. Koessler, and S. Zelingher. "Practical Applications of FACTS Technology For System Control," Paper APT 216-10-29, IEEE/NTUA Athens Power Tech Conference, September 1993.
- [13] M. La Scala, R. Sbrizzai, F. Torelli and M. Trovato. "Enhancement of Interconnected Power System Stability Using A Control Strategy Involving Static Phase Shifters," *Electrical Power and Energy Systems*, Vol. 15, No. 6, 1993, pp. 227-236.
- [14] P. M. Anderson and A. A. Fouad. *Power System Control and Stability*, New York: IEEE Press, 1994.
- [15] K. R. Padiyar and K. K. Ghosh. "Direct Stability Evaluation of Power Systems With Detailed Generator Models Using Structure-Preserving Energy Functions," *Electrical Power and Energy Systems*, Vol. 11, No. 1, January 1989, pp. 47-56.
- [16] M. A. Pai. *Energy Function Analysis For Power System Stability*, Boston: Kluwer Academic Publishers, 1989.
- [17] IEEE Committee Report. "Computer Representation of Excitation Systems," *IEEE Transactions on Power Apparatus and Systems*, June 1968.
- [18] MATLAB<sup>®</sup> for Windows, Version 4.2c.1. The MathWorks, Inc., Natick, MA, 1994.
- [19] A. G. Phadke. "Synchronized Phasor Measurements in Power Systems," *IEEE Computer Applications in Power*, Vol. 6, No. 2, April 1993, pp. 10-15.
- [20] R. O. Burnett, Jr., M. M. Butts, T. W. Cease, V. Centeno, G. Michel, R. J. Murphy, and A. G. Phadke. "Synchronized Phasor Measurements of a Power System Event," *IEEE Transactions on Power Systems*, Vol. 9, No. 3, August 1994, pp. 1643-1649.
- [21] T. L. Saaty and K. P. Kearns. *Analytical Planning: The Organization of Systems*. New York: Pergamon Press, 1985, pp. 19-62.

## APPENDIX A

### Numeric Coefficient Matrices

#### A.1 Current Coefficient Matrices

		1 Eq1	2 Ed1	3 Eq2	4 Ed2	5 Eq3	6 Ed3	7 delta12	8 delta13
1	Iq1	0.834136	3.012001	-1.101558	-1.023412	-0.801957	-0.915188	1.492073	1.203257
2	Id1	-3.012001	0.834136	1.023412	-1.101558	0.915188	-0.801957	0.231708	0.044179
3	Iq2	1.393549	-0.564643	0.399427	2.772691	0.323263	-1.0206	-1.178059	0.581605
4	Id2	0.564643	1.393549	-2.772691	0.399427	1.0206	0.323263	2.357449	-0.885393
5	Iq3	1.053606	-0.608785	0.069708	-1.068299	0.265545	2.394397	0.7988	-1.441882
6	Id3	0.608785	1.053606	1.068299	0.069708	-2.394397	0.265545	-0.719555	1.832517

**Figure A.1: Current Coefficient Matrix for Uncompensated System**

		1 Eq1	2 Ed1	3 Eq2	4 Ed2	5 Eq3	6 Ed3	7 delta12	8 delta13	9 X45
1	Iq1	0.834136	3.012001	-1.101558	-1.023412	-0.801957	-0.915188	1.492073	1.203257	0.882872
2	Id1	-3.012001	0.834136	1.023412	-1.101558	0.915188	-0.801957	0.231708	0.044179	-0.676396
3	Iq2	1.393549	-0.564643	0.399427	2.772691	0.323263	-1.0206	-1.178059	0.581605	0.34157
4	Id2	0.564643	1.393549	-2.772691	0.399427	1.0206	0.323263	2.357449	-0.885393	0.670046
5	Iq3	1.053606	-0.608785	0.069708	-1.068299	0.265545	2.394397	0.7988	-1.441882	0.103354
6	Id3	0.608785	1.053606	1.068299	0.069708	-2.394397	0.265545	-0.719555	1.832517	0.070593

**Figure A.2: Current Coefficient Matrix for FACTS Compensated System**

#### A.2 State Coefficient Matrices

The coefficients of the A state matrices for both the uncompensated and FACTS compensated test systems are shown on the following two pages.

	1	2	3	4	5	6	7	8	9	10	11	12	13	14	15	16	17	18	19	20
	Eq1	Ed1	Eq2	Ed2	Eq3	Ed3	delta12	delta13	omega1	omega2	omega3	Vr1	Efd1	Va11	Vr2	Ed2	Va2	Vr3	Efd3	Va13
1	Eq1	-0.1402	0.00793	-0.00973	-0.0105	0.0087	-0.00763	0.002203	0.00042	0	0	0	0	0.111607	0	0	0	0	0	0
2	Ed1	0	-2	0	0	0	0	0	0	0	0	0	0	0	0	0	0	0	0	0
3	Eq2	0.07303	0.18023	-0.5253	0.05166	0.132	0.041809	0.304897	-0.1145	0	0	0	0	0	0	0.16667	0	0	0	0
4	Ed2	-1.9398	0.78596	-0.556	-5.7286	-0.45	1.420637	1.639814	-0.8096	0	0	0	0	0	0	0	0	0	0	0
5	Eq3	0.11692	0.20235	0.20517	0.01339	-0.6296	0.050999	-0.13819	0.35194	0	0	0	0	0	0	0	0	0	0.169779	0
6	Ed3	-1.8903	1.09226	-0.1251	1.91671	-0.4764	-5.96261	-1.43318	2.58698	0	0	0	0	0	0	0	0	0	0	0
7	delta12	0	0	0	0	0	0	0	1	-1	0	0	0	0	0	0	0	0	0	0
8	delta13	0	0	0	0	0	0	0	1	0	-1	0	0	0	0	0	0	0	0	0
9	omega1	-12.375	-22.96	9.27819	8.61998	6.75471	7.708438	-12.5674	-10.135	-7.9736	0	0	0	0	0	0	0	0	0	0
10	omega2	-22.01	38.6435	-87.523	-19.057	11.1946	29.61941	70.54712	-29.727	0	-29.452	0	0	0	0	0	0	0	0	0
11	omega3	-26.844	70.4621	38.4204	54.0804	-145.19	-69.5637	-66.5347	140.966	0	-62.623	0	0	0	0	0	0	0	0	0
12	Vr1	-3.6622	-0.0284	-0.2475	0.32608	-0.2262	0.241996	-0.10312	-0.0445	0	0	-4.46429	-2.1271	4.46429	0	0	0	0	0	0
13	Efd1	0	0	0	0	0	0	0	0	0	0	1.945325	0.301556	0	0	0	0	0	0	0
14	Va11	0	0	0	0	0	0	0	0	0	0	0	0.560554	-1.1765	0	0	0	0	0	0
15	Vr2	-1.9311	-0.1188	-3.5605	2.45459	-0.9422	1.004973	0.057661	-0.1832	0	0	0	0	0	-7.5	-0.8029	7.5	0	0	0
16	Ed2	0	0	0	0	0	0	0	0	0	0	0	0	0	1.14943	-1.0263	0	0	0	0
17	Va2	0	0	0	0	0	0	0	0	0	0	0	0	0	0	0.12595	-1.1765	0	0	0
18	Vr3	-4.5326	-0.1396	-2.3178	3.2473	-6.9681	4.564941	-1.11799	0.97048	0	0	0	0	0	0	0	0	-16.667	-2.11765	16.66667
19	Efd3	0	0	0	0	0	0	0	0	0	0	0	0	0	0	0	0	0.6603	-0.58976	0
20	Va13	0	0	0	0	0	0	0	0	0	0	0	0	0	0	0	0	0	0.149481	-1.17647

Figure A.3: Numeric State Matrix Coefficients for Uncompensated Test System

	1	2	3	4	5	6	7	8	9	10	11	12	13	14	15	16	17	18	19	20	21
	Eq1	Ed1	Eq2	Ed2	Eq3	Ed3	delta12	delta13	X45	omega1	omega2	omega3	Vr1	Ed1	Vd1	Vr2	Ed2	Vd2	Vr3	Ed3	Vd3
1	Eq1	-0.1402	0.00793	0.00973	-0.0105	0.0087	-0.00763	0.002203	0.00042	-0.0064	0	0	0	0.11161	0	0	0	0	0	0	0
2	Ed1	-0.0602	-2.2175	0.07943	0.07389	0.0579	0.066077	-0.10773	-0.0869	-0.0637	0	0	0	0	0	0	0	0	0	0	0
3	Eq2	0.07303	0.18023	-0.5253	0.05166	0.132	0.041809	0.304897	-0.1145	0.08666	0	0	0	0	0	0	0.16667	0	0	0	0
4	Ed2	-1.9398	0.78596	-0.556	-5.7286	-0.45	1.420637	1.639814	-0.8096	-0.4755	0	0	0	0	0	0	0	0	0	0	0
5	Eq3	0.11692	0.20235	0.20517	0.01339	-0.6296	0.050999	-0.13819	0.35194	0.01356	0	0	0	0	0	0	0	0	0	0.169779	0
6	Ed3	-1.8903	1.09226	-0.1251	1.91671	-0.4764	-5.96261	-1.43318	2.58698	-0.1854	0	0	0	0	0	0	0	0	0	0	0
7	delta12	0	0	0	0	0	0	0	0	1	-1	0	0	0	0	0	0	0	0	0	0
8	delta13	0	0	0	0	0	0	0	0	1	0	-1	0	0	0	0	0	0	0	0	0
9	X45	0	0	0	0	0	0	0	0	-0.02	-1	1	0	0	0	0	0	0	0	0	0
10	omega1	-12.375	-22.96	9.27819	8.61998	6.75471	7.708438	-12.5674	-10.135	-7.4362	-7.9736	0	0	0	0	0	0	0	0	0	0
11	omega2	-22.01	38.6435	-87.523	-19.057	11.1946	29.61941	70.54712	-29.727	4.34645	0	-29.452	0	0	0	0	0	0	0	0	0
12	omega3	-26.844	70.4621	38.4204	54.0804	-145.19	-69.5637	-66.5347	140.966	-2.2081	0	0	-62.6231	0	0	0	0	0	0	0	0
13	Vr1	-3.6622	-0.0284	-0.2475	0.32608	-0.2262	0.241996	-0.10312	-0.0445	0.15936	0	0	-4.46429	-2.1271	4.46429	0	0	0	0	0	0
14	Ed1	0	0	0	0	0	0	0	0	0	0	0	1.945525	0.30156	0	0	0	0	0	0	0
15	Vd1	0	0	0	0	0	0	0	0	0	0	0	0	0.56055	-1.1765	0	0	0	0	0	0
16	Vr2	-1.9311	-0.1188	-3.5605	2.45459	-0.9422	1.004973	0.057661	-0.1832	-0.7687	0	0	0	0	0	-7.5	-0.8029	7.5	0	0	0
17	Ed2	0	0	0	0	0	0	0	0	0	0	0	0	0	0	1.14943	-1.0263	0	0	0	0
18	Vd2	0	0	0	0	0	0	0	0	0	0	0	0	0	0	0	0.12595	-1.1765	0	0	0
19	Vr3	-4.5326	-0.1396	-2.3178	3.2473	-6.9681	4.564941	-1.11799	0.97048	-0.466	0	0	0	0	0	0	0	0	-16.6667	-2.11765	16.6667
20	Ed3	0	0	0	0	0	0	0	0	0	0	0	0	0	0	0	0	0	0.660502	-0.58976	0
21	Vd3	0	0	0	0	0	0	0	0	0	0	0	0	0	0	0	0	0	0	0.149481	-1.17647

Figure A.4: Numeric State Matrix Coefficients for FACTS Compensated Test System

## APPENDIX B

### Source Code Listings

#### B.1 MATLAB Data Files

```
%*****
% LINEDATA.M
%
% MATLAB Script file that contains initial line impedance data for
% Anderson & Fouad's Nine Bus, Three Machine Power System
%
% Mark A. Smith
% November 10, 1994
%*****
%
Z=zeros(9,9);
R=zeros(9,9);
X=zeros(9,9);
Y=zeros(9,9);
Ybus=zeros(9,9);
%
% Initial System Impedance Data
R(1,4)=0;
X(1,4)=0.1184;
R(2,7)=0;
X(2,7)=0.1823;
R(3,9)=0;
X(3,9)=0.2399;
R(4,5)=0.0100;
X(4,5)=0.0850;
R(4,6)=0.0170;
X(4,6)=0.0920;
R(5,7)=0.0320;
X(5,7)=0.1610;
R(6,9)=0.0390;
X(6,9)=0.1700;
R(7,8)=0.0085;
X(7,8)=0.0720;
R(8,9)=0.0119;
X(8,9)=0.1008;
%
%
% End of LINEDATA.M
%*****
```



```

%*****
% GENDATA.M
%
% MATLAB Script file that contains two-axis generator model data,
% excitation system data, and calculates initial conditions for generators
% in Anderson & Fouad's Nine Bus, Three Machine Power System
%
% Mark A. Smith
% November 10, 1994
%*****
%
%*****
%           Power System Data for Three-Machine, Nine Bus System
%           Source:      Power System Control and Stability
%                       by Paul M. Anderson & A. A. Fouad
%
%
%           Unit 1           Unit 2           Unit 3
%*****
%Unit Type:           Hydro           Fossil           Fossil
%Unit MVA:            247.5 (250)      192             128 (125)
%Unit kV:             16.5 (18)        18             13.8 (15.5)
%Excitation System Type      A           A           A
%Excitation System Name      ASEA        GE NA101      GE NA101
%*****
VRmax      =      [      1,              1,              1      ];
VRmin      =      [     -1,             -1,             -1      ];
Vref       =      [      1,              1,              1      ];
xd         =      [  0.1460,            0.8958,            1.3125  ];
xdprime    =      [  0.0608,            0.1198,            0.1813  ];
xq         =      [  0.0969,            0.8645,            1.2578  ];
xqprime    =      [  0.0969,            0.1969,            0.25     ];
Td0        =      [  8.96,              6.000,            5.89     ];
Tq0        =      [  0.500,            0.5350,            0.6000  ];
Pm         =      [  71.6,             163.0,            85.0     ];
H          =      [  23.64,            6.4,             3.01     ];
Pgen       =      [  0.716,            1.63,             0.85     ];
Qgen       =      [  0.270,            0.067,            -0.109  ];
Vt0        =      [  1.04,            1.025,            1.025  ];
Beta       =      [  0.0,              9.3*2*PI/360,      4.7*2*PI/360  ];
D          =      [      1,              1,              1      ];
%*****
% Excitation System Data (Adjusted to Make System Marginally Stable)
Ka         =      [  25,              15,              20      ];
Ke         =      [ -1.155,           -0.1071,           -0.1071  ];
Kf         =      [  0.405,            0.091,            0.108  ];
Ta         =      [  5.6,              2.0,             1.2     ];
Te         =      [  0.5140,           0.8700,           1.5140  ];
Tf         =      [  0.85,            0.85,             0.85  ];
%*****
%
% Calculate Generator Initial Conditions
for k=1:3,
    Ir(k)      =  Pgen(k)/Vt0(k);
    Ix(k)      = -Qgen(k)/Vt0(k);
    phi(k)     = -atan(-Qgen(k)/Pgen(k));
    delta_0(k) = atan((xq(k)*Ir(k))/(Vt0(k)-xq(k)*Ix(k)))+Beta(k);
    Vq0(k)     = real(Vt0(k)*exp(i*(Beta(k)-delta_0(k))));
    Vd0(k)     = imag(Vt0(k)*exp(i*(Beta(k)-delta_0(k))));
    Iq0(k)     = real(abs(Ir(k)+i*Ix(k))*exp(-i*(delta_0(k)-Beta(k)+phi(k))));

```

```

    Id0(k)      = imag(abs(Ir(k)+i*Ix(k))*exp(-i*(delta_0(k)-Beta(k)+phi(k))));
    Eq0(k)      = Vq0(k)-xdprime(k)*Id0(k);
    Ed0(k)      = Vd0(k)+xqprime(k)*Iq0(k);
    E(k)        = Eq0(k)+i*Ed0(k);
end;
%
% Calculate Initial Difference in Rotor Angles
delta12_0=delta_0(1)-delta_0(2);
delta13_0=delta_0(1)-delta_0(3);
delta23_0=delta_0(2)-delta_0(3);
%
%
% End of GENDATA.M
%*****

%*****
% REDUCE.M
%
% MATLAB script file used to calculate the reduced admittance matrix Yred
% for Anderson & Fouad's Nine Bus, Three Machine Power System
%
% Mark A. Smith
% November 10, 1994
%*****
%
% Load Bus Power Data (in pu on 100 MVA base)
SLoadA=1.25+i*0.50; % Original Data
SLoadB=0.90+i*0.30; % Original Data
SLoadC=1.00+i*0.35; % Original Data
SLoadC=SLoadC+i*0.35;
%
% Load Bus Voltages (pu)
VLoadA=0.996;
VLoadB=1.013;
VLoadC=1.016;
%
% Shunt Susceptance Data
LineB(7,8)=0.0745;
LineB(7,5)=0.1530;
LineB(8,9)=0.1045;
LineB(9,6)=0.1790;
LineB(6,4)=0.0790;
LineB(4,5)=0.0880;
%
% Convert Loads to Admittances
YLoadA=real(SLoadA)/((VLoadA)^2)-i*imag(SLoadA)/((VLoadA)^2);
YLoadB=real(SLoadB)/((VLoadB)^2)-i*imag(SLoadB)/((VLoadB)^2);
YLoadC=real(SLoadC)/((VLoadC)^2)-i*imag(SLoadC)/((VLoadC)^2);
%
% Total Shunt Admittance Data (Calculated from Raw Data)
Y0(5)=YLoadA+i*(LineB(7,5)+LineB(4,5));
Y0(6)=YLoadB+i*(LineB(9,6)+LineB(6,4));
Y0(8)=YLoadC+i*(LineB(7,8)+LineB(8,9));
Y0(4)=i*(LineB(6,4)+LineB(4,5));
Y0(7)=i*(LineB(7,8)+LineB(7,5));
Y0(9)=i*(LineB(8,9)+LineB(9,6));
%
% Compute Z and Y matrices
for k=1:9,
    for l=1:9,
        Z(k,l)=R(k,l)+i*X(k,l);

```

```

        if Z(k,l) ~= 0+j*0
            Y(k,l)=inv(Z(k,l));
        end;
    end;
end;
%
% Compute Ybus matrix
for k=1:9,
    for l=1:9,
        % Compute diagonal terms
        Ybus(k,k)=Ybus(k,k)+Y(k,l);
        if Y(k,l) ~= Y(l,k)
            Ybus(k,k)=Ybus(k,k)+Y(l,k);
        end;
        % Compute off-diagonal terms
        if k~=l
            Ybus(k,l)=Ybus(k,l)-Y(k,l)-Y(l,k);
        end;
    end;
    % Add in shunt admittance data to diagonal terms
    Ybus(k,k)=Ybus(k,k)+Y0(k);
end;
%
% Partition Ybus matrix
Ynn=Ybus(1:3,1:3);
Ynr=Ybus(1:3,4:9);
Yrn=Ybus(4:9,1:3);
Yrr=Ybus(4:9,4:9);
%
% Compute Reduced Network Admittance Matrix
Yred=Ynn-Ynr*inv(Yrr)*Yrn;
%
%
% End of REDUCE.M
%*****

```

## B.2 Uncompensated System Simulations

```

%*****
% RUN20.M
%
% Main MATLAB script file for the uncompensated version of the test system.
% Calls all other script files necessary to calculate the state matrix for
% Anderson & Fouad's Nine Bus, Three Machine Power System
%
% Mark A. Smith
% November 10, 1994
%*****
%
PI =3.141592654;
OMEGA_R= 2*PI*60;
%
% Initialize all impedance and admittance matrices
Z=zeros(9,9);
R=zeros(9,9);
X=zeros(9,9);
Y=zeros(9,9);
Ybus=zeros(9,9);
%
% Load Generator and Excitation System Data

```

```

gendata;
%
% Load Initial System Impedance Data
linedata;
%
% Value for Simulation of Mechanical Compensation (50%)
% X(4,5)=0.0425;
%
% Calculate Reduced Network Parameters
reduce;
%
% Calculate A matrix (20 x 20 case)
acalc20;
%
% Format I matrix and print to a text file for later printing
fid=fopen('Imat20.txt', 'wt');
for k=1:6,
    for l=1:8,
        fprintf(fid,'%f\t',I(k,l));
    end;
    fprintf(fid,'\n');
end;
fclose(fid);
%
% Format A matrix and print to a text file for later printing
fid=fopen('Amat20.txt', 'wt');
for k=1:20,
    for l=1:20,
        fprintf(fid,'%f\t',A(k,l));
    end;
    fprintf(fid,'\n');
end;
fclose(fid);
%
% Format A matrix and print to file for use in C programs
fid=fopen('Amat20.c', 'wt');
fprintf(fid, '/*Amat20.c: Coefficients of Stable A matrix from runle.m*/\n');
for i=1:20,
    for j=1:20,
        dummy=sprintf('%f\n',A(i,j));
        fprintf(fid,dummy);
    end;
end;
fclose(fid);
%
%
% Set Pre-Disturbance Forcing Function Constants
for k=1:20,
    B1(k)=0;
end;
%
% Format Pre-Disturbance B matrix coefficients for use in DIFFEQ20.C
fid=fopen('Bmat20_1.c', 'wt');
fprintf(fid, '/*B1 matrix coefficients (20) from MATLAB script run20.m*/\n');
for k=1:20,
    fprintf(fid,'%f\n',B1(k));
end;
fclose(fid);
%
% Set Post-Disturbance Forcing Function Constants
for k=1:20,
    B2(k)=0;
end;

```

```

B2(2)=(OMEGA_R)/(2*H(1))*0.02;
%
% Format Disturbance B matrix coefficients for use in DIFFEQ20.C
fid=fopen('Bmat20_2.c', 'wt');
fprintf(fid, '/*B2 matrix coefficients (20) from MATLAB script run20.m*/\n');
for k=1:20,
    fprintf(fid, '%f\n', B2(k));
end;
fclose(fid);
%
% Set Initial Conditions to Zero
for k=1:20,
    x0(k)=0;
end;
%
% Format Initial Conditions and print to file for use in C programs
fid=fopen('Initcond.c', 'wt');
fprintf(fid, '/*Initial Conditions from MATLAB script runld.m*/\n');
for k=1:20,
    fprintf(fid, '%f\n', x0(k));
end;
fclose(fid);
%
%
% End of RUN20.M
%*****

%*****
% ACALC20.M
%
% MATLAB Script file that calculates state and current coefficient matrices
% for the uncompensated version of Anderson & Fouad's Nine Bus, Three
% Machine Power System
%
% Mark A. Smith
% November 10, 1994
%*****
%
%
% Form Transformation Matrices T and M
clear i;
T=[exp(i*delta_0(1)) 0 0; 0 exp(i*delta_0(2)) 0; 0 0 (i*delta_0(3))];
M=inv(T)*Yred*T;
M(1,1)=Yred(1,1);
M(1,2)=Yred(1,2)*exp(-i*delta12_0);
M(1,3)=Yred(1,3)*exp(-i*delta13_0);
M(2,1)=Yred(2,1)*exp(i*delta12_0);
M(2,2)=Yred(2,2);
M(2,3)=Yred(2,3)*exp(-i*delta23_0);
M(3,1)=Yred(3,1)*exp(i*delta13_0);
M(3,2)=Yred(3,2)*exp(i*delta23_0);
M(3,3)=Yred(3,3);
%
%*****
% Calculate the current coefficient matrix for the uncompensated system
%*****
%
I=M;
I(1,4)=-i*(M(1,2)*E(2));
I(1,5)=-i*(M(1,3)*E(3));
I(2,4)=-i*(-(M(2,1))*E(1)-M(2,3)*E(3));
I(2,5)=-i*(M(2,3)*E(3));

```

```

I(3,4)=-i*(M(3,2)*E(2));
I(3,5)=-i*((-M(3,1)*E(1)-M(3,2)*E(2)));
%
% Separate Real and Imaginary Parts of Currents
%
for k=1:3,
    for l=1:3,
        Inew(2*k-1,2*l-1)=real(I(k,l));
        Inew(2*k-1,2*l)=-imag(I(k,l));
        Inew(2*k,2*l-1)=imag(I(k,l));
        Inew(2*k,2*l)=real(I(k,l));
    end;
    for l=7:8,
        Inew(2*k-1,l)=real(I(k,l-3));
        Inew(2*k,l)=imag(I(k,l-3));
    end;
end;
I=Inew;
%
% Save I matrix for use in Power Calculations
save I1.mat I;
%
%*****
% Calculate the state matrix A for the uncompensated system
%*****
%
% Two-Axis Model Coefficients
%
% Unit 1
A(1,:)=(1/Td0(1))*(xd(1)-xdprime(1))*I(2,:);
A(1,1)=A(1,1)-(1/Td0(1));
A(2,:)=(1/Tq0(1))*(-1)*(xq(1)-xqprime(1))*I(1,:);
A(2,2)=A(2,2)-(1/Tq0(1));
A(9,:)=(OMEGA_R/(2*H(1)))*(-Eq0(1))*I(1,:);
A(9,:)=A(9,:)+(OMEGA_R/(2*H(1)))*(-Ed0(1))*I(2,:);
A(9,1)=A(9,1)-(OMEGA_R/(2*H(1)))*Iq0(1);
A(9,2)=A(9,2)-(OMEGA_R/(2*H(1)))*Id0(1);
%
% Unit 2
A(3,:)=(1/Td0(2))*(xd(2)-xdprime(2))*I(4,:);
A(3,3)=A(3,3)-(1/Td0(2));
A(4,:)=(1/Tq0(2))*(-1)*(xq(2)-xqprime(2))*I(3,:);
A(4,4)=A(4,4)-(1/Tq0(2));
A(10,:)=(OMEGA_R/(2*H(2)))*(-Eq0(2))*I(3,:);
A(10,:)=A(10,:)+(OMEGA_R/(2*H(2)))*(-Ed0(2))*I(4,:);
A(10,3)=A(10,3)-(OMEGA_R/(2*H(2)))*Iq0(2);
A(10,4)=A(10,4)-(OMEGA_R/(2*H(2)))*Id0(2);
%
% Unit 3
A(5,:)=(1/Td0(3))*(xd(3)-xdprime(3))*I(6,:);
A(5,5)=A(5,5)-(1/Td0(3));
A(6,:)=(1/Tq0(3))*(-1)*(xq(3)-xqprime(3))*I(5,:);
A(6,6)=A(6,6)-(1/Tq0(3));
A(11,:)=(OMEGA_R/(2*H(3)))*(-Eq0(3))*I(5,:);
A(11,:)=A(11,:)+(OMEGA_R/(2*H(3)))*(-Ed0(3))*I(6,:);
A(11,5)=A(11,5)-(OMEGA_R/(2*H(3)))*Iq0(3);
A(11,6)=A(11,6)-(OMEGA_R/(2*H(3)))*Id0(3);
%
%
% Rotor Angle Coefficients
%
A(7,9)=1;
A(7,10)=-1;

```

```

A(8,9)=1;
A(8,11)=-1;
%
%
% Damping Coefficients
%
A(9,9)=-D(1)*OMEGA_R/(2*H(1));
A(10,10)=-D(2)*OMEGA_R/(2*H(2));
A(11,11)=-D(3)*OMEGA_R/(2*H(3));
%
%
% Excitation System Coefficients
%
% Unit 1
%
unit=1;
for k=1:8,
    A(12,k) = -(Ka(unit)/Ta(unit))*(-1*(Vd0(unit)/Vt0(unit))*xqprime(unit)*...
        I(1,k)+(Vq0(unit)/Vt0(unit))*xdprime(unit)*I(2,k));
end;
% Add additional coefficient components due to Eq and Ed
A(12,1)=A(12,1)-(Ka(unit)/Ta(unit))*(Vq0(unit)/Vt0(unit));
A(12,2)=A(12,2)-(Ka(unit)/Ta(unit))*(Vd0(unit)/Vt0(unit));
% Calculate Remaining Coefficients for this unit
A(1,13)=1/Td0(1);
A(12,12)=-Ka(unit)/Ta(unit);
A(12,13)=-Ka(unit)*Kf(unit)/(Ta(unit)*Tf(unit));
A(12,14)=Ka(unit)/Ta(unit);
A(13,12)=1/Te(unit);
A(13,13)=-(1+Ke(unit))/Te(unit);
A(14,13)=Kf(unit)/Tf(unit)/Tf(unit);
A(14,14)=-1/Tf(unit);
%
% Unit 2
%
unit=2;
% Calculate Coefficients due to Vt
for k=1:8,
    A(15,k)=- (Ka(unit)/Ta(unit))*(-1*(Vd0(unit)/Vt0(unit))*xqprime(unit)*I(3,k)+...
        (Vq0(unit)/Vt0(unit))*xdprime(unit)*I(4,k));
end;
% Add additional coefficient components due to Eq and Ed
A(15,3)=A(15,3)-(Ka(unit)/Ta(unit))*(Vq0(unit)/Vt0(unit));
A(15,4)=A(15,4)-(Ka(unit)/Ta(unit))*(Vd0(unit)/Vt0(unit));
% Calculate Remaining Coefficients for this unit
A(3,16)=1/Td0(2);
A(15,15)=-Ka(unit)/Ta(unit);
A(15,16)=-Ka(unit)*Kf(unit)/(Ta(unit)*Tf(unit));
A(15,17)=Ka(unit)/Ta(unit);
A(16,15)=1/Te(unit);
A(16,16)=-(1+Ke(unit))/Te(unit);
A(17,16)=Kf(unit)/Tf(unit)/Tf(unit);
A(17,17)=-1/Tf(unit);
%
% Unit 3
%
unit=3;
% Calculate Coefficients due to Vt
for k=1:8,
    A(18,k)=- (Ka(unit)/Ta(unit))*(-1*(Vd0(unit)/Vt0(unit))*xqprime(unit)*I(5,k)+...
        (Vq0(unit)/Vt0(unit))*xdprime(unit)*I(6,k));
end;
% Add additional coefficient components due to Eq and Ed

```

```

A(18,5)=A(18,5)-(Ka(unit)/Ta(unit))*(Vq0(unit)/Vt0(unit));
A(18,6)=A(18,6)-(Ka(unit)/Ta(unit))*(Vd0(unit)/Vt0(unit));
% Calculate Remaining Coefficients for this unit
A(5,19)=(1/Td0(3));
A(18,18)=-Ka(unit)/Ta(unit);
A(18,19)=-Ka(unit)*Kf(unit)/(Ta(unit)*Tf(unit));
A(18,20)=Ka(unit)/Ta(unit);
A(19,18)=1/Te(unit);
A(19,19)=-(1+Ke(unit))/Te(unit);
A(20,19)=Kf(unit)/Tf(unit)/Tf(unit);
A(20,20)=-1/Tf(unit);
%
%
% End of ACALC20.M
%*****

//*****
// DIFFEQ20.C
//
// C Program used to solve differential equations represented in the state
// matrix calculated by the MATLAB script file RUN20.M. Resulting solution
// is for the uncompensated version of Anderson & Fouad's Nine Bus,
// Three Machine Power System
//
// Compiled using Borland C++ Compiler version 3.1 in conjunction with
// Phar Lap's DOS Extender version 2.1
//
// Mark A. Smith
// November 10, 1994
//*****

#include <stdlib.h>
#include <stdio.h>
#include <math.h>
#include <string.h>

#define LDCHANGE 10
#define LOOPS 80000
#define DT 0.005
#define SKIP 500
#define ASIZE LOOPS/SKIP+1

/* Define Functions */
void c_to_mat(float huge var[ASIZE][22], char *varname, char *filename);
void ReadAmat(char *filename, float var[22][22]);

/* Define Global Variable */
static float huge x[ASIZE][22];
float xnew[22];
float xold[22];
float A[22][22];
float B1[22];
float B2[22];
FILE *fp;

void main(int argc, char *argv[])
{
    int count, index, i, j;
    unsigned long int iter;
    char dummy[80];

```



```

if(argc<2) argv[1]="";

/* Read in Initial Conditions for state variables */
printf("Reading initial conditions for state variables...\n\n");
if((fp = fopen("initcond.c", "rt"))==NULL)
{
    printf("Cannot open %s\n", "initcond.c");
    exit(1);
}
/* Skip over file header */
fgets(dummy, 79, fp);
printf("%s\n\n", dummy);
for(i=1; i<=20; i++)
{
    fgets(dummy, 79, fp);
    xold[i]=atof(dummy);
    //printf("xold[%d]=%f\n", i, xold[i]);
}
fclose(fp);

/* Read in B1 matrix coefficients */
printf("Reading coefficients for B matrix...\n\n");
if((fp = fopen("bmat20_1.c", "rt"))==NULL)
{
    printf("Cannot open %s\n", "bmat20_1.c");
    exit(1);
}
/* Skip over file header */
fgets(dummy, 79, fp);
for(i=1; i<=20; i++)
{
    fgets(dummy, 79, fp);
    B1[i]=atof(dummy);
}
fclose(fp);

/* Read in B2 matrix coefficients */
printf("Reading coefficients for B matrix...\n\n");
if((fp = fopen("bmat20_2.c", "rt"))==NULL)
{
    printf("Cannot open %s\n", "bmat20_2.c");
    exit(1);
}
/* Skip over file header */
fgets(dummy, 79, fp);
for(i=1; i<=20; i++)
{
    fgets(dummy, 79, fp);
    B2[i]=atof(dummy);
}
fclose(fp);

/* Read in A matrix coefficients */
ReadAmat("amat20.c", A);

count=SKIP;
index=0;
printf("Solving Differential Equations...\n\n");
iter=1;

/* Set Initial Conditions */
for(j=1; j<=20; j++)

```

```

{
    x[1][j]=xold[j];
}

/* Start Main Loop for Solving Differential Equations Using Euler's Method */
while(iter<LOOPS)
{
    for(j=1;j<=20;j++)
    {
        if((iter*DT) < LDCHANGE)
        {
            xnew[j] = (DT)*(A[j][ 1]*xold[ 1]+A[j][ 2]*xold[2]+
                A[j][ 3]*xold[ 3]+A[j][ 4]*xold[4]+
                A[j][ 5]*xold[ 5]+A[j][ 6]*xold[6]+
                A[j][ 7]*xold[ 7]+A[j][ 8]*xold[8]+
                A[j][ 9]*xold[ 9]+A[j][10]*xold[10]+
                A[j][11]*xold[11]+A[j][12]*xold[12]+
                A[j][13]*xold[13]+A[j][14]*xold[14]+
                A[j][15]*xold[15]+A[j][16]*xold[16]+
                A[j][17]*xold[17]+A[j][18]*xold[18]+
                A[j][19]*xold[19]+A[j][20]*xold[20]+
                B1[j])*xold[j];
        }
        if((iter*DT) >= LDCHANGE )
        {
            xnew[j] = (DT)*(A[j][ 1]*xold[ 1]+A[j][ 2]*xold[2]+
                A[j][ 3]*xold[ 3]+A[j][ 4]*xold[4]+
                A[j][ 5]*xold[ 5]+A[j][ 6]*xold[6]+
                A[j][ 7]*xold[ 7]+A[j][ 8]*xold[8]+
                A[j][ 9]*xold[ 9]+A[j][10]*xold[10]+
                A[j][11]*xold[11]+A[j][12]*xold[12]+
                A[j][13]*xold[13]+A[j][14]*xold[14]+
                A[j][15]*xold[15]+A[j][16]*xold[16]+
                A[j][17]*xold[17]+A[j][18]*xold[18]+
                A[j][19]*xold[19]+A[j][20]*xold[20]+
                B2[j])*xold[j];
        }
    }
    /* Compress Data and Store in New Variable */
    if(count==SKIP)
    {
        for(j=1;j<=20;j++)
        {
            x[index][j]=xnew[j];
        }
        count=0;
        index++;
    }

    /* Set values for next iteration */
    for(j=1;j<=20;j++)
    {
        xold[j]=xnew[j];
    }
    count++;
    iter++;
}

/* Repeat last point to avoid reset to zero */
for(j=1;j<=20;j++)
{
    x[index][j]=x[index-1][j];
}

```

```

    }

    /* If "-mat" option specified, convert results to MATLAB format */
    if(strcmp(argv[1], "-mat") == 0)
    {
        c_to_mat(x, "x", "xmat.m");
    }
}

void ReadAmat(char *filename, float matrix[22][22])
{
    int i,j;
    char dummy[80];

    /* Read in A matrix coefficients */
    printf("Reading coefficients for A matrix...\n\n");
    if((fp = fopen(filename, "rt"))==NULL)
    {
        printf("Cannot open %s\n", filename);
        exit(1);
    }
    /* Skip over file header */
    fgets(dummy, 79, fp);
    for(i=1; i<=20; i++)
    {
        for(j=1; j<=20; j++)
        {
            fgets(dummy, 79, fp);
            matrix[i][j]=atof(dummy);
        }
    }
    fclose(fp);
}

void c_to_mat(float huge var[ASIZE][22], char *varname, char *filename)
{
    int i,j;

    printf("Converting results to MATLAB format...\n\n");

    if((fp = fopen(filename, "w"))==NULL)
    {
        printf("Cannot open %s\n", filename);
        exit(1);
    }
    fprintf(fp, "time = [");

    for(i=0; i<ASIZE-1; i++)
    {
        fprintf(fp, "%f\n", (DT)*SKIP*i);
    }
    fprintf(fp, "%f ];\n\n", (DT)*SKIP*(ASIZE-1));

    fprintf(fp, "%s = [", varname);

    for(i=0; i<ASIZE-1; i++)
    {
        for(j=1; j<20; j++)
        {
            fprintf(fp, "%f, ", var[i][j]);

```

```

    }
    fprintf(fp,"%f;\n",var[i][20]);
}
for(j=1;j<20;j++)
{
    fprintf(fp,"%f, ",var[ASIZE-1][j]);
}
fprintf(fp,"%f ];\n\n", var[ASIZE-1][20]);

fclose(fp);
}

// End of DIFFEQ20.C
//*****

%*****
% POWER20.M
%
% MATLAB script file used for calculating incremental electrical power for
% each generator in the uncompensated version of Anderson & Fouad's
% Nine Bus, Three Machine Power System
%
% Mark A. Smith
% November 10, 1994
%*****
%
clear;
%
% Load in Generator Data
gendata;
%
% Load in Results from DIFFEQ20.C
xmat;
%
% Define times at which events occur
DT=0.005;
SKIP=500;
LDCHANGE=10/(SKIP*DT)+1;
ENDTIME =400/(SKIP*DT)+1;
%
% Load Pre-event Current Coefficient Matrix
load I1.mat;
%
% Initialize Current Variables
Id1=0;
Iq1=0;
Id2=0;
Iq2=0;
Id3=0;
Iq3=0;
%
% Compute Incremental Current Vectors
for k=1:8,
    Id1=Id1+I(2,k)*x(1:LDCHANGE,k);
    Iq1=Iq1+I(1,k)*x(1:LDCHANGE,k);
    Id2=Id2+I(4,k)*x(1:LDCHANGE,k);
    Iq2=Iq2+I(3,k)*x(1:LDCHANGE,k);
    Id3=Id3+I(6,k)*x(1:LDCHANGE,k);
    Iq3=Iq3+I(5,k)*x(1:LDCHANGE,k);
end;
%
```

```

% Compute Pre-Disturbance Incremental Power for each Unit
Pe1(1:LDCHANGE)=(Iq0(1)*x(1:LDCHANGE,1)+Eq0(1)*Iq1(:))+...
    (Ed0(1)*Id1(:)+Id0(1)*x(1:LDCHANGE,2));
Pe2(1:LDCHANGE)=(Iq0(2)*x(1:LDCHANGE,3)+Eq0(2)*Iq2(:))+...
    (Ed0(2)*Id2(:)+Id0(2)*x(1:LDCHANGE,4));
Pe3(1:LDCHANGE)=(Iq0(3)*x(1:LDCHANGE,5)+Eq0(3)*Iq3(:))+...
    (Ed0(3)*Id3(:)+Id0(3)*x(1:LDCHANGE,6));

%
% Load Event Current Coefficient Matrix
load I2.mat;
%
% Initialize Current Variables
Id1=0;
Iq1=0;
Id2=0;
Iq2=0;
Id3=0;
Iq3=0;
%
% Compute Incremental Current Vectors
for k=1:8,
    Id1=Id1+I(2,k)*x(LDCHANGE+1:ENDTIME,k);
    Iq1=Iq1+I(1,k)*x(LDCHANGE+1:ENDTIME,k);
    Id2=Id2+I(4,k)*x(LDCHANGE+1:ENDTIME,k);
    Iq2=Iq2+I(3,k)*x(LDCHANGE+1:ENDTIME,k);
    Id3=Id3+I(6,k)*x(LDCHANGE+1:ENDTIME,k);
    Iq3=Iq3+I(5,k)*x(LDCHANGE+1:ENDTIME,k);
end;
%
% Compute Post-Disturbance Incremental Power for each Unit
Pe1(LDCHANGE+1:ENDTIME)=(Iq0(1)*x(LDCHANGE+1:ENDTIME,1)+Eq0(1)*Iq1(:))+...
    (Ed0(1)*Id1(:)+Id0(1)*x(LDCHANGE+1:ENDTIME,2));
Pe2(LDCHANGE+1:ENDTIME)=(Iq0(2)*x(LDCHANGE+1:ENDTIME,3)+Eq0(2)*Iq2(:))+...
    (Ed0(2)*Id2(:)+Id0(2)*x(LDCHANGE+1:ENDTIME,4));
Pe3(LDCHANGE+1:ENDTIME)=(Iq0(3)*x(LDCHANGE+1:ENDTIME,5)+Eq0(3)*Iq3(:))+...
    (Ed0(3)*Id3(:)+Id0(3)*x(LDCHANGE+1:ENDTIME,6));

%
% Group Resulting Power, Rotor Angle, and Frequency Data
Peltot=Pe1+Pgen(1);
Pe2tot=Pe2+Pgen(2);
Pe3tot=Pe3+Pgen(3);
Pe=[Peltot; Pe2tot; Pe3tot]';
omega=[x(:,9) x(:,10) x(:,11)];
delta=[x(:,7) x(:,8)];
%
%
% End of POWER20.M
%*****

```

### B.3 FACTS Compensated System Simulations

```

%*****
% RUN21.M
%
% Main MATLAB script file for the FACTS compensated test system.
% Calls all other script files necessary to calculate the state matrix for
% Anderson & Fouad's Nine Bus, Three Machine Power System

```

```

%
% Mark A. Smith
% November 8, 1994
%*****
%
PI =3.141592654;
OMEGA_R= 2*PI*60;
%
% Load Generator and Excitation System Data
gendata;
%
% Set FACTS Controller Gain and Time Constant
Kx = -50;
Tx = 50;
%
% Load Initial Line Impedance Data
linedata;
% Calculated Reduce Network Admittance Matrix
reduce;
%
% Load dY/dX values
load c:\thesis\dydxmean.mat;
for k=1:3,
    for l=1:3,
        dY(k,l)=dYmean(3*(k-1)+l);
    end;
end;
alpha=angle(dY);
dYdX=abs(dY);
%
% Calculate A matrix
acalc21;
%
% Format I matrix and print to a text file for later printing
fid=fopen('Imat21.txt', 'wt');
for k=1:6,
    for l=1:9,
        fprintf(fid,'%f\t',I(k,l));
    end;
    fprintf(fid,'\n');
end;
fclose(fid);
%
% Format A matrix and print to a text file
fid=fopen('Amat21.txt', 'wt');
for i=1:21,
    for j=1:21,
        fprintf(fid,'%f\t',A(i,j));
    end;
    fprintf(fid,'\n');
end;
fclose(fid);
%
% Format A matrix and print to file for use in C programs
fid=fopen('Amat21.c', 'wt');
fprintf(fid, '/*Amat21.c: Coefficients of A matrix from run21.m*/\n');
for i=1:21,
    for j=1:21,
        dummy=sprintf('%f\n',A(i,j));
        fprintf(fid,dummy);
    end;
end;
fclose(fid);

```

```

%
% Set Pre-Disturbance forcing function constants
for k=1:21,
    B1(k)=0;
end;
%
% Format Pre-Disturbance B matrix coefficients for use in C programs
fid=fopen('Bmat1.c', 'wt');
fprintf(fid, '/*B1 matrix coefficients for state variables from run21.m*/\n');
for k=1:21,
    fprintf(fid, '%f\n', B1(k));
end;
fclose(fid);
%
% Set Pre-Disturbance forcing function constants
for k=1:21,
    B2(k)=0;
end;
B2(10)=(OMEGA_R)/(2*H(1))*0.02;
%
% Format Post-Disturbance B matrix coefficients for use in C programs
fid=fopen('Bmat2.c', 'wt');
fprintf(fid, '/*B2 matrix coefficients for state variables from run21.m*/\n');
for k=1:21,
    fprintf(fid, '%f\n', B2(k));
end;
fclose(fid);
%
% Set Initial Conditions to Zero
for k=1:21,
    x0(k)=0;
end;
%
% Format Initial Conditions and print to file for use in C programs
fid=fopen('Initcond.c', 'wt');
fprintf(fid, '/*Initial Conditions from MATLAB script run1d.m*/\n');
for k=1:21,
    fprintf(fid, '%f\n', x0(k));
end;
fclose(fid);
%
%
% End of RUN21.M
%*****

%*****
% ACALC21.M
%
% MATLAB Script file that calculates state and current coefficient matrices
% for the FACTS compensated version of Anderson & Fouad's Nine Bus, Three
% Machine Power System
%
% Mark A. Smith
% November 10, 1994
%*****
%
%
% Form Transformation Matrices T and M
%
clear i;
T=[exp(i*delta_0(1)) 0 0; 0 exp(i*delta_0(2)) 0; 0 0 (i*delta_0(3))];
M=inv(T)*Yred*T;
M(1,1)=Yred(1,1);

```

```

M(1,2)=Yred(1,2)*exp(-i*delta12_0);
M(1,3)=Yred(1,3)*exp(-i*delta13_0);
M(2,1)=Yred(2,1)*exp(i*delta12_0);
M(2,2)=Yred(2,2);
M(2,3)=Yred(2,3)*exp(-i*delta23_0);
M(3,1)=Yred(3,1)*exp(i*delta13_0);
M(3,2)=Yred(3,2)*exp(i*delta23_0);
M(3,3)=Yred(3,3);
%
%*****
% Calculate the current coefficient matrix for the FACTS compensated system
%*****
%
I=M;
I(1,4)=-i*(M(1,2)*E(2));
I(1,5)=-i*(M(1,3)*E(3));
I(1,6)= E(1)*dYdX(1,1)*exp(i*alpha(1,1))+...
        E(2)*dYdX(1,2)*exp(i*(alpha(1,2)-delta12_0))+...
        E(3)*dYdX(1,3)*exp(i*(alpha(1,3)-delta13_0));
I(2,4)=-i*(-(M(2,1))*E(1)-M(2,3)*E(3));
I(2,5)=-i*(M(2,3)*E(3));
I(2,6)= E(1)*dYdX(2,1)*exp(i*(alpha(2,1)+delta12_0))+...
        E(2)*dYdX(2,2)*exp(i*alpha(2,2))+...
        E(2)*dYdX(2,3)*exp(i*(alpha(2,3)-delta23_0));
I(3,4)=-i*(M(3,2)*E(2));
I(3,5)=-i*(-(M(3,1))*E(1)-M(3,2)*E(2));
I(3,6)= E(1)*dYdX(3,1)*exp(i*(alpha(3,1)+delta13_0))+...
        E(2)*dYdX(3,2)*exp(i*(alpha(3,2)+delta23_0))+...
        E(3)*dYdX(3,3)*exp(i*alpha(3,3));
%
% Separate Real and Imaginary Parts of Currents
%
for k=1:3,
    for l=1:3,
        Inew(2*k-1,2*l-1)=real(I(k,l));
        Inew(2*k-1,2*l)=-imag(I(k,l));
        Inew(2*k,2*l-1)=imag(I(k,l));
        Inew(2*k,2*l)=real(I(k,l));
    end;
    for l=7:9,
        Inew(2*k-1,l)=real(I(k,l-3));
        Inew(2*k,l)=imag(I(k,l-3));
    end;
end;
I=Inew;
%
% Save I matrix for use in Power Calculations
save I1.mat I;
%
%*****
% Calculate the state matrix A for the FACTS compensated system
%*****
%
% Two-Axis Model Coefficients
%
% Unit 1
A(1,:)=(1/Td0(1))*(xd(1)-xdprime(1))*I(2,:);
A(1,1)=A(1,1)-(1/Td0(1));
A(2,:)=(1/Tq0(1))*(-1)*(xq(1)-xdprime(1))*I(1,:);
A(2,2)=A(2,2)-(1/Tq0(1));
A(10,:)=(OMEGA_R/(2*H(1)))*(-Eq0(1))*I(1,:);
A(10,:)=A(10,:)+(OMEGA_R/(2*H(1)))*(-Ed0(1))*I(2,:);
A(10,1)=A(10,1)-(OMEGA_R/(2*H(1)))*Iq0(1);

```



```

A(10,2)=A(10,2)-(OMEGA_R/(2*H(1)))*Id0(1);
%
% Unit 2
A(3,:)=(1/Td0(2))*(xd(2)-xdprime(2))*I(4,:);
A(3,3)=A(3,3)-(1/Td0(2));
A(4,:)=(1/Tq0(2))*(-1)*(xq(2)-xdprime(2))*I(3,:);
A(4,4)=A(4,4)-(1/Tq0(2));
A(11,:)=(OMEGA_R/(2*H(2)))*(-Eq0(2))*I(3,:);
A(11,:)=A(11,:)+(OMEGA_R/(2*H(2)))*(-Ed0(2))*I(4,:);
A(11,3)=A(11,3)-(OMEGA_R/(2*H(2)))*Iq0(2);
A(11,4)=A(11,4)-(OMEGA_R/(2*H(2)))*Id0(2);
%
% Unit 3
A(5,:)=(1/Td0(3))*(xd(3)-xdprime(3))*I(6,:);
A(5,5)=A(5,5)-(1/Td0(3));
A(6,:)=(1/Tq0(3))*(-1)*(xq(3)-xdprime(3))*I(5,:);
A(6,6)=A(6,6)-(1/Tq0(3));
A(12,:)=(OMEGA_R/(2*H(3)))*(-Eq0(3))*I(5,:);
A(12,:)=A(12,:)+(OMEGA_R/(2*H(3)))*(-Ed0(3))*I(6,:);
A(12,5)=A(12,5)-(OMEGA_R/(2*H(3)))*Iq0(3);
A(12,6)=A(12,6)-(OMEGA_R/(2*H(3)))*Id0(3);
%
%
% Rotor Angle Coefficients
A(7,10)=1;
A(7,11)=-1;
A(8,10)=1;
A(8,12)=-1;
%
%
% Damping Coefficients
A(10,10)=-D(1)*OMEGA_R/(2*H(1));
A(11,11)=-D(2)*OMEGA_R/(2*H(2));
A(12,12)=-D(3)*OMEGA_R/(2*H(3));
%
%
% FACTS Coefficients
A(9,9) = -1/Tx;
A(9,10) = Kx/Tx;
A(9,11) = -Kx/Tx;
%
%
% Excitation System Coefficients
%
% Unit 1
%
unit=1;
for k=1:9,
    A(13,k) = -(Ka(unit)/Ta(unit))*(-1*(Vd0(unit)/Vt0(unit))*xqprime(unit)*...
        I(1,k)+(Vq0(unit)/Vt0(unit))*xdprime(unit)*I(2,k));
end;
% Add additional coefficient components due to Eq and Ed
A(13,1)=A(13,1)-(Ka(unit)/Ta(unit))*(Vq0(unit)/Vt0(unit));
A(13,2)=A(13,2)-(Ka(unit)/Ta(unit))*(Vd0(unit)/Vt0(unit));
% Calculate Remaining Coefficients for this unit
A(1,14)=1/Td0(1);
A(13,13)=-Ka(unit)/Ta(unit);
A(13,14)=-Ka(unit)*Kf(unit)/(Ta(unit)*Tf(unit));
A(13,15)=Ka(unit)/Ta(unit);
A(14,13)=1/Te(unit);
A(14,14)=- (1+Ke(unit))/Te(unit);
A(15,14)=Kf(unit)/Tf(unit)/Tf(unit);
A(15,15)=-1/Tf(unit);

```

```

%
% Unit 2
%
unit=2;
% Calculate Coefficients due to Vt
for k=1:9,
    A(16,k)=- (Ka(unit)/Ta(unit))*(-1*(Vd0(unit)/Vt0(unit))*xqprime(unit)*I(3,k)+...
        (Vq0(unit)/Vt0(unit))*xdprime(unit)*I(4,k));
end;

% Add additional coefficient components due to Eq and Ed
A(16,3)=A(16,3)-(Ka(unit)/Ta(unit))*(Vq0(unit)/Vt0(unit));
A(16,4)=A(16,4)-(Ka(unit)/Ta(unit))*(Vd0(unit)/Vt0(unit));
% Calculate Remaining Coefficients for this unit
A(3,17)=1/Td0(2);
A(16,16)=-Ka(unit)/Ta(unit);
A(16,17)=-Ka(unit)*Kf(unit)/(Ta(unit)*Tf(unit));
A(16,18)=Ka(unit)/Ta(unit);
A(17,16)=1/Te(unit);
A(17,17)=- (1+Ke(unit))/Te(unit);
A(18,17)=Kf(unit)/Tf(unit)/Tf(unit);
A(18,18)=-1/Tf(unit);
%
% Unit 3
%
unit=3;
% Calculate Coefficients due to Vt
for k=1:9,
    A(19,k)=- (Ka(unit)/Ta(unit))*(-1*(Vd0(unit)/Vt0(unit))*xqprime(unit)*I(5,k)+...
        (Vq0(unit)/Vt0(unit))*xdprime(unit)*I(6,k));
end;

% Add additional coefficient components due to Eq and Ed
A(19,5)=A(19,5)-(Ka(unit)/Ta(unit))*(Vq0(unit)/Vt0(unit));
A(19,6)=A(19,6)-(Ka(unit)/Ta(unit))*(Vd0(unit)/Vt0(unit));
% Calculate Remaining Coefficients for this unit
A(5,20)=(1/Td0(3));
A(19,19)=-Ka(unit)/Ta(unit);
A(19,20)=-Ka(unit)*Kf(unit)/(Ta(unit)*Tf(unit));
A(19,21)=Ka(unit)/Ta(unit);
A(20,19)=1/Te(unit);
A(20,20)=- (1+Ke(unit))/Te(unit);
A(21,20)=Kf(unit)/Tf(unit)/Tf(unit);
A(21,21)=-1/Tf(unit);
%
%
% End of ACALC21.M
%*****

//*****
// DIFFEQ21.C
//
// C Program used to solve differential equations represented in the state
// matrix calculated by the MATLAB script file RUN21.M. Resulting solution
// is for the FACTS compensated version of Anderson & Fouad's Nine Bus,
// Three Machine Power System
//
// Compiled using Borland C++ Compiler version 3.1 in conjunction with
// Phar Lap's DOS Extender version 2.1
//
// Mark A. Smith
// November 10, 1994

```

```

//*****

#include <stdlib.h>
#include <stdio.h>
#include <math.h>
#include <string.h>

#define LDCHANGE 10
#define LOOPS 40000
#define DT 0.01
#define SKIP 250
#define ASIZE LOOPS/SKIP+1
#define TOL 0.005

/* Declare Functions */
void c_to_mat(float huge var[ASIZE][22], char *varname, char *filename);
void ReadAmat(char *filename, float var[22][22]);
void findpeak(float huge trace[ASIZE]);

/* Declare Global Variables */
static float huge x[ASIZE][22];
static float huge facts[ASIZE];
static float huge localmax[ASIZE];
static float huge localmin[ASIZE];
static float huge localavg[ASIZE];
float xnew[22];
float xold[22];
float A[22][22];
float Atemp[22][22];
float B1[22];
float B2[22];
float factsmax, factsmin;
FILE *fp;

/* Set Value of Initial Line Reactance for Line Containing FACTS Device */
float X45_init=0.0850;

void main(int argc, char *argv[])
{
    int count, index, i, j;
    int flag;
    unsigned long int iter;
    int pkcount;
    float oldmax, oldmin;
    char dummy[80];
    float set_time;

    flag=0;
    pkcount=0;
    set_time=500.0;

    if(argc<2) argv[1]="";

    for(i=0;i<ASIZE;i++)
    {
        localmax[i]=1;
        localmin[i]=-1;
    }

    /* Read in Initial Conditions for state variables */
    printf("Reading initial conditions for state variables...\n\n");

```

```

if((fp = fopen("initcond.c", "rt"))==NULL)
{
    printf("Cannot open %s\n", "initcond.c");
    exit(1);
}
/* Skip over file header */
fgets(dummy, 79, fp);
printf("%s\n\n", dummy);
for(i=1; i<=21; i++)
{
    fgets(dummy, 79, fp);
    xold[i]=atof(dummy);
    //printf("xold[%d]=%f\n", i, xold[i]);
}
fclose(fp);

/* Read in B1 matrix coefficients */
printf("Reading coefficients for B1 matrix...\n\n");
if((fp = fopen("bmat1.c", "rt"))==NULL)
{
    printf("Cannot open %s\n", "bmat1.c");
    exit(1);
}
/* Skip over file header */
fgets(dummy, 79, fp);
for(i=1; i<=21; i++)
{
    fgets(dummy, 79, fp);
    B1[i]=atof(dummy);
}
fclose(fp);

/* Read in B2 matrix coefficients */
printf("Reading coefficients for B2 matrix...\n\n");
if((fp = fopen("bmat2.c", "rt"))==NULL)
{
    printf("Cannot open %s\n", "bmat2.c");
    exit(1);
}
/* Skip over file header */
fgets(dummy, 79, fp);
for(i=1; i<=21; i++)
{
    fgets(dummy, 79, fp);
    B2[i]=atof(dummy);
}
fclose(fp);

/* Read in A matrix coefficients */
ReadAmat("amat21.c", A);

count=SKIP;
index=0;
printf("Solving Differential Equations...\n\n");
iter=1;

for(j=1; j<=21; j++)
{
    x[1][j]=xold[j];
}

/* Start Main Loop for Solving Differential Equations Using Euler's Method */

```

```

while(iter<LOOPS)
{
    for(j=1;j<=21;j++)
    {
        if((iter*DT) < LDCHANGE)
        {
            xnew[j] = (DT)*(A[j][ 1]*xold[ 1]+A[j][ 2]*xold[2]+
                A[j][ 3]*xold[ 3]+A[j][ 4]*xold[4]+
                A[j][ 5]*xold[ 5]+A[j][ 6]*xold[6]+
                A[j][ 7]*xold[ 7]+A[j][ 8]*xold[8]+
                A[j][ 9]*xold[ 9]+A[j][10]*xold[10]+
                A[j][11]*xold[11]+A[j][12]*xold[12]+
                A[j][13]*xold[13]+A[j][14]*xold[14]+
                A[j][15]*xold[15]+A[j][16]*xold[16]+
                A[j][17]*xold[17]+A[j][18]*xold[18]+
                A[j][19]*xold[19]+A[j][20]*xold[20]+
                A[j][21]*xold[21]+B1[j])*xold[j];
        }
        if((iter*DT) >= LDCHANGE )
        {
            xnew[j] = (DT)*(A[j][ 1]*xold[ 1]+A[j][ 2]*xold[2]+
                A[j][ 3]*xold[ 3]+A[j][ 4]*xold[4]+
                A[j][ 5]*xold[ 5]+A[j][ 6]*xold[6]+
                A[j][ 7]*xold[ 7]+A[j][ 8]*xold[8]+
                A[j][ 9]*xold[ 9]+A[j][10]*xold[10]+
                A[j][11]*xold[11]+A[j][12]*xold[12]+
                A[j][13]*xold[13]+A[j][14]*xold[14]+
                A[j][15]*xold[15]+A[j][16]*xold[16]+
                A[j][17]*xold[17]+A[j][18]*xold[18]+
                A[j][19]*xold[19]+A[j][20]*xold[20]+
                A[j][21]*xold[21]+B2[j])*xold[j];
        }
    }
}
/* Compress Data and Store in New Variable */
if(count==SKIP)
{
    for(j=1;j<=21;j++)
    {
        x[index][j]=xnew[j];
    }
    facts[index]=xnew[9];

    /* Check for local maxima and minima */
    if((iter*DT) > LDCHANGE )
    {
        if((facts[index-1] > facts[index-2]) && (facts[index] < facts[index-1]))
        {
            localmax[pkcount]=facts[index-1];
            //printf("Local Max[%d]=%f\n",pkcount,localmax[pkcount]);
        }

        if((facts[index-1] < facts[index-2]) && (facts[index] > facts[index-1]))
        {
            localmin[pkcount]=facts[index-1];
            //printf("Local Min[%d]=%f\n",pkcount,localmin[pkcount]);

            localavg[pkcount]=((localmax[pkcount]+localmin[pkcount])/2.0);
            //printf("Average of Min and Max=%f\n",localavg[pkcount]);

            // If all values within response envelope of FACTS Device
            // are less than required tolerance %, settling time has
            // been reached

```

```

        if((fabs(localavg[pkcount]) <= TOL*X45_init)
            && (fabs(localmin[pkcount]) <= TOL*X45_init)
            && (fabs(localmax[pkcount]) <= TOL*X45_init)
            && (flag == 0))
        {
            set_time=(DT)*SKIP*(index-1);
            flag=1;
        }
        pkcount++;
    }

    count=0;
    index++;
}

for(j=1;j<=21;j++)
{
    xold[j]=xnew[j];
}
count++;
iter++;
}

// Repeat last point to avoid reset to zero
for(j=1;j<=21;j++)
{
    x[index][j]=x[index-1][j];
}

/* If "-mat" option specified, convert results to MATLAB format */
if(strcmp(argv[1], "-mat") == 0)
{
    c_to_mat(x, "x", "xmat.m");
}

findpeak(facts);
printf("\n\n*****\n");
printf("Min = %f%%, Max = %f%%\n", factsmin, factsmax);
printf("Settling Time is %f seconds\n", set_time);
printf("\n\n*****\n");

/* Write Response Data to File */
if((fp = fopen("response.out", "at"))==NULL)
{
    printf("Cannot open %s\n", "response.out");
    exit(1);
}

fprintf(fp, "%f\t\t%f\t\t%f\n", factsmax, factsmin, set_time);
fclose(fp);

exit(1);
}

void ReadAmat(char *filename, float matrix[22][22])
{
    int i,j;
    char dummy[80];

```

```

/* Read in A matrix coefficients */
printf("Reading coefficients for A matrix...\n\n");
if((fp = fopen(filename,"rt"))==NULL)
{
    printf("Cannot open %s\n", filename);
    exit(1);
}
/* Skip over file header */
fgets(dummy,79,fp);
for(i=1;i<=21;i++)
{
    for(j=1;j<=21;j++)
    {
        fgets(dummy,79,fp);
        matrix[i][j]=atof(dummy);
    }
}
fclose(fp);
}

void c_to_mat(float huge var[ASIZE][22], char *varname, char *filename)
{
    int i,j;

    printf("Converting results to MATLAB format...\n\n");

    if((fp = fopen(filename,"w"))==NULL)
    {
        printf("Cannot open %s\n", filename);
        exit(1);
    }

    fprintf(fp,"time = [");

    for(i=0;i<ASIZE-1;i++)
    {
        fprintf(fp,"%f;\n", (DT)*SKIP*i);
    }
    fprintf(fp,"%f ];\n\n", (DT)*SKIP*(ASIZE-1));

    fprintf(fp,"%s = [", varname);

    for(i=0;i<ASIZE-1;i++)
    {
        for(j=1;j<21;j++)
        {
            fprintf(fp,"%f, ", var[i][j]);
        }
        fprintf(fp,"%f;\n",var[i][21]);
    }
    for(j=1;j<21;j++)
    {
        fprintf(fp,"%f, ",var[ASIZE-1][j]);
    }
    fprintf(fp,"%f ];\n\n", var[ASIZE-1][21]);

    fclose(fp);
}

```

```

void findpeak(float huge trace[ASIZE])
{
    int i;
    float min, max;

    min=0;
    max=0;

    for(i=0;i<=ASIZE;i++)
    {
        if(trace[i] >= max)
        {
            max=trace[i];
        }
        if(trace[i] <= min)
        {
            min=trace[i];
        }
    }
    factsmax=max/X45_init;
    factsmin=min/X45_init;
}

// End of DIFFEQ21.C
//*****

%*****
% POWER21.M
%
% MATLAB script file used for calculating incremental electrical power for
% each generator in the FACTS compensated version of Anderson & Fouad's
% Nine Bus, Three Machine Power System
%
% Mark A. Smith
% November 10, 1994
%*****
%
% clear;
%
% Load in Generator Data
gendata;
%
% Load Results from DIFFEQ21.C
xmat;
%
% Define Event Times and Time Step Information
DT=0.01;
SKIP=250;
LDCHANGE=10/(SKIP*DT)+1;
ENDTIME =400/(SKIP*DT)+1;
%
% Load Pre-Disturbance Incremental Current Coefficient Matrix
load I1.mat;
%
% Initialize Current Variables
Id1=0;
Iq1=0;
Id2=0;
Iq2=0;
Id3=0;
Iq3=0;

```



```

%
% Calculate Incremental Current Vector
for k=1:9,
    Id1=Id1+I(2,k)*x(1:LDCHANGE,k);
    Iq1=Iq1+I(1,k)*x(1:LDCHANGE,k);
    Id2=Id2+I(4,k)*x(1:LDCHANGE,k);
    Iq2=Iq2+I(3,k)*x(1:LDCHANGE,k);
    Id3=Id3+I(6,k)*x(1:LDCHANGE,k);
    Iq3=Iq3+I(5,k)*x(1:LDCHANGE,k);
end;
%
% Calculate Pre-Disturbance Electrical Power for each Generator
Pe1(1:LDCHANGE)=(Iq0(1)*x(1:LDCHANGE,1)+Eq0(1)*Iq1(:))+...
    (Ed0(1)*Id1(:)+Id0(1)*x(1:LDCHANGE,2));
Pe2(1:LDCHANGE)=(Iq0(2)*x(1:LDCHANGE,3)+Eq0(2)*Iq2(:))+...
    (Ed0(2)*Id2(:)+Id0(2)*x(1:LDCHANGE,4));
Pe3(1:LDCHANGE)=(Iq0(3)*x(1:LDCHANGE,5)+Eq0(3)*Iq3(:))+...
    (Ed0(3)*Id3(:)+Id0(3)*x(1:LDCHANGE,6));
%
% Load Pre-Disturbance Incremental Current Coefficient Matrix
load I2.mat;
%
% Re-initialize Current Variables
Id1=0;
Iq1=0;
Id2=0;
Iq2=0;
Id3=0;
Iq3=0;
%
% Calculate Incremental Current Vector
for k=1:9,
    Id1=Id1+I(2,k)*x(LDCHANGE+1:ENDTIME,k);
    Iq1=Iq1+I(1,k)*x(LDCHANGE+1:ENDTIME,k);
    Id2=Id2+I(4,k)*x(LDCHANGE+1:ENDTIME,k);
    Iq2=Iq2+I(3,k)*x(LDCHANGE+1:ENDTIME,k);
    Id3=Id3+I(6,k)*x(LDCHANGE+1:ENDTIME,k);
    Iq3=Iq3+I(5,k)*x(LDCHANGE+1:ENDTIME,k);
end;
%
% Calculate Post-Disturbance Electrical Power for each Generator
Pe1(LDCHANGE+1:ENDTIME)=(Iq0(1)*x(LDCHANGE+1:ENDTIME,1)+Eq0(1)*Iq1(:))+...
    (Ed0(1)*Id1(:)+Id0(1)*x(LDCHANGE+1:ENDTIME,2));
Pe2(LDCHANGE+1:ENDTIME)=(Iq0(2)*x(LDCHANGE+1:ENDTIME,3)+Eq0(2)*Iq2(:))+...
    (Ed0(2)*Id2(:)+Id0(2)*x(LDCHANGE+1:ENDTIME,4));
Pe3(LDCHANGE+1:ENDTIME)=(Iq0(3)*x(LDCHANGE+1:ENDTIME,5)+Eq0(3)*Iq3(:))+...
    (Ed0(3)*Id3(:)+Id0(3)*x(LDCHANGE+1:ENDTIME,6));
%
% Group Resulting Power, Rotor Angle, and Frequency Data
Peltot=Pe1+Pgen(1);
Pe2tot=Pe2+Pgen(2);
Pe3tot=Pe3+Pgen(3);
Pe=[Peltot; Pe2tot; Pe3tot]';
omega=[x(:,10) x(:,11) x(:,12)];
delta=[x(:,7) x(:,8)];
%
%
% End of POWER21.M
%*****

```

## B.4 Sensitivity Studies

```
*****
% XSENSE.M
%
% MATLAB script file used for determining the change in the real part
% of critical eigenvalues for incremental changes in the reactance of each
% line. Data arrays that are calculated are then used by DEDXCALC.M to
% calculate the average numerical critical eigenvalue derivatives with
% respect to changes in the reactance of each line.
%
% Mark A. Smith
% November 10, 1994
%*****
%
PI =3.141592654;
OMEGA_R= 2*PI*60;
%
% Load Generator and Excitation System Data
gendata;
%
% Calculate Reduced Network Parameters
linedata;
%
% Begin Sensitivity Loop
for zz=1:200,
    clear A I Inew M T Yred Ybus Ynn Ynr Yrn Yrr;
    Z=zeros(9,9);
    Y=zeros(9,9);
    Ybus=zeros(9,9);
    %
    % Reduce Network Based on Present Value of Each Line Reactance
    reduce;
    %
    % Calculate A Matrix
    acalc20;
    %
    % Calculate Real Part of Critical Eigenvalues and Store in Array
    de_dX(zz)=-min(abs(real(eig(A)))));
    if zz >= 1,
        if max(real(eig(A))) >= 0;
            de_dX(zz)=-de_dX(zz);
        end;
    end;
    %
    % Store Reactance Value and Decrement for Next Iteration
    dX(zz)=X(4,5)-0.001;
    X(4,5)=X(4,5)-0.001;
end;
%
%
% End of XSENSE.M
%*****

%*****
% DEDXCALC.M
%
% MATLAB script file used for calculating the average numerical critical
% eigenvalue derivatives with respect to changes in the reactance of each
% line based on calculations made by XSENSE.M
%
```

```

% Mark A. Smith
% November 10, 1994
%*****
%
INT=5;
dx=0.001;
%
% Set Logic Flags to Zero
flag89=0;
flag78=0;
flag57=0;
flag45=0;
flag46=0;
flag69=0;
%
% Calculate Eigenvalue Derivative With Respect to Changes in X89
load dx89.mat
for z=1:195,
    e89(z)=de_dX(z);
    dedx89(z)=(de_dX(z+INT)-de_dX(z))/(dx*INT);
    dx89(z)=dX(z);
    half89=0.5*dX(1);
    if dx89(z)<half89 & flag89 ~=1,
        flag89=1;
        dsens89=mean(dedx89(1:z));
        esens89=e89(z);
    end;
end;
clear z de_dX dX;
%
% Calculate Eigenvalue Derivative With Respect to Changes in X78
load dx78.mat
for z=1:195,
    e78(z)=de_dX(z);
    dedx78(z)=(de_dX(z+INT)-de_dX(z))/(dx*INT);
    dx78(z)=dX(z);
    half78=0.5*dX(1);
    if dx78(z)<half78 & flag78 ~=1,
        flag78=1;
        dsens78=mean(dedx78(1:z));
        esens78=e78(z);
    end;
end;
clear z de_dX dX;
%
% Calculate Eigenvalue Derivative With Respect to Changes in X57
load dx57.mat
for z=1:195,
    e57(z)=de_dX(z);
    dedx57(z)=(de_dX(z+INT)-de_dX(z))/(dx*INT);
    dx57(z)=dX(z);
    half57=0.5*dX(1);
    if dx57(z)<half57 & flag57 ~=1,
        flag57=1;
        dsens57=mean(dedx57(1:z));
        esens57=e57(z);
    end;
end;
clear z de_dX dX;
%
% Calculate Eigenvalue Derivative With Respect to Changes in X45
load dx45.mat
for z=1:195,

```

```

e45(z)=de_dX(z);
dedx45(z)=(de_dX(z+INT)-de_dX(z))/(dx*INT);
dx45(z)=dX(z);
half45=0.5*dX(1);
if dx45(z)<half45 & flag45 ~=1,
    flag45=1;
    dsens45=mean(dedx45(1:z));
    esens45=e45(z);
end;
end;
clear z de_dX dX;
%
% Calculate Eigenvalue Derivative With Respect to Changes in X46
load dx46.mat
for z=1:195,
    e46(z)=de_dX(z);
    dedx46(z)=(de_dX(z+INT)-de_dX(z))/(dx*INT);
    dx46(z)=dX(z);
    half46=0.5*dX(1);
    if dx46(z)<half46 & flag46 ~=1,
        flag46=1;
        dsens46=mean(dedx46(1:z));
        esens46=e46(z);
    end;
end;
clear z de_dX dX;
%
% Calculate Eigenvalue Derivative With Respect to Changes in X69
load dx69.mat
for z=1:195,
    e69(z)=de_dX(z);
    dedx69(z)=(de_dX(z+INT)-de_dX(z))/(dx*INT);
    dx69(z)=dX(z);
    half69=0.5*dX(1);
    if dx69(z)<half69 & flag69 ~=1,
        flag69=1;
        dsens69=mean(dedx69(1:z));
        esens69=e69(z);
    end;
end;
clear z de_dX dX;
%
% Calculate Eigenvalue Derivative With Respect to Changes in X89
%
% Group Sensitivity Results
dsens=[dsens45;dsens57;dsens78;dsens89;dsens69;dsens46];
esens=[esens45;esens57;esens78;esens89;esens69;esens46];
%
%
% End of DEDXCALC.M
%*****

%*****
% YSENSE.M
%
% MATLAB script file used for determining the change in the elements of
% the reduce admittance matrix for Anderson & Fouad's Nine Bus System due
% to incremental changes in the reactance of the line connecting buses
% 4 and 5 (FACTS reactance). Data arrays that are calculated are then used
% by DYDXCALC.M to calculate the derivatives of each reduced admittance
% matrix term with respect to changes in the FACTS reactance.
%

```

```

% Mark A. Smith
% November 10, 1994
%*****
%
tic;          % Start Timer
format short e; % Set Numeric Display Format
%
dX=0.001;     % Impedance Change in per unit
STEPS=100;    % Number of increment steps
%
for r=1:3,
    for s=1:3,
        varname=sprintf('Yred%d%d',r,s);
        filename=sprintf('%s.m',varname);
        fid=fopen(filename,'wt');
        fprintf(fid,'%s =[' , varname);
        %
        % Create Arrays of Yred Elements and Store for Use By DYDXCALC.M
        for q=1:STEPS,
            clear A I M Ybus R Z X Yred Ynn Yrn Ynr Yrr N;
            linedata;
            X(4,5)=X(4,5)-q*dX;
            reduce;      % runlc;
            dummy=sprintf('%s(%d)=Yred(%d,%d);\n',varname,q,r,s);
            eval(dummy);
            dummy1=sprintf('real(Yred%d%d(%d))\n',r,s,q);
            dummy2=sprintf('imag(Yred%d%d(%d))\n',r,s,q);
            if q < STEPS
                fprintf(fid,'%f+{%f}*i;\n',eval(dummy1),eval(dummy2));
            end;
            if q == STEPS
                fprintf(fid,'%f+{%f}*i];\n',eval(dummy1),eval(dummy2));
            end;
        end;
        fclose(fid);
    end;
end;
%
toc      % Stop timer;
%
%
% End of YSENSE.M
%*****

%*****
% DYDXCALC.M
%
% MATLAB script file used for calculating the derivatives of each reduced
% admittance matrix term with respect to changes in the FACTS reactance.
% Uses data created by YSENSE.M
%
% Mark A. Smith
% November 10, 1994
%*****
%
clear;
%
dX=0.001;      % impedance in per unit
STEPS=100;     % Number of increment steps
INT = 5;
%
% Load Yred element arrays created by YSENSE.M

```

```

yred11;
yred12;
yred13;
yred21;
yred22;
yred23;
yred31;
yred32;
yred33;
%
% Calculate derivatives of each Yred element with respect to X45
for z=1:(STEPS-INT),
    dY_dX11(z)=(Yred11(z+INT)-Yred11(z))/(dX*INT);
    dY_dX12(z)=(Yred12(z+INT)-Yred12(z))/(dX*INT);
    dY_dX13(z)=(Yred13(z+INT)-Yred13(z))/(dX*INT);
    dY_dX21(z)=(Yred21(z+INT)-Yred21(z))/(dX*INT);
    dY_dX22(z)=(Yred22(z+INT)-Yred22(z))/(dX*INT);
    dY_dX23(z)=(Yred23(z+INT)-Yred23(z))/(dX*INT);
    dY_dX31(z)=(Yred31(z+INT)-Yred31(z))/(dX*INT);
    dY_dX32(z)=(Yred32(z+INT)-Yred32(z))/(dX*INT);
    dY_dX33(z)=(Yred33(z+INT)-Yred33(z))/(dX*INT);
end;
%
% Group elements together in array
dY_dX=[dY_dX11; dY_dX12; dY_dX13; dY_dX21; dY_dX22; dY_dX23; dY_dX31;dY_dX32;dY_dX33];
Yred=[Yred11,Yred12,Yred13,Yred21,Yred22,Yred23,Yred31,Yred32,Yred33]';
%
for zz=1:(STEPS-INT),
    dX(zz)=-0.001*zz;
end;
%
% Calculate Mean Derivatives over 50% compensation range
for zz=1:9,
    dYmean(zz)=mean(dY_dX(zz,1:40));
end;
%
%
% End of DYDXCALC.M
%*****

%*****
% KSENSE.M
%
% MATLAB Script file that checks eigenvalue sensitivity to changes in FACTS
% gain (or Time Constant) by creating an array of gain (or time constant)
% values versus critical eigenvalues.
%
% Mark A. Smith
% November 10, 1994
%*****
%
clear;
PI =3.141592654;
OMEGA_R= 2*PI*60;
%
% Load Generator Data
gendata;
%
% Set Initial FACTS Controller Gain and Time Constant
Kx = -100;
Tx = 100;
%
% Calculate Reduced Network Parameters

```

```

linedata;
reduce;
%
% Load dY/dX values
load c:\thesis\dydxmean.mat;
for k=1:3,
    for l=1:3,
        dY(k,l)=dYmean(3*(k-1)+l);
    end;
end;
alpha=angle(dY);
dYdX=abs(dY);
%
% Begin Sensitivity Loop
for zz=1:40,
    clear i;
    % Calculate A matrix for FACTS Compensated System
    acalc21;
    %
    % Calculate Real Part of Critical Eigenvalues and Store in Array
    de_dk(zz)=-min(abs(real(eig(A)))));
    if zz >= 1,
        if max(real(eig(A))) >= 0;
            de_dk(zz)=-de_dk(zz);
        end;
    end;
    dk(zz)=Kx;
    dt(zz)=Tx;
    %
    % Set New Value of Kx (or Tx) for next iteration and Reset Variables
    Kx=Kx-5;
    %Tx=Tx+0.5;
    clear A I Inew M T;
end;
%
%
% End of KSENSE.M
%*****

%*****
% RESPONSE.M
%
% MATLAB script file used in conjunction with DIFFEQ21.C for calculating
% and tabulating the time response attributes of the FACTS device for
% varying values of gain and time constant. Resulting table is stored in
% RESPONSE.OUT.
%
% Mark A. Smith
% November 10, 1994
%*****
%
clear;
PI =3.141592654;
OMEGA_R= 2*PI*60;
%
% Load Generator Data
gendata;
%
% Set Initial FACTS Controller Gain and Time Constant
Kx = -1;
Tx = 10;
%

```

```

% Calculate Reduced Network Parameters
linedata;
reduce;
%
% Load dY/dX values
load c:\thesis\dydxmean.mat;
for k=1:3,
    for l=1:3,
        dY(k,l)=dYmean(3*(k-1)+1);
    end;
end;
alpha=angle(dY);
dYdX=abs(dY);
%
% Format Output File
fid=fopen('response.out', 'wt');
fprintf(fid, '*****\n');
fprintf(fid, '                RESPONSE.OUT: Output File from RESPONSE.M\n\n');
fprintf(fid, '                Includes data for maximum value of FACTS reactance,\n');
fprintf(fid, '                minimum value of FACTS reactance, and time required\n');
fprintf(fid, '                for the device to settle to 0.5% of the nominal line\n');
fprintf(fid, '                reactance for varying values of Kx and Tx, the FACTS\n');
fprintf(fid, '                controller gain and time constant.\n\n');
fprintf(fid, '                Note: "500" second settling time indicates reactance\n');
fprintf(fid, '                did not settle in the studied time interval.\n');
fprintf(fid, '*****\n\n');
fprintf(fid, ' Kx\t\t\t\tTx\t\t\t\tMax\t\t\t\tMin\t\t\t\tTime(sec)\n\n');
fclose(fid);
%
% Begin Sensitivity Loop
for zz=1:11,
    % Print Values of Kx and Tx in a Text File
    fid=fopen('response.out', 'At');
    fprintf(fid, '%3d\t\t\t\t3.0f\t\t\t\t', Kx, Tx);
    fclose(fid);
    clear i;
    %
    % Calculate A matrix
    acalc21;
    %
    % Format A matrix and print to file for use in C programs
    fid=fopen('Amat21.c', 'wt');
    fprintf(fid, '/*Amat21.c: Coefficients of A matrix from response.m*/\n');
    for i=1:21,
        for j=1:21,
            dummy=sprintf('%f\n', A(i,j));
            fprintf(fid, dummy);
        end;
    end;
    fclose(fid);
    %
    % Call DIFFEQ21.EXE to find Max, Min, and Settling Time
    !diffeq21
    %
    % Set New Value of Kx for next iteration and Reset Variables
    Kx=Kx-10;
    %
    clear A I Inew M T;
end;
% End of RESPONSE.M
%*****

```



## VITA

Mark Allen Smith is originally from Charleston, Illinois where he graduated first in his class from Charleston High School in 1987. After high school he attended the University of Illinois at Urbana-Champaign where he received a Bachelor of Science Degree in Electrical Engineering with honors in 1991. After graduating, he joined American Electric Power Service Corporation in Columbus, Ohio where he worked in System Measurements Section. In August of 1993, he left AEPSC to pursue his Master of Science Degree at Virginia Polytechnic Institute and State University. After graduating with his Master's Degree, he will be working for the Tennessee Valley Authority in Chattanooga, Tennessee. He is a member of Tau Beta Pi and Eta Kappa Nu honor societies.

*Mark A. Smith*